TECHNICAL REPORT DOCUMENTATION PAGE

1. Report No.	2. Government Accession No.	3. Recipient's Catalog No.
FHWA/TX-95/1359-1F		

4. Title and Subtitle	5. Report Date
CORROSION EFFECTS OF CEMENT STABILIZED BACKFILL ON GALVANIZED STEEL EARTH REINFORCEMENTS	November 1994
	6. Performing Organization Code

7. Author(s)	8. Performing Organization Report No.
Derek V. Morris and Branko N. Popov	Research Report 1359-1F

9. Performing Organization Name and Address	10. Work Unit No.
Texas Transportation Institute The Texas A&M University System College Station, Texas 77843-3135	11. Contract or Grant No. Study No. 0-1359

12. Sponsoring Agency Name and Address	13. Type of Report and Period Covered
Texas Department of Transportation Research and Technology Transfer Office P. O. Box 5080 Austin, Texas 78763-5080	Final: September 1992 - August 1994
	14. Sponsoring Agency Code

15. Supplementary Notes

Research performed in cooperation with the Texas Department of Transportation and the U.S. Department of Transportation, Federal Highway Administration.
Research Study Title: Corrosion Effects of Cement Stabilized Backfill on Galvanized Steel Earth Reinforcements

16. Abstract

Cement stabilization of backfill has been used for some time in mechanically stabilized earth type retaining walls. However, there has been no data on the corrosion life of galvanized steel reinforcement in this environment, which is intermediate in pH between normal soil and pure cement. Field observations had indicated a potential corrosion problem at a particular site in District 12.

As a result of the test program conducted during this project, it has been concluded that:

(a) Cement addition to backfill in the usual quantities (i.e. 7% or more) raised the pH environment to values close to that of normal concrete. At these levels corrosion rates of zinc coatings were not significantly accelerated -- if anything, corrosion rates were less than for unstabilized fill.

(b) Very small amounts of cement addition, of the order of 1% to 4% producing pH values significantly less than 12, could cause limited acceleration of corrosion. It is, therefore, advisable to control minimum cement levels and to encourage efficient mixing.

(c) Elevated corrosion rates were associated primarily with the presence of inorganic ions, both for stabilized and unstabilized fill. In the case of the problem site in District 12, this appeared to be the result primarily of unusually high sulfate content in the fill.

(d) The use of crushed concrete as backfill did not accelerate corrosion. This material, therefore, appears to be acceptable for this application.

17. Key Words	18. Distribution Statement
Soil Corrosion, Soil Cement, Retaining Walls, Earth Retaining Structures, Tiebacks, Retained Earth, Reinforced Earth, Galvanized Steel Corrosion	No restrictions. This document is available to the public through NTIS: National Technical Information Service 5285 Port Royal Road Springfield, Virginia 22161

19. Security Classif. (of this report)	20. Security Classif. (of this page)	21. No. of Pages	22. Price
Unclassified	Unclassified	152	

Form DOT F 1700.7 (8-72) Reproduction of completed page authorized

CORROSION EFFECTS OF CEMENT STABILIZED BACKFILL ON GALVANIZED STEEL EARTH REINFORCEMENTS

by

Derek V. Morris, P.E.
Associate Research Engineer
Texas Transportation Institute

and

Branko N. Popov
Research Scientist
Texas Transportation Institute

Research Report 1359-1F
Research Study Number 0-1359
Research Study Title: Corrosion Effects of Cement Stabilized Backfill on Galvanized Steel Earth Reinforcements

Sponsored by the
Texas Department of Transportation
In Cooperation with
U.S. Department of Transportation
Federal Highway Administration

November 1994

TEXAS TRANSPORTATION INSTITUTE
The Texas A&M University System
College Station, Texas 77843-3135

IMPLEMENTATION STATEMENT

The results of this project are potentially relevant to retaining walls constructed with cement stabilization in the fill, and implementation in principle involves all walls built with stabilized backfill. The presence of cement stabilized fill is sufficiently widespread that information on corrosion life is significant to almost every district in the TxDOT system. Before this project, data on the subject was entirely absent, so that the hard data generated on the subject is of interest to highway departments across the country.

The conclusions from this study are also pertinent to new wall construction using cement stabilization. This includes, for instance, the North Central Expressway in Dallas, where adverse information concerning corrosion rates would have had a major impact on the project. Fortunately, the results of this study have indicated that there should be no problem. The study has concluded that the use of cement addition to retaining wall backfill does not need to be discouraged or discontinued from a corrosion point of view, so long as reasonable concentrations of cement are used (the normal minimum of 7% cement being acceptable). Widespread reconstruction and repair might otherwise have been necessary. In the event, existing construction designs need not be compromised, which has a major beneficial effect on departmental planning since there are currently large retaining wall projects being built almost entirely with cement stabilized backfill.

It now also appears likely that the use of crushed concrete in the backfill can be permitted, as far as corrosion is concerned, and the specifications for backfill relaxed to allow this material to be used. This should result in some economies in some cases. The prime cause of accelerated corrosion at this location is attributed to high concentrations of ionic salts, and in this respect, the project will almost certainly encourage and amplify the recent changes to backfill corrosivity specifications to specifically measure ionic concentrations, rather than just using backfill resistivity as a general overall measure as has been the tendency in the past.

On a national level, the generation of real data and a satisfactory understanding of actual corrosion rates under these circumstances is likely to be of significant interest to other highway departments also. The potential benefits both to TxDOT and elsewhere are likely to be substantial since cement stabilization has, in some cases, been quite widespread and is liable to continue to be a popular technique in the future.

T.T.I. will coordinate with department personnel in ensuring that results and recommendations will be incorporated into TxDOT practice as expeditiously and effectively as possible.

DISCLAIMER

The contents of this report reflect the views of the first author, Dr. Derek V. Morris (Texas P.E. # 63681), who is responsible for the opinions, findings, and conclusions presented herein. The contents do not necessarily reflect the official views or policies of the Texas Department of Transportation (TxDOT) or the Federal Highway Administration (FHWA). This report does not constitute a standard, specification, or regulation, nor is it intended for construction, bidding, or permit purposes.

ACKNOWLEDGMENT

The help and assistance of the Bridge Division of the Texas Department of Transportation (Mark P. McClelland, technical panel chairman) and the Federal Highway Administration (Donald E. Harley, Field Technical Coordinator, Texas Division) is gratefully acknowledged in carrying out this project. The District 12 field and maintenance staff (George Gonzales, Charles Fry, and Ronald Smith) was also of major assistance in the field work. The later portions of the laboratory corrosion testing were carried out by the second author at the University of South Carolina Chemical Engineering Department.

TABLE OF CONTENTS

Page

LIST OF FIGURES

LIST OF TABLES

SUMMARY

For some time, it has been possible for contractors engaged in the construction of mechanically stabilized earth walls to incorporate cement stabilization into backfill material. Although no specific research had ever been conducted into the effect of this on the corrosivity of the backfill, it was generally assumed to be no worse than having normal soil backfill that met the standard specifications.

However, as a result of apparently accelerated corrosion observed at a retaining wall at State Highway 225 in Deer Park, District 12, it was necessary to consider examining the effects of cement stabilization on corrosion rates of the reinforcing strips. It was theorized that the pH levels generated in cement stabilized soil, which is intermediate between normal soil and pure cement, might be high enough to attack the zinc coating, without being high enough to passivate the underlying steel. It was not known what levels of cement addition might cause problems, or what was responsible for the accelerated corrosion at the Deer Park site. It was possible that rather than being an isolated incident, such corrosion might actually be widespread in many such walls.

The objectives of the study were to determine whether or not corrosion of earth reinforcement is a significant problem in cement stabilized fill, and to determine the reasons for the accelerated corrosion observed in the field. The effect of cement stabilization on galvanized and reinforcing steel was investigated in order to determine what cement concentration accelerates or inhibits corrosion. Additional data was also generated on the use of crushed concrete as a backfill material, which so far has been excluded since the inherent pH of this material is outside the range of normal fill specifications. Field sampling and chemical testing were carried out to identify the conditions responsible for the corrosion at Deer Park.

As a result of the test program documented in this report, it was concluded that cement addition to backfill in the usual quantities (i.e. 7% or more) raised the pH environment to values close to that of normal concrete. At these levels corrosion rates of zinc coatings were not significantly accelerated -- if anything, corrosion rates were less than for unstabilized fill.

Very small amounts of cement addition, of the order of 1% to 4% producing pH values significantly less than 12, could cause limited acceleration of corrosion. It is, therefore, advisable to control minimum cement levels and to encourage efficient mixing. The overall conclusion is that the use of cement addition to retaining wall backfill does not need to be discouraged or discontinued from a corrosion point of view, if reasonable concentrations of cement are used -- the normal minimum value of 7% (sometimes referred to colloquially as 2 sacks/cu. yd.) being acceptable, so long as it is uniform.

Elevated corrosion rates were associated primarily with the presence of inorganic ions, both for stabilized and unstabilized fill. In the case of the problem site in District 12, this appeared to be the result primarily of unusually high sulfate content in the fill.

The use of crushed concrete as backfill did not accelerate corrosion, and this material, therefore, appears to be acceptable for this application (at least as far as corrosion is concerned); the appropriate specifications for backfill can be relaxed to allow this material to be used.

1. INTRODUCTION

During the last 20 years, the use of mechanically stabilized earth type retaining walls (e.g., "Reinforced Earth," "Retained Earth," etc.) has gained widespread popularity because of their flexibility, ease of installation, and economic advantages. They generally use metal straps or bar mats and select backfill to form the retaining wall mass behind a precast concrete facing. In some areas, stabilizing cement is added to the backfill, both as an aid to construction and to reduce reinforcement lengths where necessary.

Obviously, the long-term durability of such a structure depends on the ability of the reinforcement to adequately withstand corrosion attack over the design life of the structure. A considerable amount of research has been done on the corrosion resistance of reinforcing materials in natural soil. Aluminum and stainless steel materials have been used as reinforcement material, but for various reasons have been found to be less satisfactory than traditional galvanization, at least in unstabilized backfill material. Predictions of 100 to 200 years have been made for the service life of galvanized steel reinforcement in normal select backfill.

Similarly, extensive research has been done on the corrosion performance of reinforcing steel in pure concrete, and the techniques for evaluating this are now fairly well established. There are now examples of mild steel reinforcement in concrete that are almost 150 years old, and which are still performing satisfactorily.

No research has ever been conducted into the effect of cement stabilization on the corrosivity of the backfill. It has generally been assumed that this was no worse than having normal soil backfill that met the standard specifications. Since unprotected steel reinforcement is known to be reasonably well protected by the highly alkaline conditions present in conventional reinforced concrete, the assumption has been that the increase in alkalinity caused by the addition of a small percentage of cement would also be beneficial in inhibiting premature corrosion of protected reinforcement. The situation appeared to be intermediate between pure soil backfill and pure concrete, for which there was apparently satisfactory corrosion data available in both cases.

These assumptions were thrown into question by field observations made at a retaining wall at State Highway 225 in Deer Park, District 12. This had to be partially dismantled temporarily in order to allow the height of the wall to be extended. Visual inspection of the exposed reinforcing strips indicated that a significant amount of corrosion had already taken place in less than 5 years, much more rapidly than had been assumed previously. As a result of the apparently accelerated corrosion observed at this retaining wall, it was necessary to consider examining the effects of cement stabilization on corrosion rates of the reinforcing strips in order to determine what levels of cement addition might cause enhanced corrosion, and what effect the soil chemistry and other factors may have on the overall situation.

This project was intended to address these concerns by establishing the true nature and extent of the problem.

2. ESTABLISHMENT OF INITIAL CONDITIONS

2.1 GENERAL

As one of the initial tasks on the project, it was desirable to investigate the conditions at the field project before proceeding much further. This would assist in determining the electro-chemical corrosion properties at the problem site in order to determine whether or not the rapid corrosion observed at Deer Park was simply an abnormality, or whether it might represent more widespread conditions within cement stabilized retaining walls. It was also the recommendation of the Federal Highway Administration that conditions at the Deer Park site be clearly established before other tasks were started to see whether conditions there were in reality an anomaly or in violation of existing specifications for corrosive properties.

As a result, in the first instance the normal test data obtained during construction testing was examined, and is described below.

2.2 FIELD DATA ON INITIAL CONSTRUCTION

Archival data was obtained relating to the original construction of the State Highway 225 retaining wall between December 1985 and January 1986 (project CSJ 502-01-134), and these are summarized in Table 2.1. At the time, the corrosivity specifications for the backfill were that the pH should be within the range 5.5 to 9.0 (test method Tex-128-E), and that the material resistivity (as measured by test method Tex-129-E) should not be less than 1,500 ohm-cm.

As can be seen, the original fill properties displayed pH values close to the upper limit of the specifications, but not exceeding them (ranging from 8.6 to 8.8). The resistivity values were on the low side, but only one sample actually tested below 1,500 ohm-cm, which was the limit in use at that time. Since this was the only non-conforming result, construction was not halted.

On this basis, the fill properties were evidently marginal in terms of meeting corrosivity specifications, but were not clearly in overall violation, as in reality these fill properties were not particularily unusual for the area.

2.3 FIELD CONDITIONS ON RAISING WALL

In 1990/91, the wall was raised (this was when the accelerated corrosion of some of the reinforcing straps was noticed). Further fill was placed for this purpose, and the usual testing conducted as part of construction control (project CSJ 502-01-131). Archival data from this period is again shown in Table 2.1. Many more samples were tested at this time, and on this occasion the backfill resistivity was in compliance for every sample tested (ranging upwards from 3,365 ohm-cm, which was the lowest resistivity measured for nine samples). However, two of the nine samples tested outside the pH limits - one low at 5.1 and one high at 9.4, while the other seven samples met specifications current at that time.

This second material tested is, of course, not the same as the fill originally used when the wall was first built, which is the material associated primarily with the accelerated corrosion. However, local sources of fill may presumably be similar, so this information is also useful as an extra indication of the properties of the material in the wall. Certainly, it does not appear as though the field staff made a serious mistake in approving the fill used, as the measured properties were not consistently out of line, and would not at that time have been considered to represent a seriously high corrosivity regime.

TABLE 2.1 - HISTORIC FIELD DATA

	pH	Resistivity
1985/86	8.6	1,534 ohm-cm
	8.8	1,167
	8.7	2,101
1990/91	5.8	5,336 ohm-cm
	5.8	23,345
	6.8	9,338
	5.1	9,338
	9.4	14,007
	6.3	9,338
	7.6	3,365
	6.8	10,005
	7.5	14,007

2.4 SPECIFICATIONS FOR CORROSIVITY OF EARTH FILLS

As far as the reinforcement material is concerned, an extensive amount of experience (e.g., Darbin, Jailloux, and Montuelle, 1978; Swamy, 1990) has resulted in galvanized steel being by far the most common choice for reinforcing strips (although epoxy coating and aluminum have occasionally been used).

When embedded in normal backfill materials, studies (e.g., Elias, 1990) have shown corrosion loss rates from buried metal of between 0.002 to 0.01 mm per year. Rates have been found to decrease with time. Since galvanization thicknesses are usually around 0.086 mm,

(corresponding to what is often referred to as 2 oz./sq.ft.), the zinc coating is usually assumed to protect the steel for around 15 years. Metal dimensions are usually chosen so that an additional 100 to 150 years worth of corrosion can take place before the cross-section becomes critically stressed (during which time any remaining zinc coating can act as a sacrificial anode). Therefore, a design life of around 150 years is commonly quoted for current designs, and this has so far been considered acceptable.

Since specific corrosion testing for individual circumstances is a long and arduous procedure, current practice for controlling the corrosivity environment, and for rejecting unsuitable fill material, is to specify the electro-chemical environment indirectly. It is normally assumed that specifying a permissible range of physicochemical properties of the soil is sufficient to hold corrosion down to reasonable levels.

At the time of initial construction and also at the time of wall raising, the appropriate backfill material specifications for backfill material (in addition to gradation, plasticity, density, moisture content, and friction angle requirements) were simply that the pH should be within the range 5.5 to 9.0, and the minimum resistivity should be 1,500 ohm-cm. If the soil fell within these limits, it was assumed that the concentration of any problem chemicals would be sufficiently low to prevent accelerated corrosion.

More recently, however, the specifications (particularily for resistivity) were revised, and are currently (effective 1993):

- pH to be in the range 5.5 to 10 (actually slightly less restrictive than in 1985/86), and
- resistivity of soil to be not less than **5,000** ohm-cm (up from 1,500 ohm-cm in 1985/86).

However, material with a resistivity of less than 5,000 ohm-cm but better than 1,500 ohm-cm is currently permitted, provided specific testing is carried out for potentially corrosive anions, notably chlorides and sulfates. Such material can still be used if the chloride content does not exceed 100 ppm (0.01 %) and the sulfate content does not exceed 200 ppm. (0.02 %) as determined by test method Tex-620-J.

This separate testing for specific chemical contaminants was not incorporated into construction control at the time this retaining wall was constructed, and undoubtedly represents an improvement in the specification, representing increased sophistication in controlling backfill corrosivity.

Although the original fill was marginally satisfactory, based on resistivity results alone, subsequent measurements have shown that it would almost certainly have failed specific testing for chloride and (especially) sulfate testing. As indicated in Chapter 9, recent tests to current standards of samples of the original backfill show chloride contents (as per the current test method) of 224 to 626 ppm (0.02 % to 0.06 %) and sulfate contents of 1248 to 2125 ppm. (0.12 % to 0.21 %). Unless these chemicals were introduced into the backfill after construction (possibly as air-borne or water-borne contaminants), it is almost certain that the fill would have failed current standards, although it did in fact meet the standards at the time of construction.

3. FIELD TESTING FOR CURRENT CONDITIONS

3.1 GENERAL

In order to obtain further information on the electro-chemical properties at the Deer Park site, it was necessary to obtain actual field samples of fill from behind the wall. As previously mentioned, historical data indicated a pH in 1985/86 close to the upper limit (8.6 to 8.8) of the standard corrosion specifications at that time, but not exceeding it (9.0). The resistivity was on the low side, but only one sample tested below the limit of 1,500 ohm-cm, at 1,167 ohm-cm. When the wall was raised in 1990/91, the resistivity of the fill used at that time was acceptable. However, two of the samples tested outside the pH limits -- one low at 5.1 and one high at 9.4, while the other samples met specifications.

Since there was no evidence that these fill properties were particularly unusual, a program of field sampling and testing was initiated in order to obtain more samples of material from a variety of locations and depths for more extensive laboratory analysis.

3.2 INITIAL SAMPLING WITH PORTABLE EQUIPMENT

Field sampling was carried out relatively straightforwardly by using a portable concrete coring drill to bore 200 mm (4 inch) diameter cores through the face of the existing retaining wall. For simplicity, it was decided initially just to obtain samples close to the facing units, because this could be done particularly economically with portable equipment. In fact, it was found to only be necessary to core through the concrete panel facing with a drill, as the fill behind could then be excavated manually to a depth of 0.15 to 0.3 m (6 to 12 inches) in selected locations in order to obtain samples of the existing cement stabilized sand backfill. It was possible to take bulk backfill samples with a hand trowel without difficulty through these holes. The facing concrete cores were then replaced to permit further sampling for more material or from deeper behind the wall. Traffic control was provided by the local TxDOT field office.

Additional samples were obtained at a later date for cement content testing. The fill behind was then excavated manually in selected locations in order to obtain bulk samples of the existing cement stabilized sand backfill (with a portable auger) through these holes. The facing concrete cores were replaced to allow further sampling in the future, if more material or samples from deeper behind the wall were required.

The detailed location of these sample points is shown on Figure 3.1. In order to represent fairly all portions of the retaining wall site, at least one sample was taken from each corner of the overpass, and in one case (the SW corner) also at two different heights.

Many of the samples appeared visually quite weak and crumbly when they were initially recovered from behind the retaining wall facing units. Also, most of the samples did not have the usual gray coloration associated with significant cement content -- indeed, all except one was primarily light orange in color so that it looked initially as if the material directly behind the facing units did not contain much stabilizing cement, although subsequent testing showed that, in fact, the correct amount of cement was present.

3.3 LOCATIONS OF SAMPLING POINTS

The first boring location was on Wall #2, 1.16 m (3.8 ft) above the finished sidewalk grade. Sample 1A was taken between 0 and 200 mm (0"-8") from the back face of the retaining wall. This sample (along with all the samples designated "A") was used for resistivity tests. Sample 1B was obtained between 200 and 300 mm (8"-12") from the back face of the retaining wall. This sample (along with all the samples designated "B") was used for cement content tests. The samples appeared to be a brown sand with little or no cement present.

Location 2 was at the same station on Wall #2 as location 1, 2.6 m (8.7 ft) above the finished sidewalk grade. Sample 2A was extracted 0 to 200 mm (0"-8") from the back face of the wall. Sample 2B was extracted 200 to 300 mm (8"-12") from the back face of the wall. The samples were described visually as a brown sand, slightly more tan than #1, with some cement present, and containing asphalt nodules.

Location 3 was at Wall #1, (using the TxDOT numbering system in use at the project, e.g., sheet #386, 502-01-131), 1 m (3.0 ft) above the finished sidewalk grade. Sample 3A was extracted 0 to 200 mm (0"-8") from the back face of the wall. Sample 3B was extracted 200 to 300 mm (8"-12") from the back face of the wall. The samples were a brown sand, easily broken-up, with little or no cement visibly present.

Location 4 was at the same station as location 3, but 2.4 m (8.0 ft) above the finished sidewalk grade. Concrete was encountered behind the face of the wall. Coring was discontinued 0.6 m (2.0 ft) behind the back face of the wall as only solid concrete was present in the depth penetrated (there must have been a solid block cast right at that location). No samples were, therefore, obtained at this location.

Location 5 was at Wall #3, 1.3 m (4.4 ft) above the finished sidewalk grade. Sample 5A was extracted 0 to 200 mm (0"-8") behind the back face of the wall. Sample 5B was extracted 200 to 300 mm (8"-12") behind the back face of the wall. The samples were a light brown sand, appearing to be highly compacted and/or cemented and stabilized.

Location 6 was at Wall #4, 1.5 m (5 ft) above the finished grade. Sample 6A was extracted 0 to 200 mm (0"-8") from the back face of the wall. Sample 6B was extracted 200 to 300 mm (8"-12") from the back face of the wall. The samples appeared as a fine, brown sand with an appearance of being cemented.

3.4 DEEP SAMPLING WITH HORIZONTAL DRILLING

Because of later concerns that the accelerated corrosion might be due at least in part to variations in cement concentration within the body of the fill, additional sampling was carried out to enable tests to be carried out on material from a considerable depth behind the retaining wall facing. This required the utilization of specialized horizontal drilling equipment at the site. It was, unfortunately, not possible to drill horizontally through the same portable core holes in the facing units, as 175 mm (7") diameter holes were required for the horizontal auger bits.

Disturbed samples were obtained in 0.6 m (2 ft) intervals by placing a large bucket at the face of the wall and recovering the drill cuttings as the horizontal auger pushed them out. The material was then collected as bulk samples in ziplock bags for transport and analysis. This was done at a total of five locations, and enabled bulk samples to be obtained as far back as 4.3 m (14 ft) behind the wall face (previously only the front 1.5 m or so of material had been tested, as this was where the problem zone was presumed to be). These samples were then tested for cement content, as described in Section 4.2.

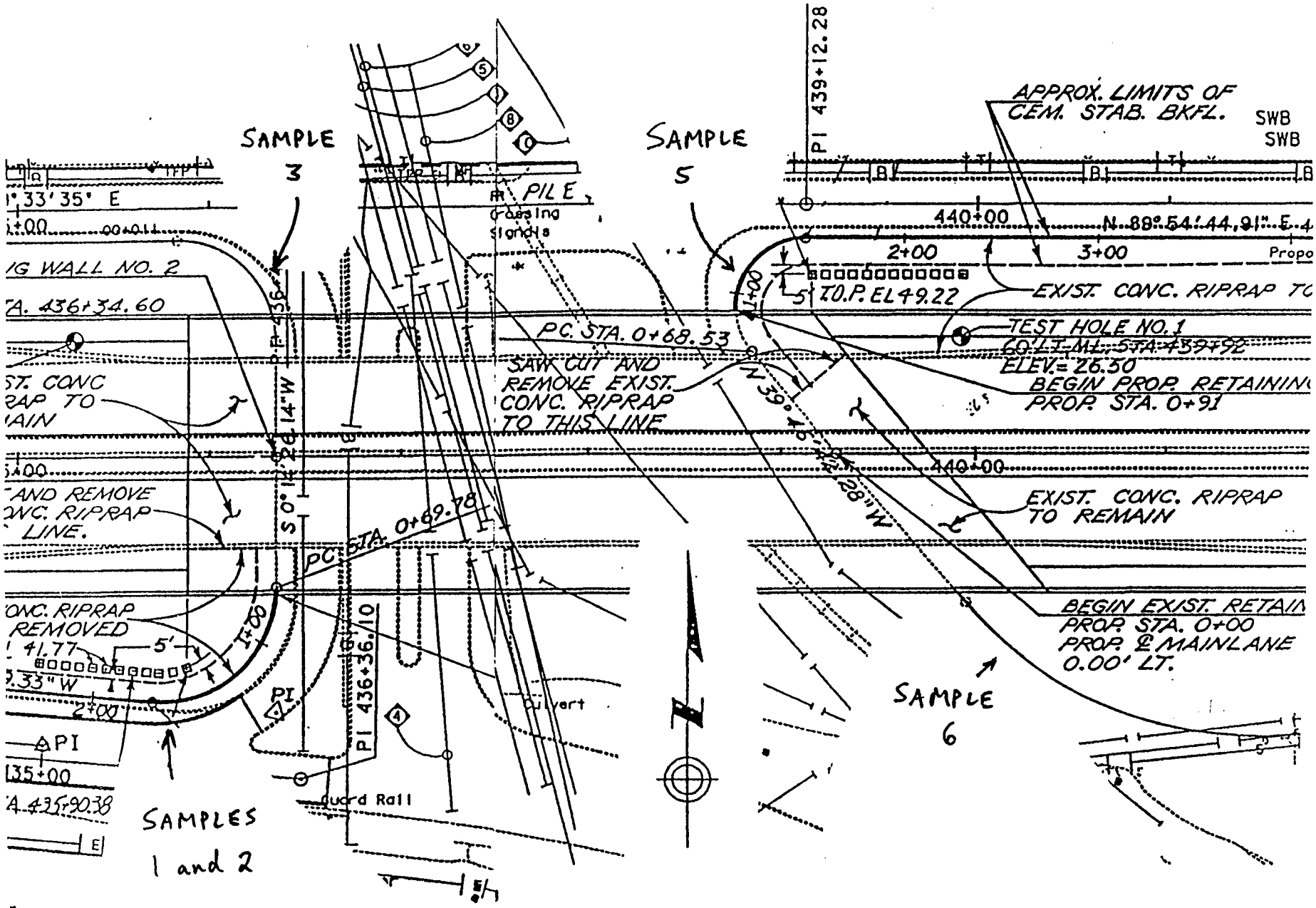

LOCATION OF RETAINING WALL SAMPLES

Fig. 3.1 - Location of Retaining Wall Samples

4. RESULTS OF FIELD TESTING

4.1 CURRENT pH AND RESISTIVITY VALUES

Following the field drilling and sampling program previously mentioned, further assessment of the post-construction conditions at the Deer Park site was carried out by post construction testing of the current pH and resistivity properties of backfill samples recovered from behind the retaining wall, as determined by standard test methods Tex-128-E (for pH) and Tex-129-E (for resistivity). Table 4.1 lists results from 5 field samples from the Deer Park retaining wall (representing at least one sample from each corner wall of the overpass, and in one location at two different heights).

TABLE 4.1 - CURRENT pH AND RESISTIVITY DATA

Sample No.	pH	Resistivity
1A	9.7	2,401 ohm-cm
2A	9.7	3,002
3A	9.3	2,268
5A	9.2	1,601
6A	9.2	1,934

As can be seen, at the present time all samples of the backfill now exceed the pH specifications for original construction (acceptable range 5.5 to 9.0), although during construction these values were reported as being between 8.6 and 8.8. However, normally these results would have been obtained before the addition of stabilizing cement, so it is not surprising that the post-construction values are higher. Probably, they were originally much higher (as the addition of even a small amount of cement will have quite a major effect on the overall pH). The effect of possible leaching of ground and rain water over the last seven years has probably contributed to the gradual post-construction lowering of pH.

Resistivity values, on the other hand, appear to have improved, as these are now all above the specified lower limit of 1,500 ohm-cm, and were originally reported as being very marginal - in the range previously of 2,101 to 1,167 ohm-cm (the latter value being in non-compliance at the time of construction).

Overall, however, in terms of identifying causes for the accelerated corrosion at this site, there is on the face of it no reason to consider the backfill material as being especially anomalous, based on the corrosivity specifications current at the time of construction. The results available to the field engineers at the time were obviously marginal, but not clearly in violation. Even now, the corrosion conditions at the site are ambiguous in terms of pH and resistivity, even though conditions in the backfill have changed with time. Initially at construction pH was in compliance, but has now moved out of compliance (almost certainly following the addition of cement). It is doubtful whether this is especially significant in this situation. Resistivity (probably the more important indicator) was marginal at construction, but is now acceptable according to the specification current at the time of construction.

As a result, the soil samples were subsequently subjected to more extensive chemical testing, and this is described in Chapter 9.

4.2 CEMENT CONTENT

Because of suggestions during the project that the accelerated corrosion might be the result of localized variations in cement concentration within the backfill, additional testing was carried out to determine exactly what this might be. Five samples were initially tested from material obtained close to the retaining wall face in the manner described in Chapter 3, and the results are summarized in Table 4.2.

TABLE 4.2 - EXISTING CEMENT CONTENTS CLOSE TO SURFACE

Sample No.	Distance	Cement Content
1B	0.25 m (10")	8.45%
2B	"	10.0%
3B	"	10.7%
5B	"	7.91%
6B	"	9.59%

This initial set of testing represented at least one sample from close to the face at each corner wall of the overpass, and also at two different heights in one location (the SW corner).

These samples were all taken between 200 and 300 mm (8"-12") from the back face of the retaining wall units, and their appearance was as follows. Those taken from Wall #2 were denoted 1B and 2B, the difference being in the vertical positions, which were 1.16 m (3.8 ft)

and 2.6 m (8.7 ft), respectively, above the finished sidewalk grade. Sample 1B appeared to be a brown sand with little or no cement visible, while sample 2B was also a brown sand, slightly more tan, with some cement evident and containing asphalt nodules. Sample 3B was from Wall #1, 1 m (3.0 ft) above the finished sidewalk grade, and was described as a brown sand, easily broken-up, with little or no cement visibly present. Sample 5B was from Wall #3, 1.3 m (4.4 ft) above the finished sidewalk grade, in appearance a light brown sand, apparently highly compacted and/or cement stabilized. Sample 6B was extracted from the back face of Wall #4, 1.5 m (5 ft) above the finished grade, described as a fine brown sand with a somewhat cemented appearance.

Although some of the samples appeared visually quite weak and crumbly when they were initially recovered, the results of this testing, nevertheless, indicated reasonably high cement contents of between 7.9% and 10.7% for these samples. Since the apparent low intact strength of field samples close to the facing units was not the result of low cement contents, it is believed that compaction densities in this region were probably low. This is not unusual, of course, and mechanically stabilized earth contractors will naturally tend to compact less close to the wall in order to avoid bulging the units there. In this instance, however, this may have exacerbated the corrosion environment at the wall face by allowing easier penetration of atmospheric oxygen and surface water in this region. It might be desirable to find some way of encouraging more effective compaction close to the facing units, although without further study it cannot be definitely said to be a contributory factor.

Since the samples initially tested were all from close to the wall face and did not display any large variations in cement content, samples from deeper within the wall were then tested, requiring horizontal drilling as described previously. Cement content tests were carried out on a total of four samples, and the results are given in Table 4.3.

TABLE 4.3 - DEEPER CEMENT CONTENTS BEHIND WALL

Location	Distance	Cement Content
1	0.6 m (2 ft)	17.4%
1	1.5 m (5 ft)	18.3%
5	1.8 m (6 ft)	14.8%
6	1.5 m (5 ft)	14.6%

(An additional sample of crushed concrete, numbered 8B, from the material subsequently used for corrosion testing on crushed concrete as described in Chapter 7, was also tested for reference under these conditions, and produced a measurement of 15.6% cement, for comparison).

These tests showed that there were indeed significant variations of cement content within the wall cross-section, with cement contents away from the wall face apparently consistently higher (in the range 15% to 18%) than those measured close to the face (typically 7.9% to 10.7%). On this basis, some laboratory testing was initiated to check the possibility of corrosion cells occurring between regions of different cement content. This is described in Chapter 8.

5. LABORATORY TESTING OF CORROSION RATES

5.1 GENERAL

In order to determine whether the addition of cement accelerates or inhibits the corrosion of reinforcement, a major testing program was undertaken in the laboratory on a large number of test samples to examine the corrosive effect of the presence of cement in the stabilized fill. The specific objectives were: (i) generation of data on the effect of cement addition on corrosion rates of reinforcing strips in sand or crushed concrete and (ii) identification of field conditions for which such corrosion is likely to be a problem.

Both uncoated steel and galvanized steel elements were subjected to test -- galvanization thicknesses were 0.069 to 0.077 mm. (commonly referred to as 1.6 to 1.8 oz/sq ft according to ASTM A53), which was comparable to field thicknesses currently used of 0.086 mm. Two fill types were used -- initially a fill sand of pH 7.1 and resistivity 22,011 ohm-cm, followed by crushed concrete (pH 8.2 and resistivity 2,201 ohm-cm). Two pH conditions were used -- the natural pH produced after immersion in distilled water, and also a maintained pH of 12 in accordance with ASTM C876 as this is the standard test method for testing reinforcing steel in concrete. In addition, samples were tested with and without the presence of chlorides at 4%.

5.2 TEST CONDITIONS

A series of samples were prepared consisting of cylinders (150 mm x 200 mm) containing a centrally placed steel or galvanized rod. The mixtures which contained sand plus water and different contents of cement were prepared at 25°C (77°F). The samples were of differing mix proportions, but generally utilized 1000 grams of sand (or crushed concrete where appropriate), 200 grams of water, and the appropriate percentage of cement (from 0 to 250 grams for 25% as the maximum percentage). The top bar was set at 3.5 cm from the top surface. The bottom bars were 3.5 cm from the bottom of the cylinder to ensure uniform distribution of the electrolyte during the storage of the samples.

The full test matrix is shown in Figure 5.1, and involved initially testing cement contents of 0, 1, 4, 6, 8, and 13 %. Later, some additional samples containing 25% cement were also prepared.

The test liquid consisted of high purity distilled water or (in the case of the later tests designed to investigate the effect of ionic concentration) distilled water with chlorides (added as sodium chloride). For two sets of samples, the pH of the test solution in contact with the soil cement was allowed to result from the composition of the sand/water/cement mixture. The pH of the other sets of samples was kept at a value of 12 as suggested by ASTM standard C-876-86. The effects of cement stabilization on reinforcing and galvanized steel were determined by measuring the corrosion current, corrosion rate, and corrosion potential in the following electrolytes: (i) distilled water at pH resulting from the composition of the mixture used (sand/cement ratio); (ii) distilled water containing $Ca(OH)_2$ at pH=12, which acted as a buffering solution; (iii) a 4% sodium chloride solution with a pH resulting from the composition of the mixture used (sand/cement ratio); and (iv) a 4% sodium chloride solution, pH=12, (the pH of the solution was adjusted with $Ca(OH_2)$.

A carbon rod with the same diameter and area as the embedded steel in the samples was used as the counter electrode. The potential was measured vs SCE as a reference electrode.

The electrochemical measurements were carried out for different durations of the storage. Several parameters were monitored during the exposure time using a computerized data acquisition system. These parameters included solution pH and resistivity, open circuit potential of the tested steel or galvanized steel, corrosion current, corrosion rate, and electrochemical impedance of the samples during the exposure of the samples in distilled water and in 4% solution of NaCl, as described below.

5.3 TEST METHODS AND PROCEDURES

5.3.1 General

In order to evaluate corrosion rates, open circuit potential measurements, linear polarization (LP), and electrochemical impedance spectroscopy (EIS) techniques were primarily used in this study. Typical values of corrosion currents in micro-amps/cm^2 and values of the corrosion rates in mm/year measured in this way (for concrete) are given in Figure 5.2. As can be seen, when corrosion rate values fall to less than about 1.1 x 10^{-3} mm/year, then this usually coincides with passivation of the metal for which no corrosion products may be observed (passive state), or the rate of attack is insignificant. For corrosion rates above about 1.1 x 10^{-3} mm/year, corrosion products may already be detected. Maximum corrosion rates in uncracked concrete measured in a very aggressive environment can approach about 10 mm/year.

In this study, open circuit potential (corrosion potential) was also used to track the corrosion of reinforcing steel, since this is the classical measurement technique to locate corroding of reinforcing steel in concrete structures. Metallic contacts are made with the samples, and a voltage reading is obtained over the surface using a voltmeter. The other lead from the test meter is attached to a reference electrode. The use and interpretation of the method is described more fully in ASTM Test Methods for half cell potentials of reinforcing steel in concrete (C-876-86).

The main techniques used to determine the corrosion rates of the samples were linear polarization (LP) and electrochemical impedance spectroscopy (EIS), briefly discussed below.

5.3.2 Corrosion Rate Determination by Linear Polarization

LP measurements are carried out by scanning a potential range which is very close to the open circuit potential (corrosion potential) of the structure. Such experiments provide nondestructive information about the nature of the corrosion process occurring at reinforcing steel. The open circuit potentials of the samples are monitored as a function of time and their corrosion rates determined by polarization resistance measurements. From the current measured close to the corrosion potential, the polarization resistance Rp and the corrosion current Icorr can be calculated from the Tafel equation slopes. In order to obtain these Tafel slopes, scan rates of 0.1 mV/s to 5 mV/s are normally performed from -150 mV from Ecorr and moving in the anodic direction to +150 mV from Ecorr.

The data of the polarization resistance measurements with the anodic and cathodic Tafel slopes (Pa and Pc) are then used to calculate the corrosion current (Icorr) by using the Stern-Geary equation:

$$Icorr = B/Rp$$

where Rp is the polarization resistance, or the inverse slope of the polarization resistance curves at open circuit potential; and B is the product of the anodic and cathodic Tafel slopes, divided by 2.3 times the sum of the anodic and cathodic Tafel slopes. Normal values of B vary from 13 to 52 in the majority of metal/solution interface systems (Andrade, 1984). In the present work, B values of 22 mV for zinc in the active state and 50 mV for zinc in the passive conditions were determined by measuring the cathodic and anodic Tafel slopes.

5.3.3 Corrosion Rate Determination by Electrochemical Impedance Spectroscopy

Whereas DC electrochemical methods provide an overall indication of the total resistance, AC impedance spectroscopy now makes it possible to obtain information specifically on the electrical resistivity and dielectric properties of the protection used for reinforcing steel (such as galvanic coating), even for electrically insulating coatings. The technique is completely non-destructive, and AC impedance data can also be obtained in an automated fashion with a 5208 two phase lock-in analyzer and a PAR potentiostat Model 273. The data can be stored and analyzed on a PC.

The electrochemical impedance spectroscopy (EIS) technique consists of applying to the working electrode a small amplitude sinusoidal voltage (5 to 10 mV) at a wide range of frequencies. The output at every frequency is another sinusoidal signal with a different amplitude and a phase shift relative to the input signal. The polarization resistance Rp is determined separately from the slope of the polarization resistance curves dI/dE, and can be calculated using the equation:

$$Rp = dE/dI - R\ equiv.$$

where in the equivalent circuit used, R equiv. represents the resistance of the electrolyte plus the resistance of the mortar layers between the metal and the calomel electrode and the resistivity of the passivating species.

The EIS data are often presented as a Nyquist plot in which the imaginary component of impedance (Z") is plotted vs the real component of impedance (Z') for each excitation frequency. At the beginning of the experiments before the solute is fully in contact with the bars, the samples are passivated and the impedance output lies in a vertical line. As the solute front arrives into the substrate, the corrosion intensity increases, and a semicircle starts to form from which one can conclude that a generalized corrosion develops on the substrate. In addition, Bode-magnitude and Bode-phase plots permit the examination of the absolute impedance. They show more clearly the characteristic features of the AC impedance data, especially in the case when more than one time constant is involved in the circuit.

5.4 DATA REDUCTION

Figures 5.3 through 5.12 show Bode-magnitude plots and Bode-phase plots for steel and galvanized steel rods for different soil/water/cement compositions in distilled water or chloride solution as appropriate. A carbon rod with the same diameter and area as the embedded steel in the samples was used as the counter electrode. The potential was measured vs SCE as a reference electrode. All electrochemical DC and AC measurements were carried out using a Model 332 Softcor-system with a PAR model 273 potentiostat. EIS data were obtained using a PAR model 5301 A with a frequency analyzer. The data were stored and analyzed using a PC.

As seen in the figures, the polarization resistance and nonfaradic resistance are functions of the concentration of cement in the mixture. In Figures 5.3 through 5.12, the polarization resistance and nonfaradic resistance have much higher values at the beginning of the testing in distilled water or 4% NaCl solution, indicating that the metal rod samples are passivated. As the solute reaches the interface, the corrosion starts to increase and after six months of exposure, as shown in Figures 5.3 and 5.4, levels off to new lower values of the polarization resistance and nonfaradic resistance (ohmic resistance) indicating higher corrosion rates. After 21 months of exposure (see Figure 5.4), an increase of both the polarization resistance and nonfaradic resistance was observed, indicating that the rods embedded in a soil/water mixture with 6% cement were passivated in water again and reached a steady state corrosion value.

As expected, the highest maximum in Bode-phase plots was observed for samples which contained 13% and 25% cement which is in agreement with the low corrosion rates observed for these samples. The peak maximum in Figure 5.5 is proportional to the polarization resistance. In theory, higher polarization resistance results in lower corrosion current and, consequently, in lower corrosion rate. Figure 5.6 shows the same results as those observed in Figure 5.4, but now drawn in a Bode-phase plot.

Similar results were observed also for galvanized steel rods, and examples obtained in different soil/water/cement compositions in water and in 4% NaCl solution are presented in Figure 5.7 through Figure 5.12. In the testing carried out in this study, the polarization resistance was estimated from Bode-magnitude plots such as those presented in Figures 5.3 through 5.12, and the results compared with values obtained from linear polarization experiments. The data were fitted using McDonald's complex nonlinear least squares algorithm, (CNLS).

LABORATORY TEST MATRIX

Metal Type	Chlorides	pH	Fill Type	Cement Content					
				0%	1%	4%	6%	8%	13%
Galv.	No	Natural	Sand						
Galv.	No	12	Sand						
Galv.	Yes	Natural	Sand						
Galv.	Yes	12	Sand						
Mild	No	Natural	Sand						
Mild	No	12	Sand						
Mild	Yes	Natural	Sand						
Mild	Yes	12	Sand						
Galv.	No	Natural	Crushed Concrete						
Galv.	No	12	Crushed Concrete						
Galv.	Yes	Natural	Crushed Concrete						
Galv.	Yes	12	Crushed Concrete						
Mild	No	Natural	Crushed Concrete						
Mild	No	12	Crushed Concrete						
Mild	Yes	Natural	Crushed Concrete						
Mild	Yes	12	Crushed Concrete						

Fig. 5.1 - Laboratory Test Matrix

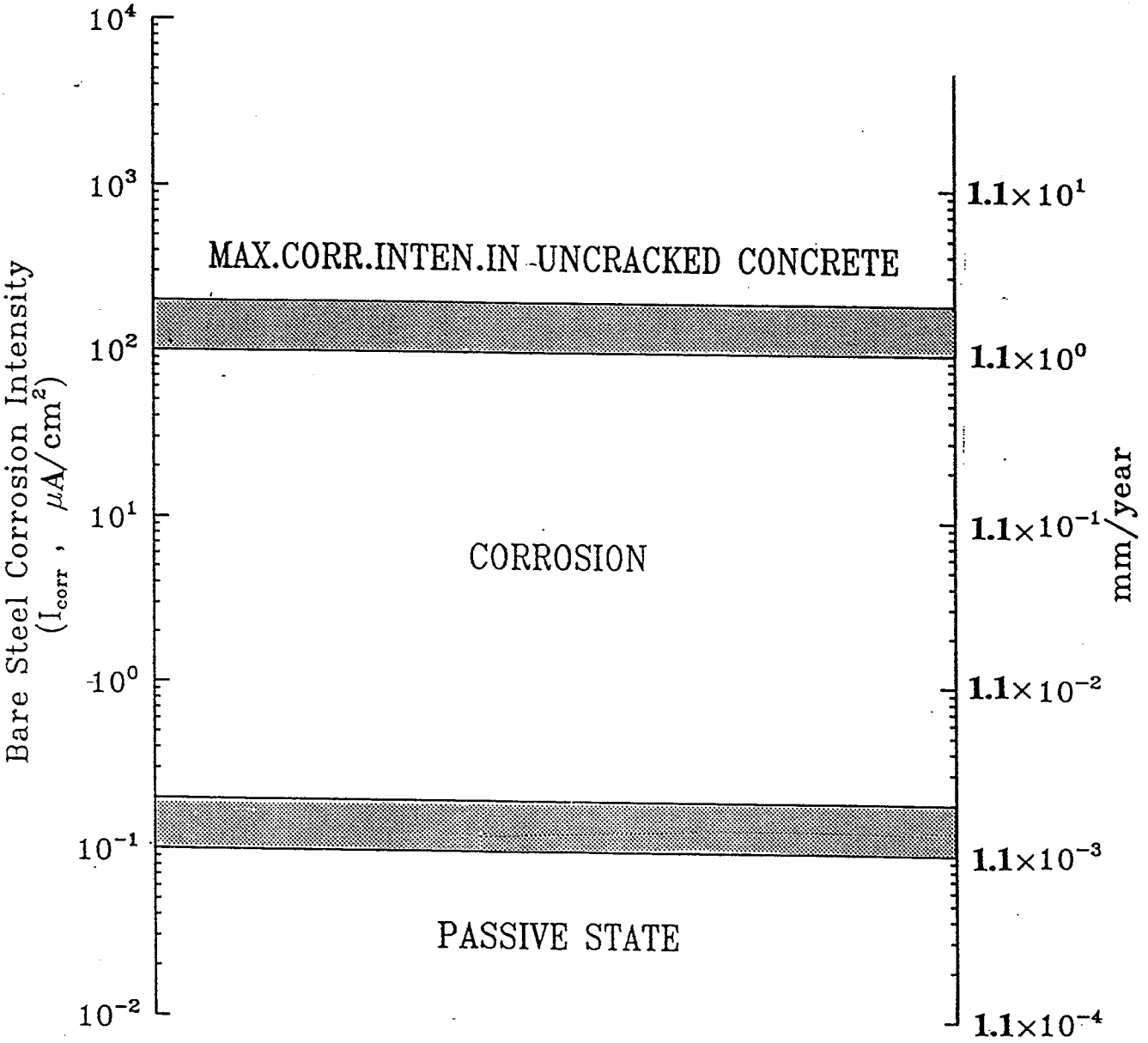

Value of corrosion intensity in $\mu A/cm^2$ and in mm/year which may be measured in concrete.

Fig. 5.2 - Typical Values of Corrosion Currents and Rates

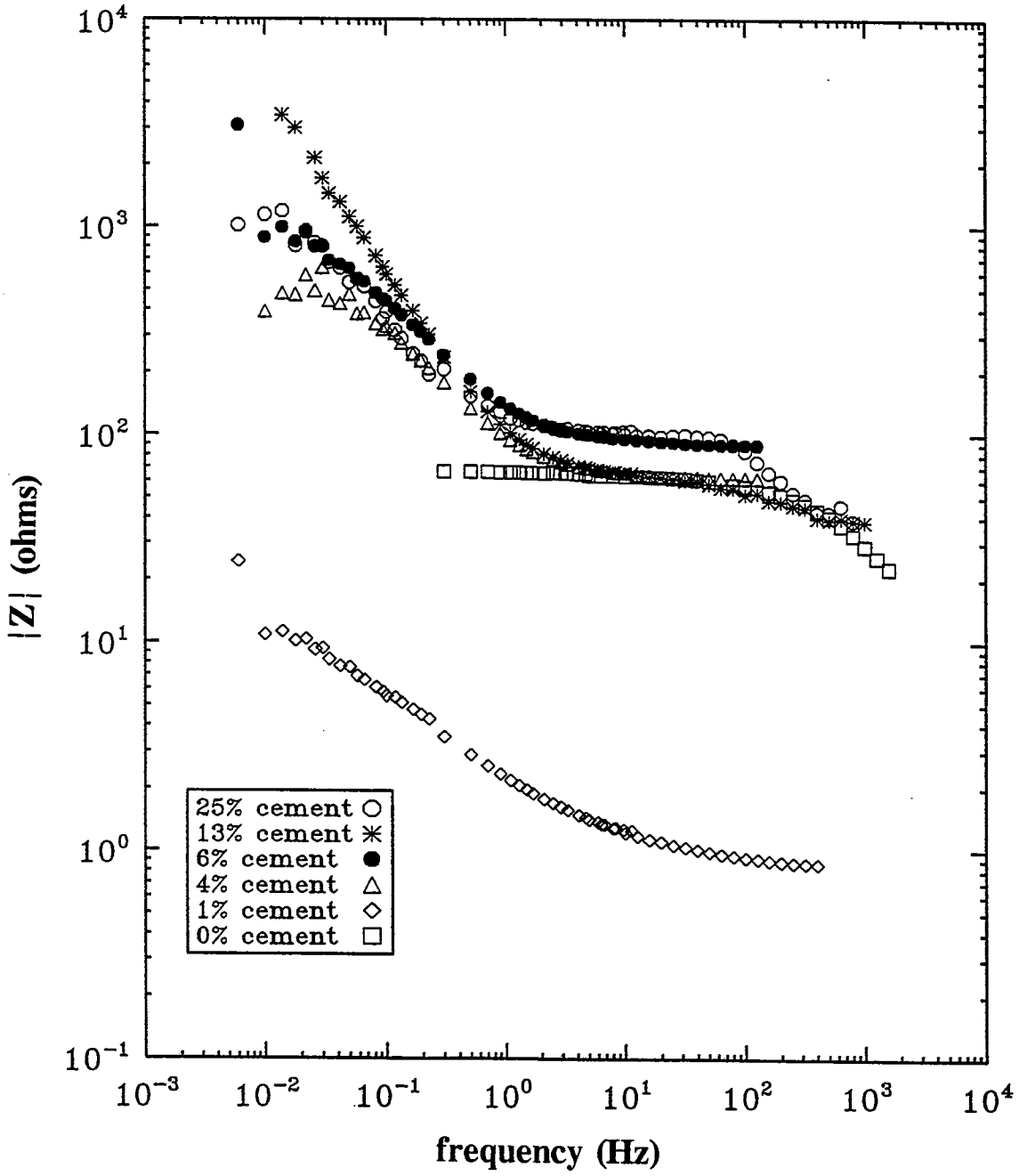

Initial Bode-Magnitude plots for steel rods in different soil/water/cement compositions in distilled water.

Fig. 5.3 - Initial Bode-Magnitude Plots (Steel Specimens, Natural pH)

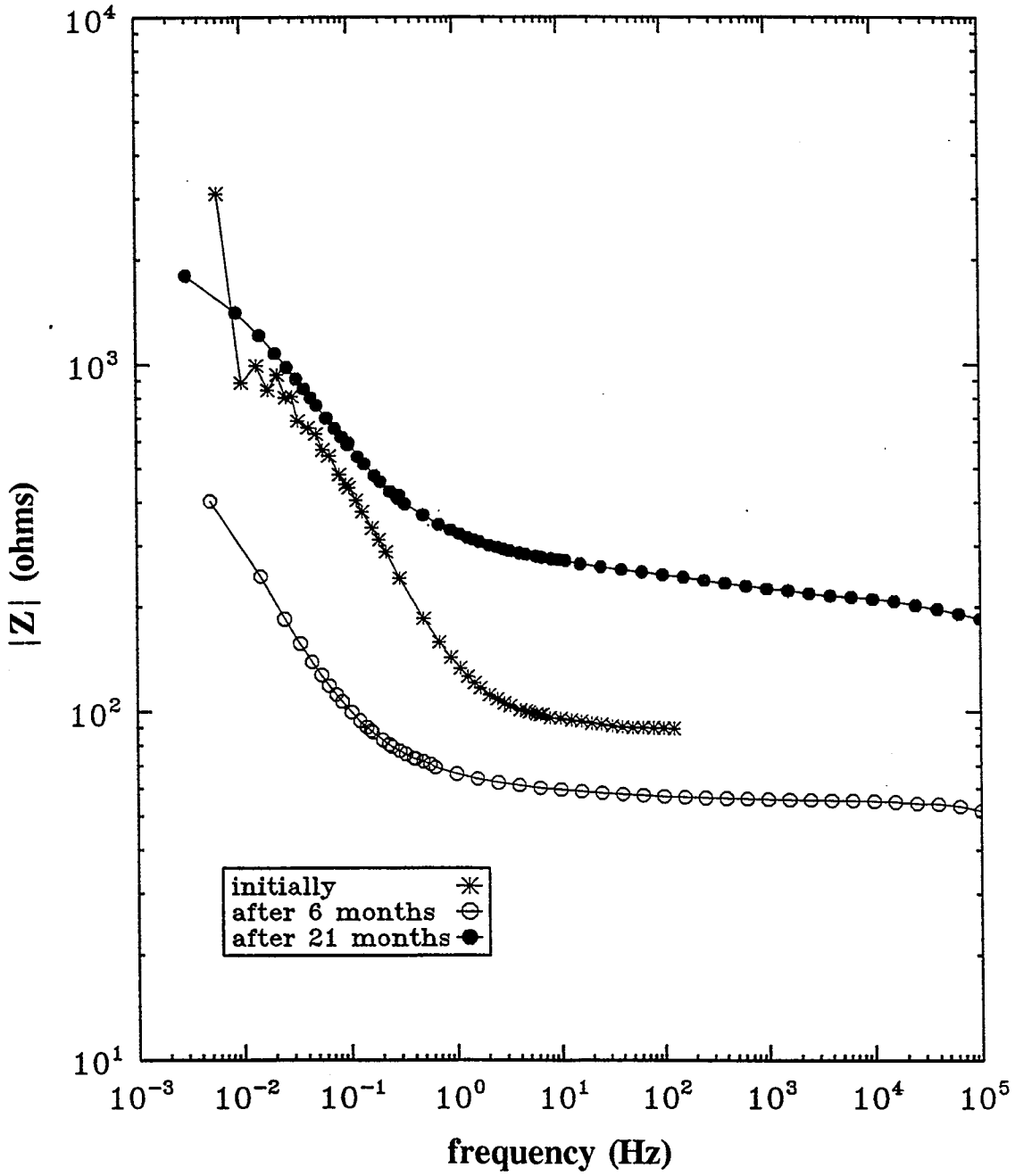

Bode-Magnitude plots for steel rods in soil/water/ mixture with 6% cement in water, as a function of time.

Fig. 5.4 - Bode-Magnitude Plots in 6% Cement, Variation with Time

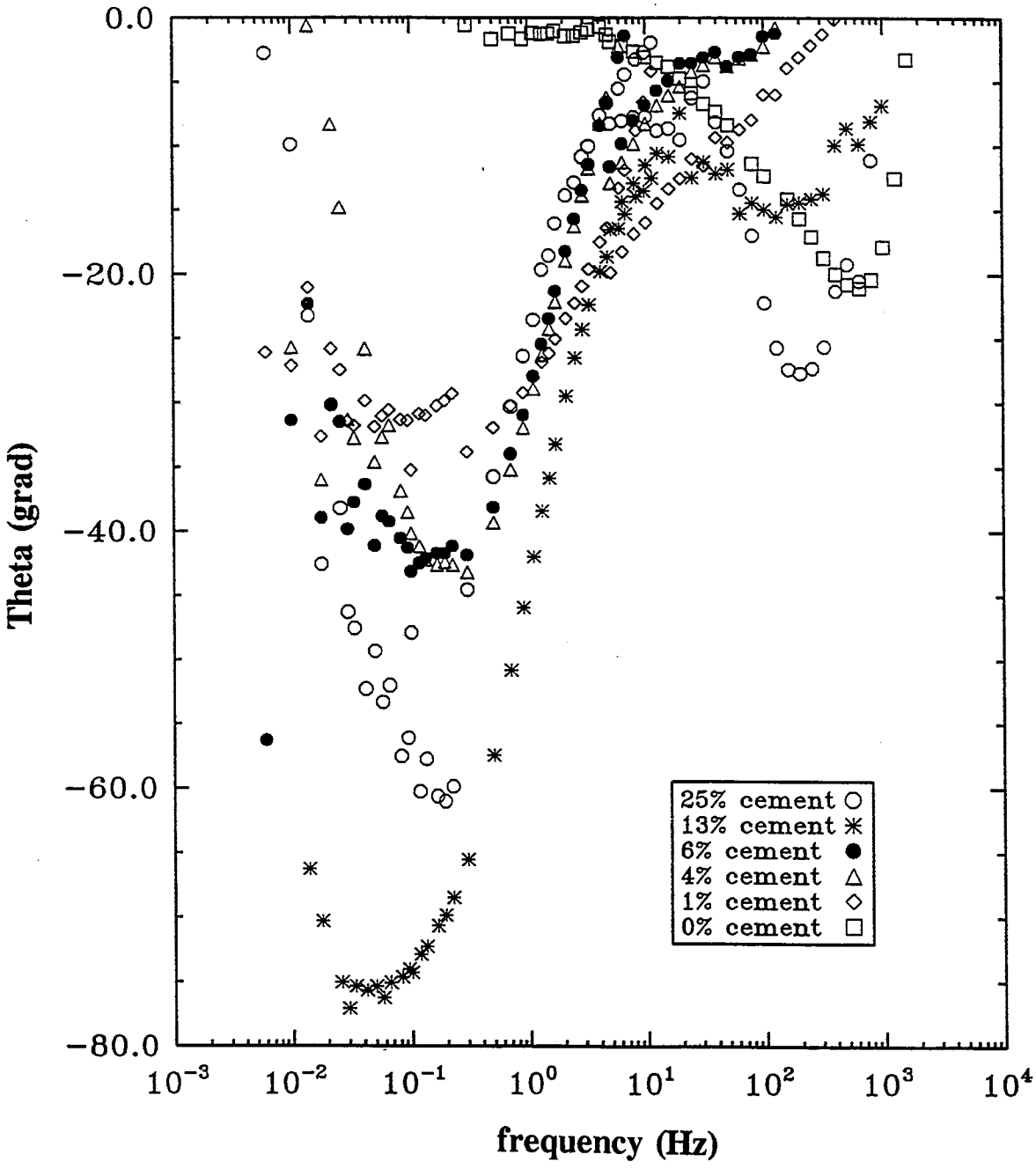

Initial Bode-Phase plots for steel rods in different soil/water/cement compositions in distilled water.

Fig. 5.5 - Initial Bode-Phase Plots for Different Cement Contents

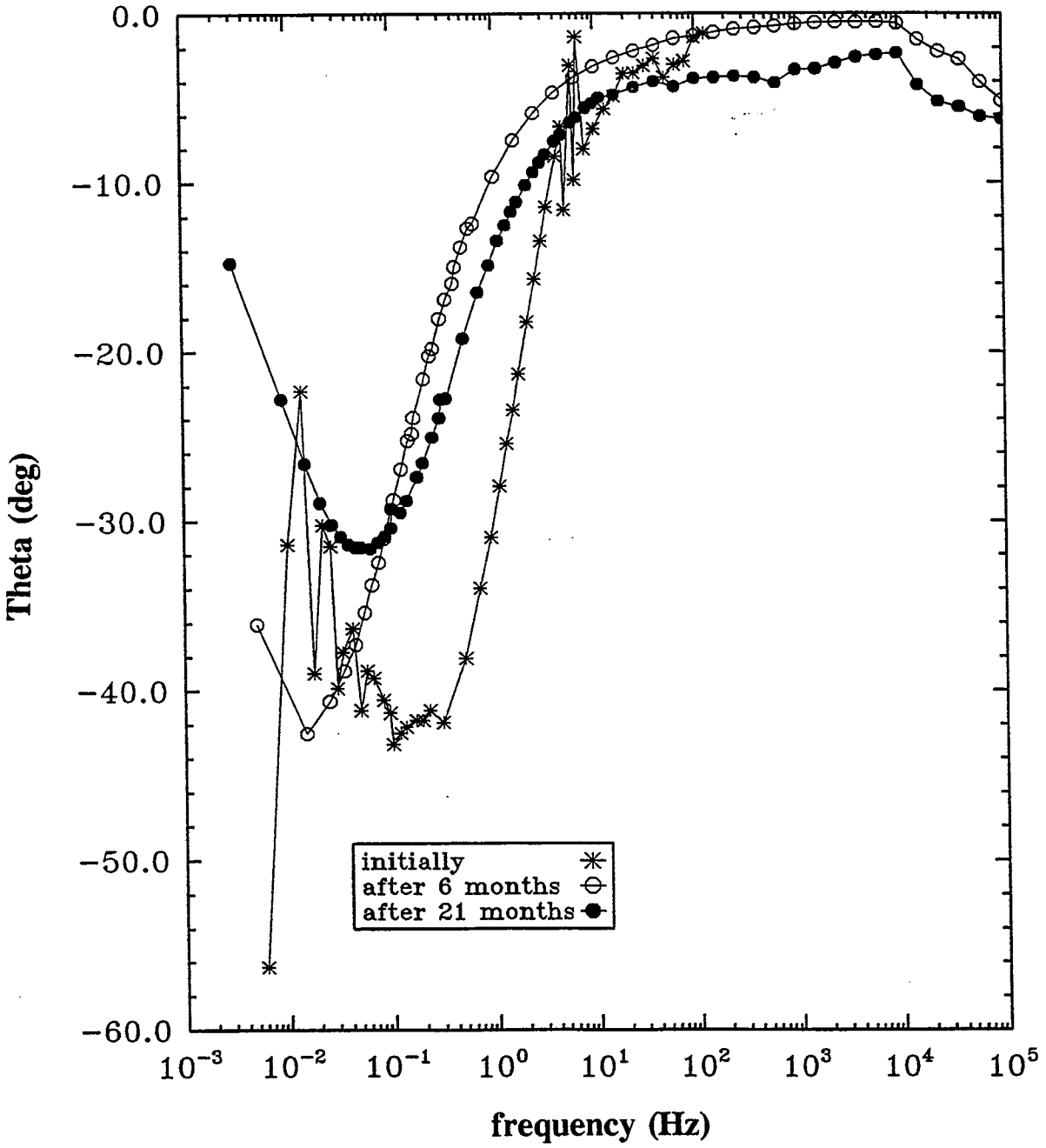

Bode-Phase plots for steel rods in 6% cement soil/water compositions in water, as a function of time.

Fig. 5.6 - Bode-Phase Plots in 6% Cement, Variation with Time

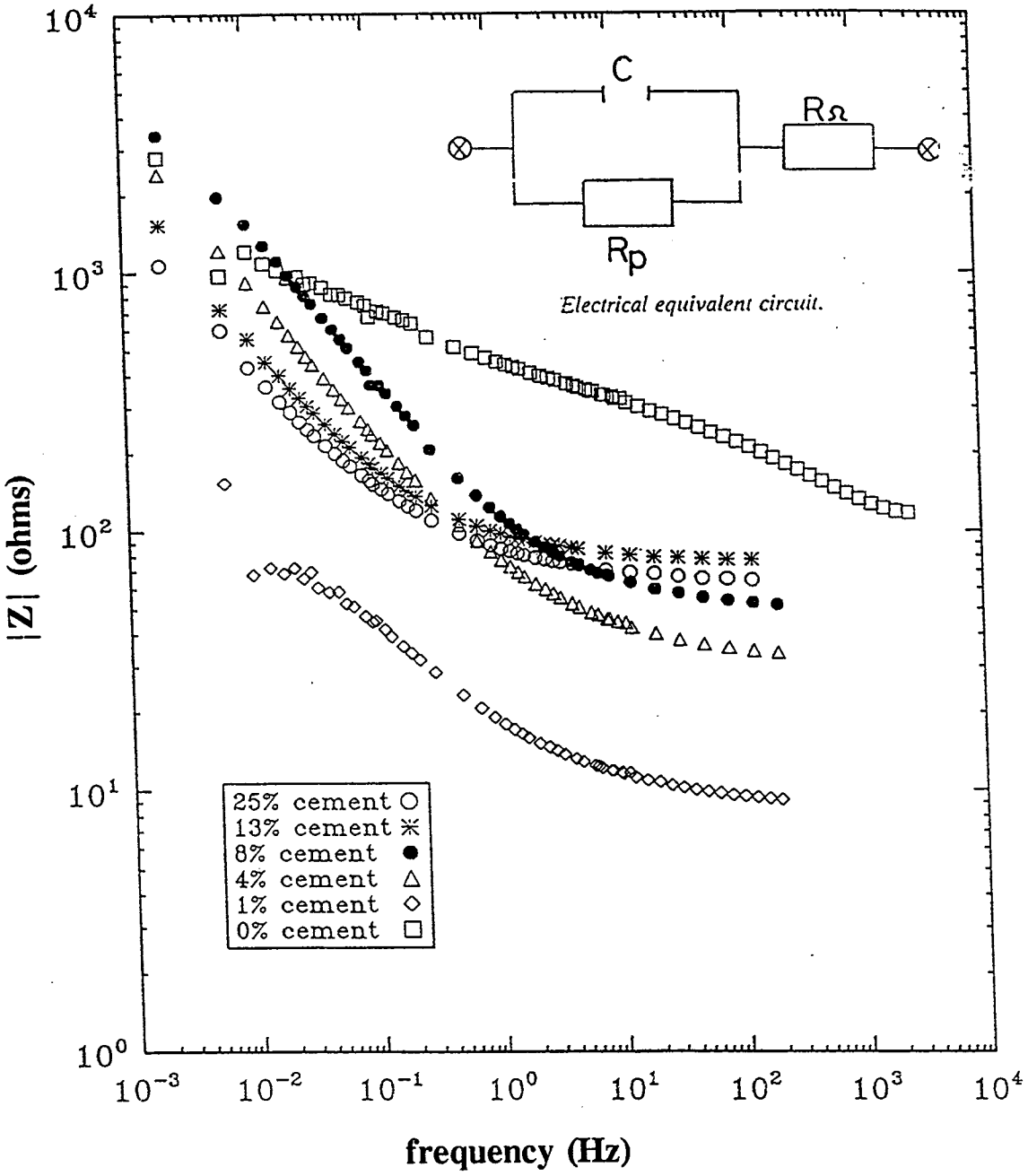

Initial Bode-Magnitude plots for galvanized steel rods in different soil/water/cement compositions in water.

Fig. 5.7 - Initial Bode-Magnitude Plots (Galvanized Specimens, Natural pH)

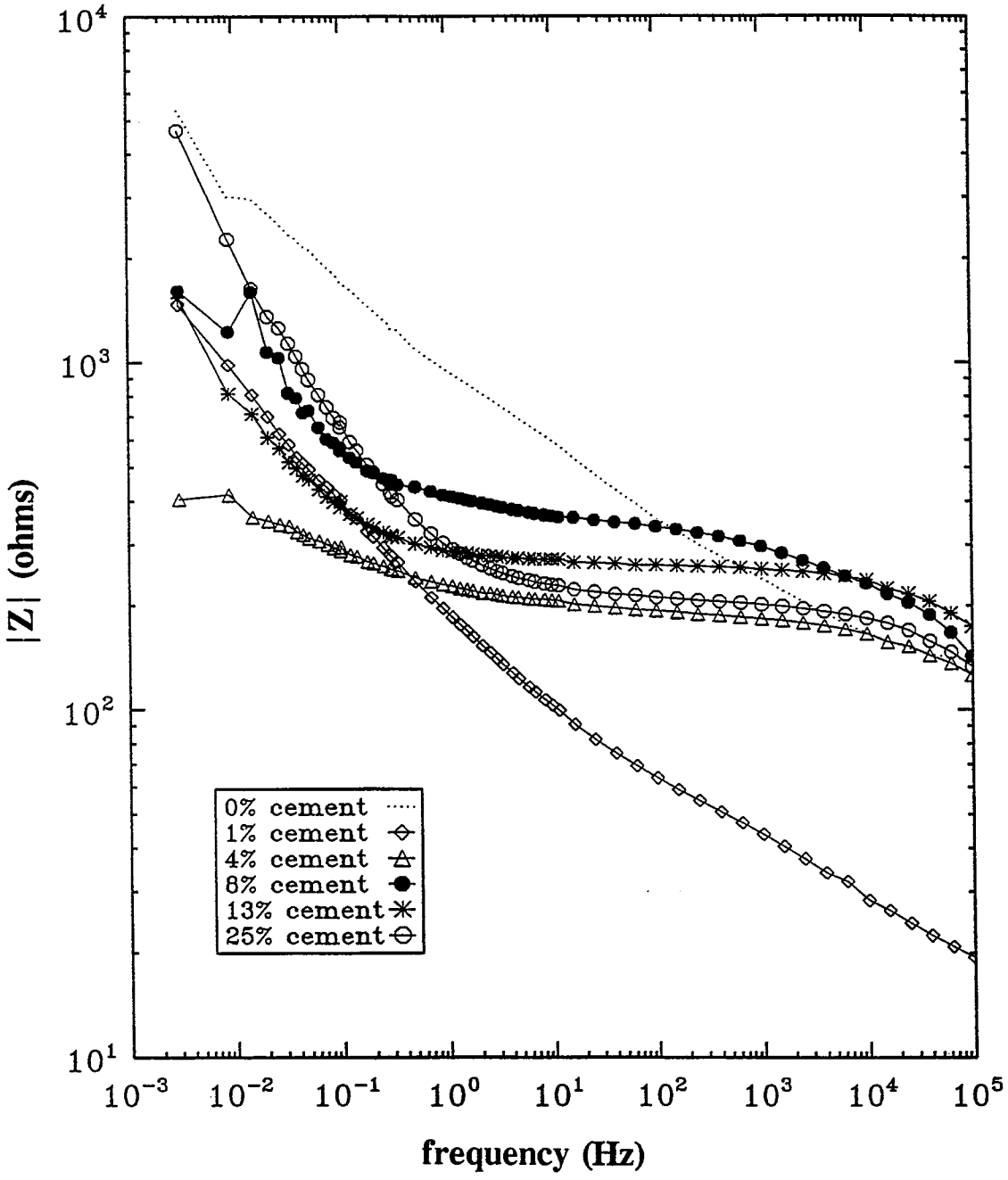

Bode-Magnitude plots for galvanized steel rods in different soil/water/cement compositions in water.

Fig. 5.8 - Bode-Magnitude Plots for Different Cement Contents

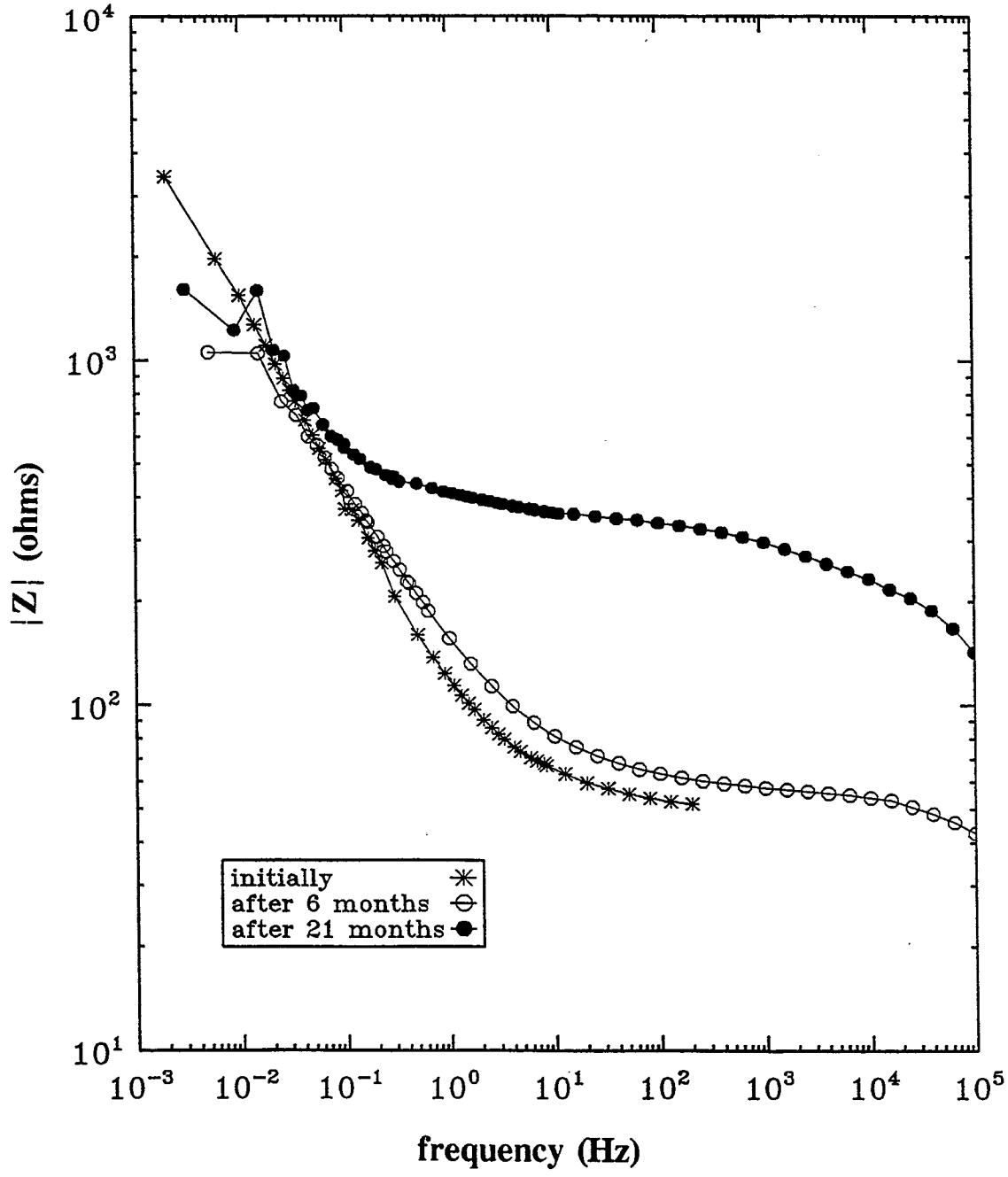

Bode-Magnitude plots for galvanized steel rods in soil/water mixture with 8% cement in water.

Fig. 5.9 - Bode-Magnitude Plots in 8% Cement, Variation with Time

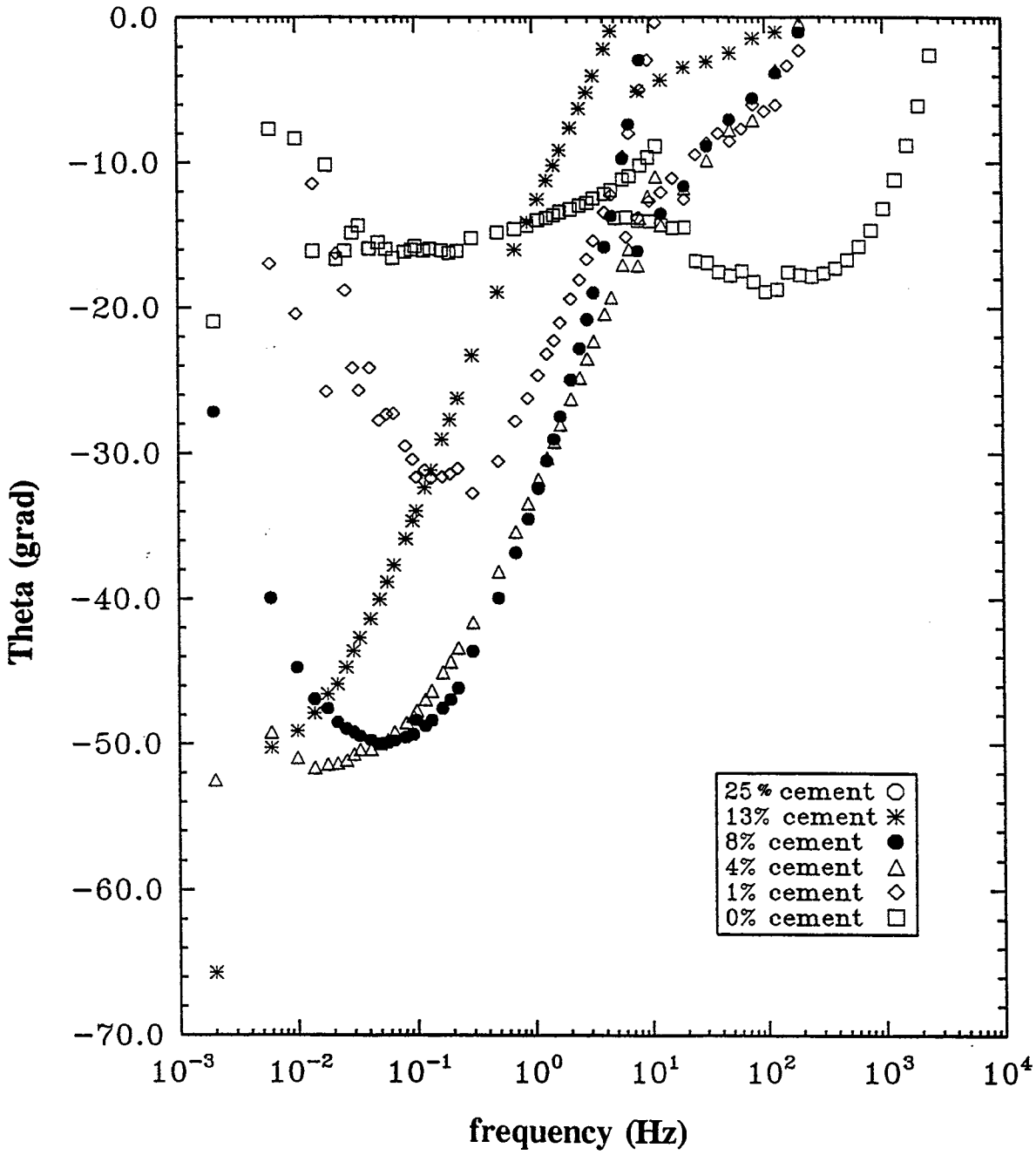

Initial Bode-Phase plots for galvanized steel rods in different soil/water/cement compositions in water.

Fig. 5.10 - Initial Bode-Phase Plots for Different Cement Contents

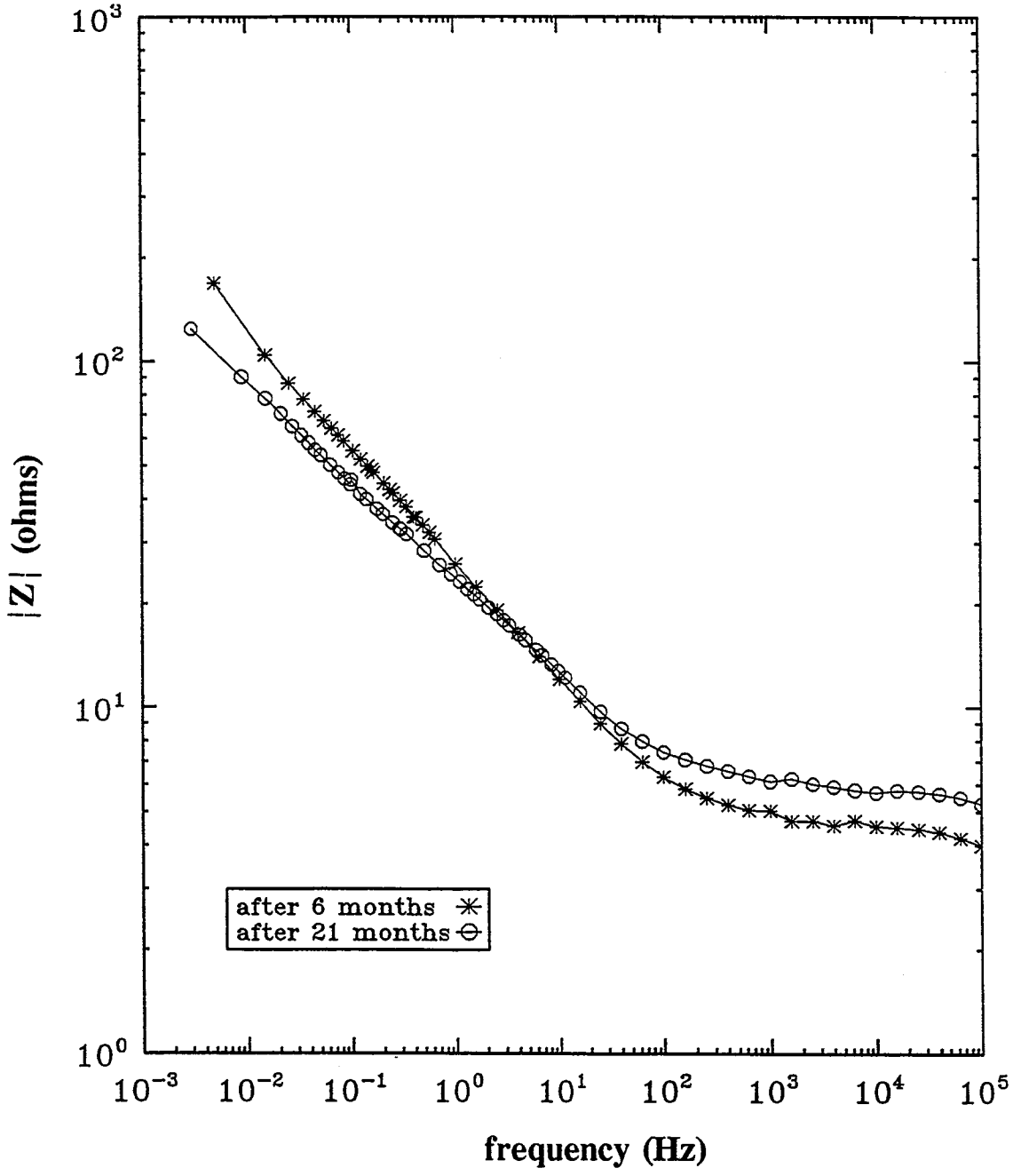

Bode-Magnitude plots for steel rods in soil with 6% cement in 4% NaCl as a function of time.

Fig. 5.11 - Bode-Magnitude Plots in 6% Cement (Steel Specimens, with Chlorides)

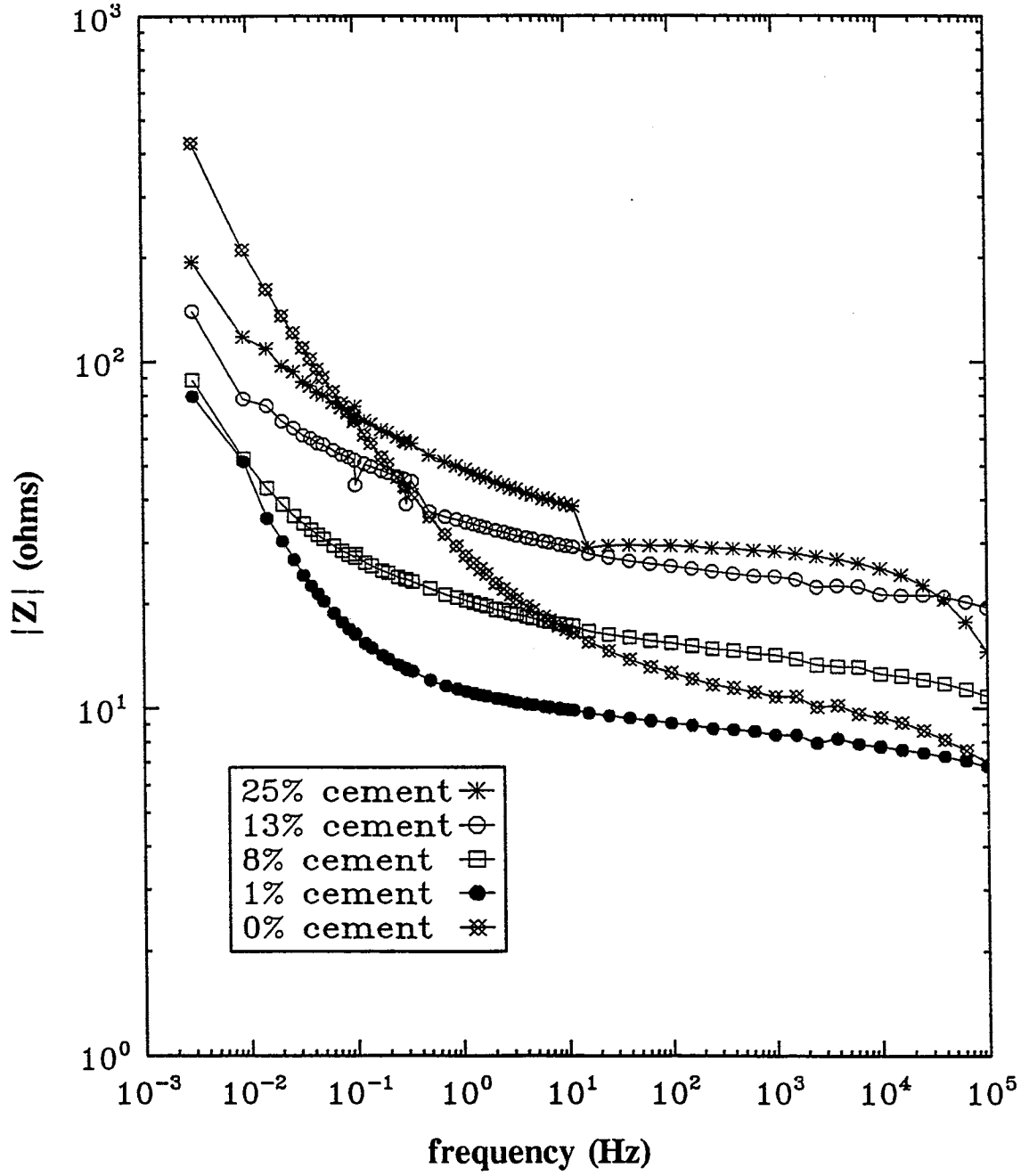

Bode-Magnitude plots for galvanized steel rods in soil/water mixture with 6% cement in 4% NaCl.

Fig. 5.12 - Bode-Magnitude Plots (Galvanized Specimens, with Chlorides)

6. RESULTS OF LABORATORY CORROSION STUDIES

6.1 GENERAL

At the onset of the project, there was a certain amount of uncertainty as to the precise overall effect of cement stabilization on the electro-chemical environment, especially the background backfill pH, as this was assumed to be responsible for any accelerated corrosion. It was not known what concentration of cement in retaining wall backfill would be sufficient to raise the pH to a level that would passivate reinforcing strips, and there was no published data on the subject. One of the early results of this study was to show that the addition of even a small amount of cement is in reality enough to raise the background level of fill pH to close to a value of 12.

Table 6.1 summarizes this effect as measured in the laboratory.

TABLE 6.1 - VARIATION OF pH WITH CEMENT ADDITION

Cement Concentration	Measured Solution pH
0 %	7
1 %	11.3 to 11.4
4 %	11.8
8 %	11.9
13 %	12.0
25 %	12.1
100 %	13*

These results correspond to the limited published data previously available on this subject, e.g., Bernsted (1983), which indicates that for sand of initial pH 7.2, 2% cement gives a pH of 11.3, and 7.5% cement addition causes pH 12.3 (*neat cement paste is usually assumed to have a pH of approximately 13).

This indicates that normal stabilized backfill situations in TxDOT practice, containing at least 7% cement, would be expected to have initial fill pH in the field of at least 11.8 and up (assuming uniform mixing), although as shown in Chapter 4, these values are liable to become more neutral with time.

6.2 CORROSION RATES

6.2.1 General

Corrosion rates were determined for all the different environments specified in the test matrix using the methods described in the previous chapter. Variations of the corrosion rate (and also corrosion potential) of the test specimens for different cement ratios as a function of time are shown in Figures 6.2 through 6.17, respectively, for each of the cases tested, and are discussed in turn in the following sections. The nature of the measurement (which is proportional to the differential with time of an initially very thin corrosion zone) results in large apparent fluctuations in corrosion rate in the short-term, so that it is, of course, the overall long-term behavior which is of significance. As mentioned in Chapter 5, for corrosion rates below about 1.1×10^{-3} mm/year, the material can either be assumed to be passive, or the rate of attack is insignificant. Above this level, corrosion products may be detected. For reference, maximum corrosion rates for concrete in very aggressive environments are as high as 10 mm/year.

Variations of corrosion potential with time were also measured as this gives an overall indication of the probability (and intensity) of corrosion. This is summarized in Figure 6.1 (after ASTM C-876-86 for half cell potentials of reinforcing steel in concrete), which shows ranges of expected corrosion intensity for different values of open circuit potential. The upper limit can range from -0.200 to -0.570 volts vs. $Cu/CuSO_4$ reference electrode.

The results can be divided conveniently into different categories, as follows.

6.2.2 Steel Specimens, Natural pH, Distilled Water

To provide reference data, Figure 6.2 shows the corrosion rates for mild steel rod samples embedded in 0%, 1%, 4%, 8%, and 25% cement, with only distilled water added, so that the electrolyte pH results only from the actual concentration of cement added (and to a very secondary extent on the initial pH of the fill sand used, although this was in reality largely neutral). The 4%, 8%, and 25% cement mixtures showed initially low corrosion rates in the electrolyte. The initial corrosion rates estimated for 4%, 8%, and 25% cement in the mixture were 0.011, 0.00984, and 0.00264 mm/year, respectively. The measured pH values for these samples at the metal/cement/solution interface were between 12.05 and 11.86 and are the main cause for the observed low corrosion rates.

After 55 days of storage of the samples in the electrolyte, the estimated corrosion rates increased and, as shown in Figure 6.2, were in the range of 0.05 mm/year and 0.02 mm/year for 4% and 25% cement content, respectively. Up to 390 days of exposure, the corrosion rates increased slowly to reach a steady state value at approximately 420 days of exposure. At 420 days, the following corrosion rates were estimated: 0.018, 0.013, and 0.004 mm/year for 4%, 8%, and 25% cement content in the mixture, respectively. These values with small changes remained constant up to 610 days of exposure.

As seen in Figure 6.2, initially, the steel rods embedded in a mixture which contained 1% cement indicated advanced corrosion. The measured corrosion rate of these samples was between 0.062 and 0.141 mm/year, which was greater than the corrosion rate of the samples without any cement, which was about 0.05 mm/year.

Figure 6.3 shows the corrosion potential of the samples embedded in 4%, 8%, and 25% cement as a function of time. This showed a trend of passivation, while the observed Ecorr values for 1% and 0% cement mixtures showed values between 3.52 V and 0.7 V, corresponding to an active corrosion state according to Figure 6.1.

6.2.3 Steel Specimens, Controlled pH, Distilled Water

Measurements of reinforcement corrosion in concrete (e.g., to ASTM C-876-86) are usually carried out at a controlled pH. A second set of samples was consequently tested under the conditions specified by this standard. This enabled the effect of pH on the corrosion to be specifically isolated, if desired, from similar measurements of the corrosion rate and corrosion potential of samples containing different contents of cement at pH=12. The experiments were carried out in distilled water containing $Ca(OH)_2$ which was used as a buffering additive to adjust the alkalinity of the solution. Under these conditions, steel is normally expected to be passivated due to the gamma ferric oxide which forms on the steel surface.

Figure 6.4 summarizes the corrosion rate values with pH=12 maintained with $Ca(OH)_2$. As can be seen, the samples embedded in 25%, 13%, 8%, and 4% cement mixtures showed initially low corrosion rates in the range of 0.001 and 0.003 mm/year (as already observed in Figure 6.2 for variable pH conditions). The similarity of results can be explained by observing that the pH at the steel/electrolyte interface was almost the same in both experiments. The data indicate that even small contents of cement in the mixture (8% to 25% cement) create favorable pH conditions at the steel/electrolyte interface which results in low corrosion rates of the substrate. The samples embedded in only 1% and 0% cement at controlled pH, however, showed significantly lower corrosion rates than the corresponding ones in natural pH conditions. The measured corrosion rate of the 1% cement sample (pH=12) after 610 days of exposure, leveled off at a value of 0.05 mm/year compared with a value of around 0.32 mm/year shown in Figure 6.2 for samples with a pH generated only from the added cement.

As expected, for most of the samples, the values of corrosion potential recorded in Figure 6.5 as a function of the time showed a trend of passivation.

6.2.4 Galvanized Specimens, Natural pH, Distilled Water

Since the primary interest in this project was on the behavior of galvanized reinforcement, the corrosion rates and corrosion potentials of galvanized steel rods in different cement contents in natural pH (i.e., with only distilled water added as an electrolyte) are shown in Figure 6.6 and Figure 6.7, respectively, as a function of time. As seen in Figure 6.6 galvanized rod samples embedded in 25%, 13%, 8%, and 4% cement showed initially low corrosion rates. These were in the range of 0.003 mm/year to 0.006 mm/year. Next, for up to 60 days, the corrosion rates showed a trend of a small increase and then leveled off, reaching values of 0.004 to 0.02 mm/year which remained almost constant up to 600 days of exposure.

An interesting phenomenon was observed for the galvanized steel rod sample containing zero cement. This sample showed initially high corrosion rates of 0.02 mm/year, which after 100 days of exposure leveled off and then decreased to a value of 0.005 mm/year. This indicates that the corrosion rates of galvanized steel in the presence and absence of cement are in the same range, implying that even cement contents up to 25% do not improve the corrosion characteristics of zinc plated steel under natural pH conditions. As shown in Figure 6.6, the most advanced corrosion was exhibited by the galvanized steel samples embedded in 1% cement, when compared with other samples at different cement contents (even 0% cement).

The variation of the corrosion potential, Ecorr as a function of the exposure time of galvanized steel rods embedded in different cement concentrations under natural Ph conditions, is presented in Figure 6.7. As can be seen for most of the samples, the corrosion potential values correspond to an overall passive regime.

6.2.5 Galvanized Specimens, Controlled pH, Distilled Water

In accordance with the test matrix, the effect of pH on the corrosion of galvanized steel rods was determined by measuring the corrosion rate and the corrosion potential of samples containing different cement contents, under constant pH conditions. Figure 6.8 summarizes the corrosion rate values obtained in distilled water with pH=12 maintained with $Ca(OH)_2$. The galvanized steel rod samples showed similar corrosion rates, regardless of the presence or absence of cement, in the range of 0.004 mm/year up to 0.03 mm/year.

The variation of corrosion potential, Ecorr, as a function of exposure time on the galvanized steel samples in different cement ratios, is shown in Figure 6.9. As can be seen, a decrease in the cement content in the mixtures causes a shift of the open circuit potential in the cathodic direction. However, in this case, this cathodic shift of the corrosion potential did not cause higher corrosion rates to be observed, by reference to Figure 6.8.

6.3 EFFECT OF ANIONIC CONTAMINATION

6.3.1 General

Although initial field testing of the fill properties at the sample site (as discussed in Chapters 2 and 4) did not initially show unusual chemical properties, it became evident at the start of the laboratory chemical analysis described in Chapter 9, that the presence of ionic contamination might be a possible explanation for the accelerated corrosion at the Deer Park retaining wall. It was for this reason that the program for the laboratory testing was expanded to include dissolved ions in the electrolyte, representing in total half of the test matrix in Figure 5.1. Even though the results of chemical analysis subsequently identified sulphates as being the particular anion present at this location, for simplicity, the ionic solution used in the laboratory was a 4% solution of sodium chloride to simulate the effects of a possibly aggressive environment on the test samples.

This portion of the corrosion rate measurements is discussed in the following sections.

6.3.2 Steel Specimens, Natural pH, with Chlorides

Figure 6.10 shows the corrosion rate as a function of time for steel rods embedded in different cement ratios in 4% NaCl solution for different pH. The pH of the electrolyte, as seen in this figure depends on the cement content in the tested samples. In this case, very high corrosion rates of between 0.8 mm/year and 1.35 mm/year were observed when the steel rods were embedded in sand/cement mixtures with 1% cement and 0% cement content with pH=1.1 and 7.01, respectively. However, the samples embedded in 4%, 8%, 13%, and 25% cement showed drastically lower corrosion rates of 0.3 mm/year, 0.09 mm/year, 0.08 mm/year, and 0.04 mm/year, respectively. The results indicated that the pH at the substrate/solution interface has a crucial role in the corrosion mechanism of steel in 4% NaCl solution and, in this case, acts so as to inhibit corrosion for cement concentrations above a certain value.

The variation of the corrosion potentials is also shown in Figure 6.11. As can be seen, there is a strong correlation between the absolute value of Ecorr observed and the cement content in the mixtures. A decrease in the cement content in the mixture gives rise to a higher corrosion potential, normally corresponding to higher corrosion rates. This is confirmed by comparison with the observed rates in Figure 6.10.

6.3.3 Steel Specimens, Controlled pH, with Chlorides

Figure 6.12 shows the corrosion rates as a function of time for steel rods embedded in different cement compositions, again in 4% NaCl solution, but this time at a controlled pH=12. All of these samples showed advanced corrosion corresponding to an active corrosion state. Samples embedded in mixtures which contained 25%, 13%, 8%, and 4% cement showed the lowest corrosion rates. Initially, for these samples, a corrosion rate of 0.005 to 0.01 mm/year was observed. As can be seen in Figure 6.12, as exposure time advances, an increase of the corrosion was observed only for the samples which contained 0%, 1%, and 4% cement content. After 610 days of exposure, corrosion rates were 0.54 mm/year, 0.9 mm/year, 0.2 mm/year, 0.1 mm/year, 0.1 mm/year, and 0.02 mm/year for steel rods embedded in 0%, 1%, 4%, 8%, 13%, and 25% cement, respectively. These results indicated that the highly alkaline environment (pH=12) created at the substrate/solution interface by the addition of $Ca(OH)_2$ decreased the corrosion rates in all tested samples when compared with the corrosion rates in Figure 6.10, which were measured under identical conditions except that the pH of the electrolyte was maintained only by the cement content in the samples.

Similarily, the variation of corrosion potential as a function of exposure time for these samples is shown in Figure 6.13. The results indicate that, for most of the samples, the corrosion potentials, Ecorr, correspond to the presence of an active corrosion state.

6.3.4 Galvanized Specimens, Natural pH, with Chlorides

Figure 6.14 shows the corrosion rate as a function of time of galvanized steel rods embedded in different cement concentrations in 4% NaCl solution at natural pH. The solution pH in these samples was generated by the amount of cement added. As shown in Figure 6.14, the highest corrosion rates were observed for the galvanized steel rods embedded in mixtures containing 4%, 1%, and 0% cement, corresponding to pH=11.80, 11.33, and 6.96, respectively. The average corrosion rates were estimated to be: 0.5 mm/year, 0.72 mm/year, and 0. 1 mm/year for 0%, 1% and 4% cement content, respectively. Overall, the presence of cement in the samples decreased the corrosion rates of galvanized steel rods in 4% NaCl electrolyte. The calculated corrosion rates for samples which contained 8%, 13%, and 25% cement content were in the range of 0.04 and 0.07 mm/year. The results indicated that cement contents above 13% further decreased the corrosion rate of galvanized steel rods in aggressive chemical environments (in this case, 4% NaCl).

The variation of corrosion potential is shown in Figure 6.15. The values of the corrosion potentials indicated that all tested samples were in the active corrosion state.

6.3.5 Galvanized Specimens, Controlled pH, with Chlorides

Figure 6.16 shows the variation of the corrosion rate as a function of time for galvanized steel rods embedded in different water/soil/cement compositions in 4% NaCl solution at a buffered pH=12. All tested samples showed advanced corrosion. Galvanized rod samples embedded in mixtures which contained 25%, 13%, and 8% cement showed again the lowest corrosion rates when compared with those with zero and 1% cement content. The estimated corrosion rates were in the range of 0.07 mm/year and 0.55 mm/year.

Values of corrosion potential with time are shown in Figure 6.17. As observed before, there is a correlation between the observed Ecorr values and the cement content in the samples. A decrease of cement content gives rise to a more cathodic potential and a greater likelihood of higher corrosion rates, which corresponds to the observations shown in Figure 6.16.

6.4 SUMMARY

In conclusion, the results of the laboratory testing can be summarized as follows. Steel rod samples embedded in 4%, 8%, and 25% cement showed initially low corrosion rates of 0.011 mm/year, 0.00984 mm/year, and 0.00264 mm/year, respectively. After 420 days of exposure in distilled water, these values rose to 0.018 mm/year, 0.013 mm/year, and 0.004 mm/year, respectively, and remained constant up to 610 days. Steel embedded in only 1% cement showed corrosion of between 0.062 and 0.14 mm/year which was, in some cases, worse than the values for no cement, which were about 0.05 mm/year (see Figures 6.2 and 6.4 for this effect).

For a controlled pH environment such as is specified in concrete rebar testing (achieved here with an electrolyte solution of distilled water with pH=12 maintained with $Ca(OH)_2$), the samples in 25%, 13%, 8%, and 4% cement showed low corrosion rates in the range of 0.001 to 0.003 mm/year. The steel rods embedded in 1% and 0% cement showed significantly lower corrosion rates than the corresponding samples in a natural pH environment. This difference is attributable only to the maintained pH conditions, for which the steel is liable to be passivated.

Galvanized samples in 25%, 13%, 8%, and 4% and 1% cement in distilled water showed low corrosion rates, in the range of 0.003 mm/year to 0.006 mm/year. These were similar for different cement concentrations, indicating that the addition of cement (at least up to 25%) does not have a major effect on the corrosion of zinc plated steel under natural pH conditions, although in some instances the initial corrosion rate in 1% cement was again worse than for no cement (Figure 6.6).

When the pH of the electrolyte was maintained at 12 with a buffering solution of $Ca(OH)_2$, galvanized samples again showed similar corrosion rates in the range of 0.004 mm/year up to 0.03 mm/year, regardless of the amount of cement present.

The really major difference in corrosion rates occurred in the presence of significant concentrations of anions in the electrolyte, achieved here with 4% NaCl solution. Corrosion rates of as high as 0.8 mm/year to 1.35 mm/year were measured for unprotected steel under these conditions with 0 or 1% cement added, and under natural pH conditions (pH=11.44 and 7.01, respectively). Higher concentrations of cement were beneficial under these circumstances, e.g., 4%, 8%, 13%, and 25% cement showed relatively reduced corrosion rates of 0.3 mm/year, 0.09 mm/year, 0.08 mm/year, and 0.04 mm/year, respectively. Controlling the pH at 12 helped to decrease the corrosion rates of rod steel in all tested samples in 4% NaCl solution, although they were still high.

The presence of anions also caused significantly accelerated corrosion of galvanized samples, although less than for unprotected metal. Corrosion rates of approximately 0.5 mm/year, 0.72 mm/year, and 0.2 mm/year were measured in 4% NaCl solution for 4%, 1%, and 0% cement in natural pH conditions (pH=11.80, 11.33 and 6.96, respectively). Addition of significant amounts of cement was, in general, actually beneficial, with typical corrosion rates for 8%, 13%, and 25% cement in the range of 0.04 to 0.07 mm/year. Controlling the pH did not make much difference in this case, typical corrosion rates for pH=12 being in the range of 0.07 mm/year to 0.7 mm/year.

In the absence of anions, the overall corrosion rates of galvanized specimens were not excessive, and did not exceed values of the order of 0.01 to 0.02 mm./year, even for extremes of cement content (Figures 6.18 and 6.19)

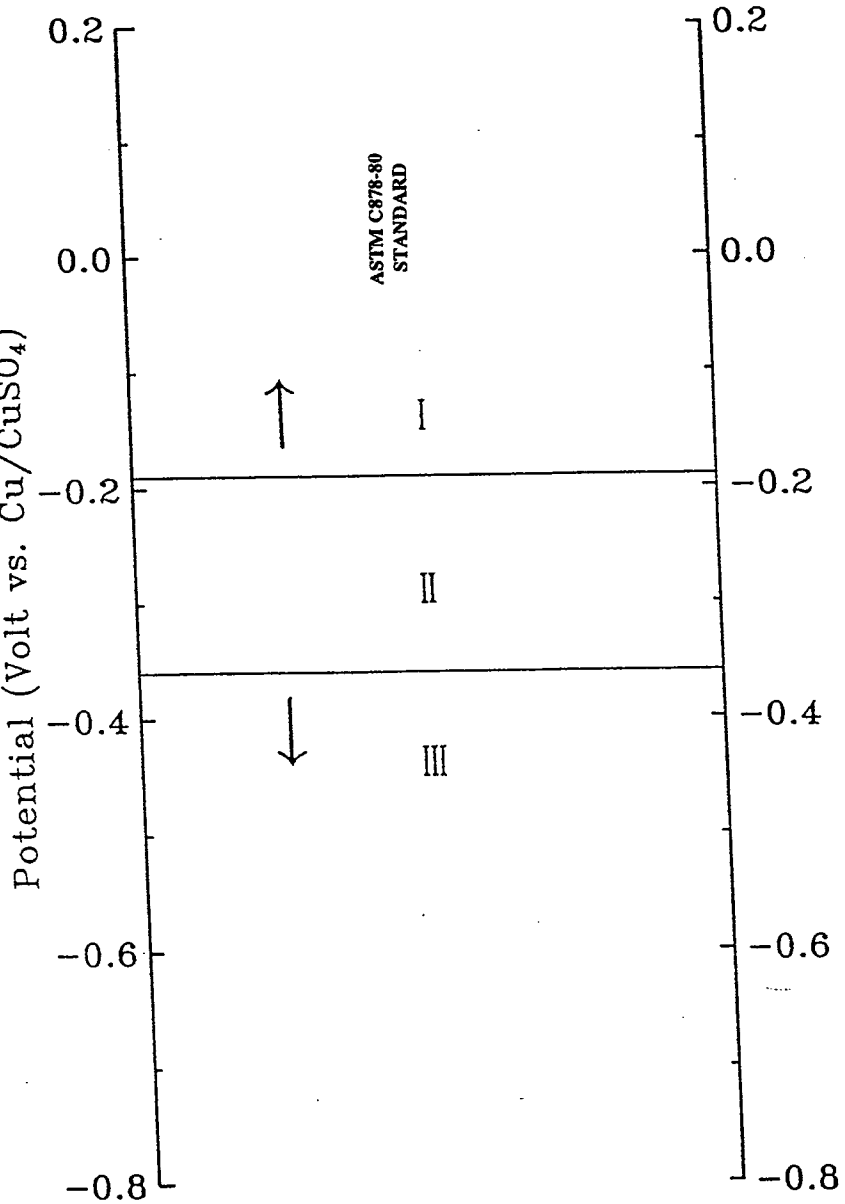

Comparison of the experimentally determined potential range indicating corrosion with the ASTM C-876-86.

- **I. Probability of corrosion < 5.**
- **II. Intermediate range (uncertain).**
- **III. Probability of corrosion 95%.**

Fig. 6.1 - Range of Corrosion Potential Values

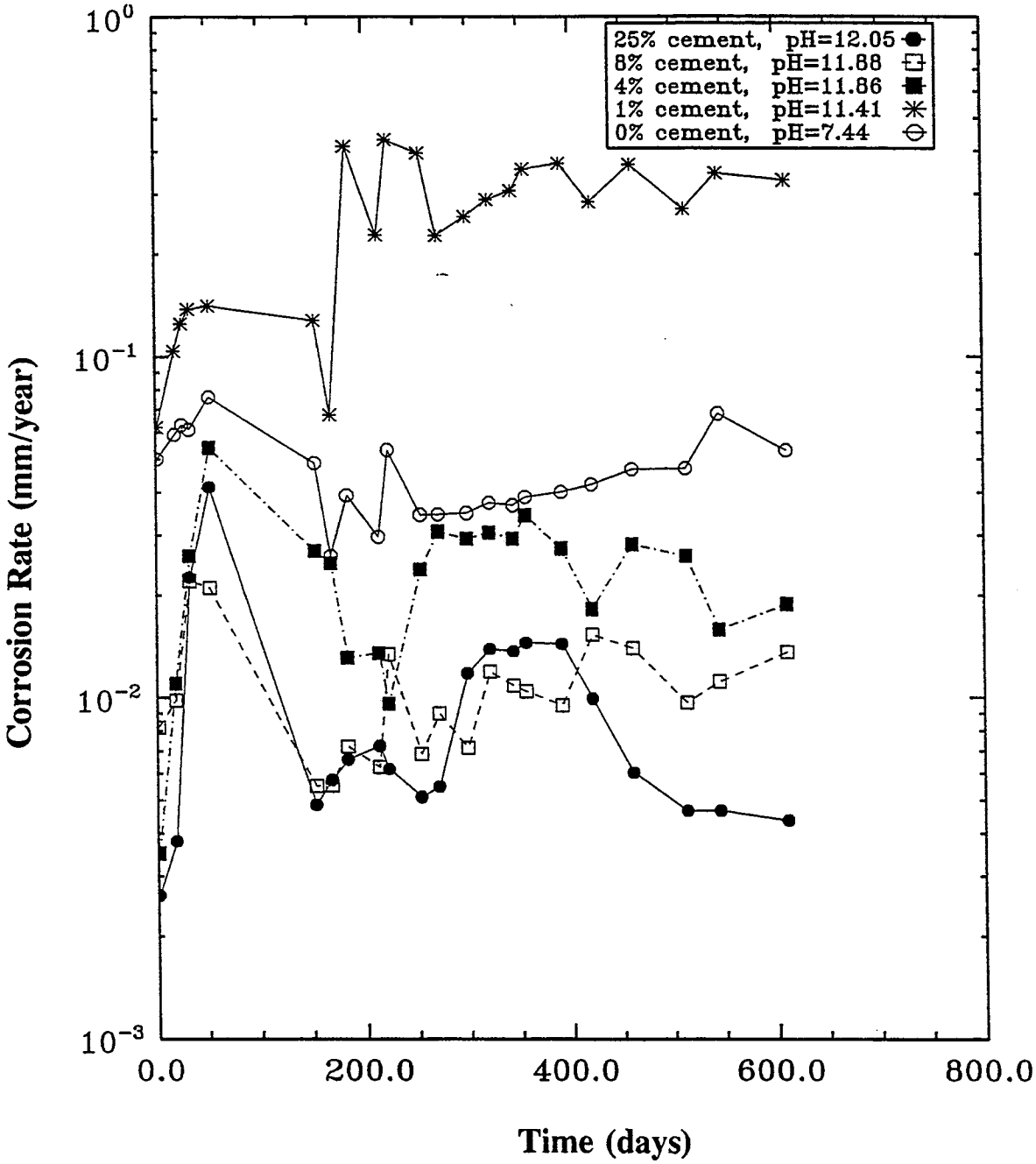

Variation of Corrosion Rate of steel rods in different soil/water/cement compositions in distilled water.

Fig. 6.2 - Corrosion Rates with Time (Steel Specimens, Natural pH)

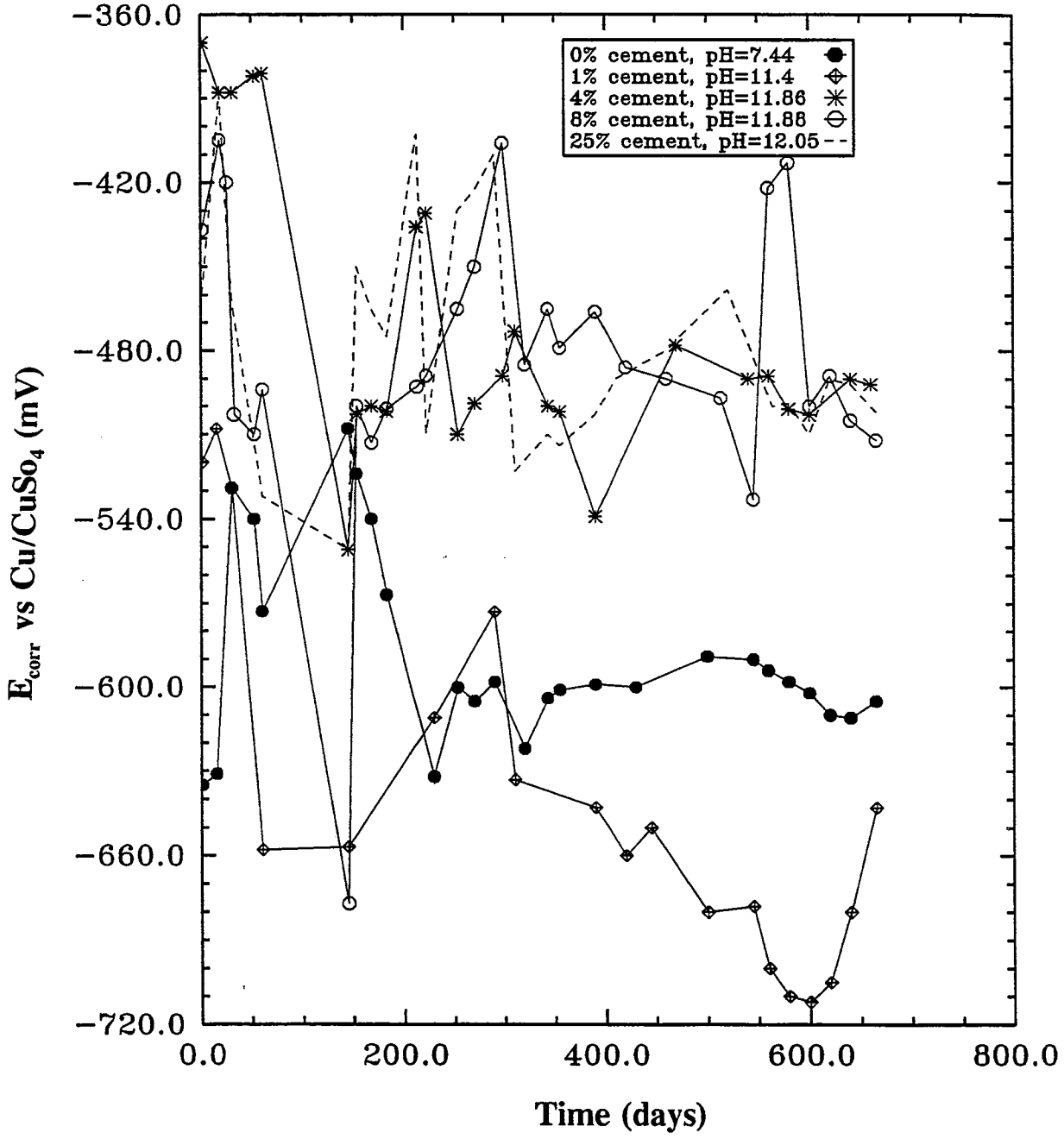

Variation of Corrosion Potential with time for steel rods in different soil/water/cement compositions in water.

Fig. 6.3 - Corrosion Potentials with Time (Steel Specimens, Natural pH)

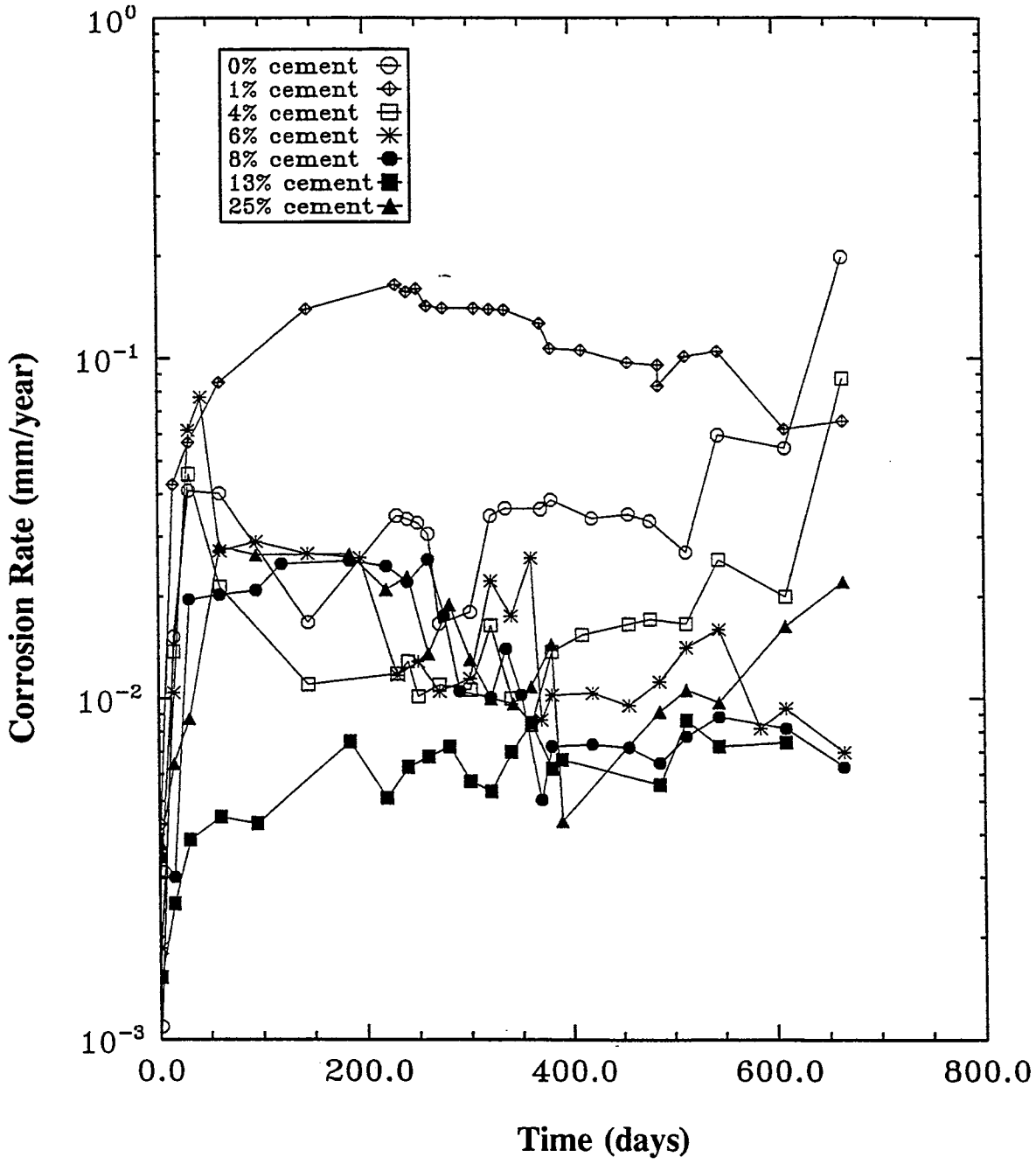

Corrosion Rate vs Time of steel rods in different soil/water/cement compositions in water at pH = 12.

Fig. 6.4 - Corrosion Rates with Time (Steel Specimens, Controlled pH)

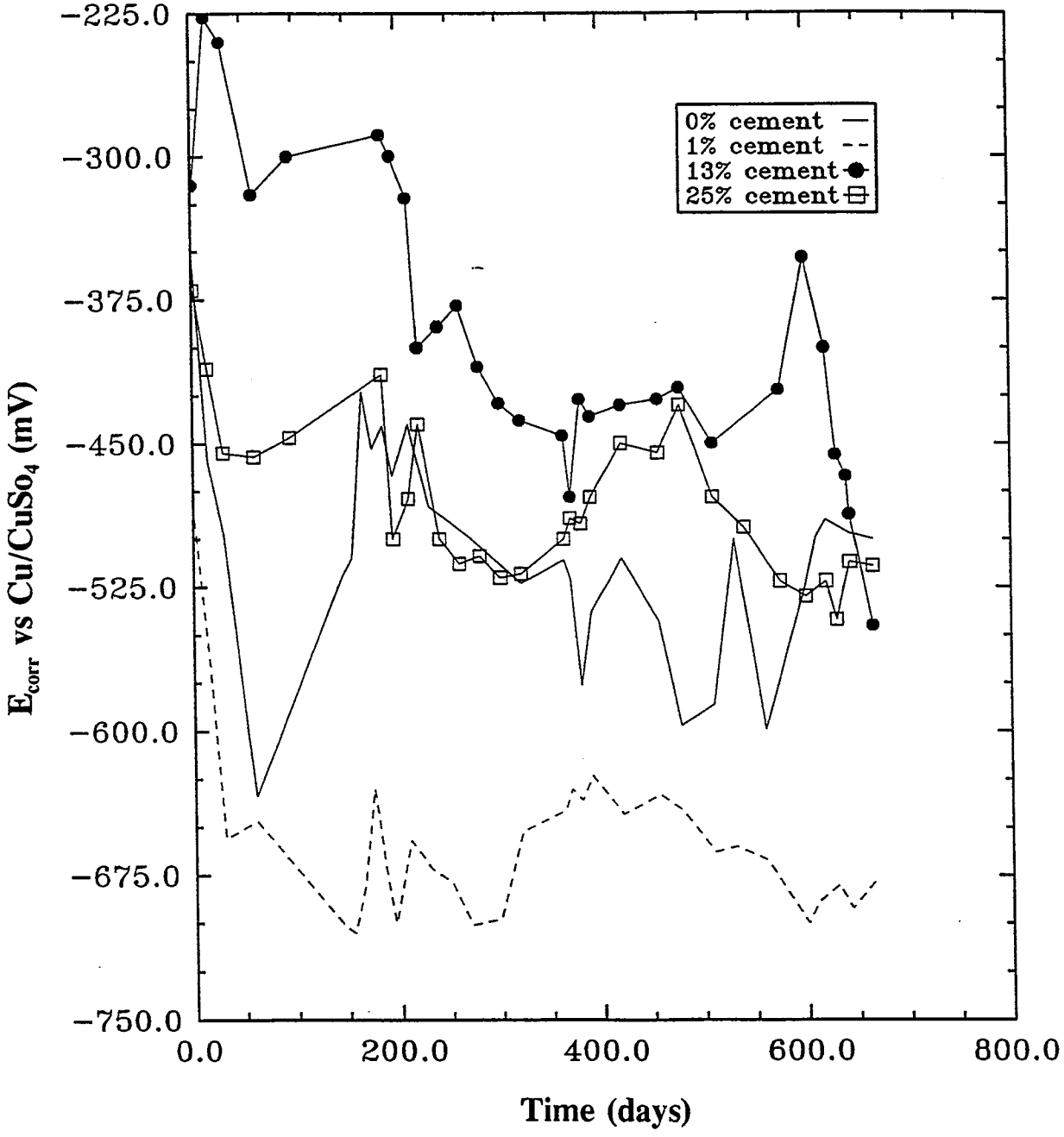

E_{corr} vs Time of steel rods in different soil/water/cement compositions in water at pH = 12.

Fig. 6.5 - Corrosion Potentials with Time (Steel Specimens, Controlled pH)

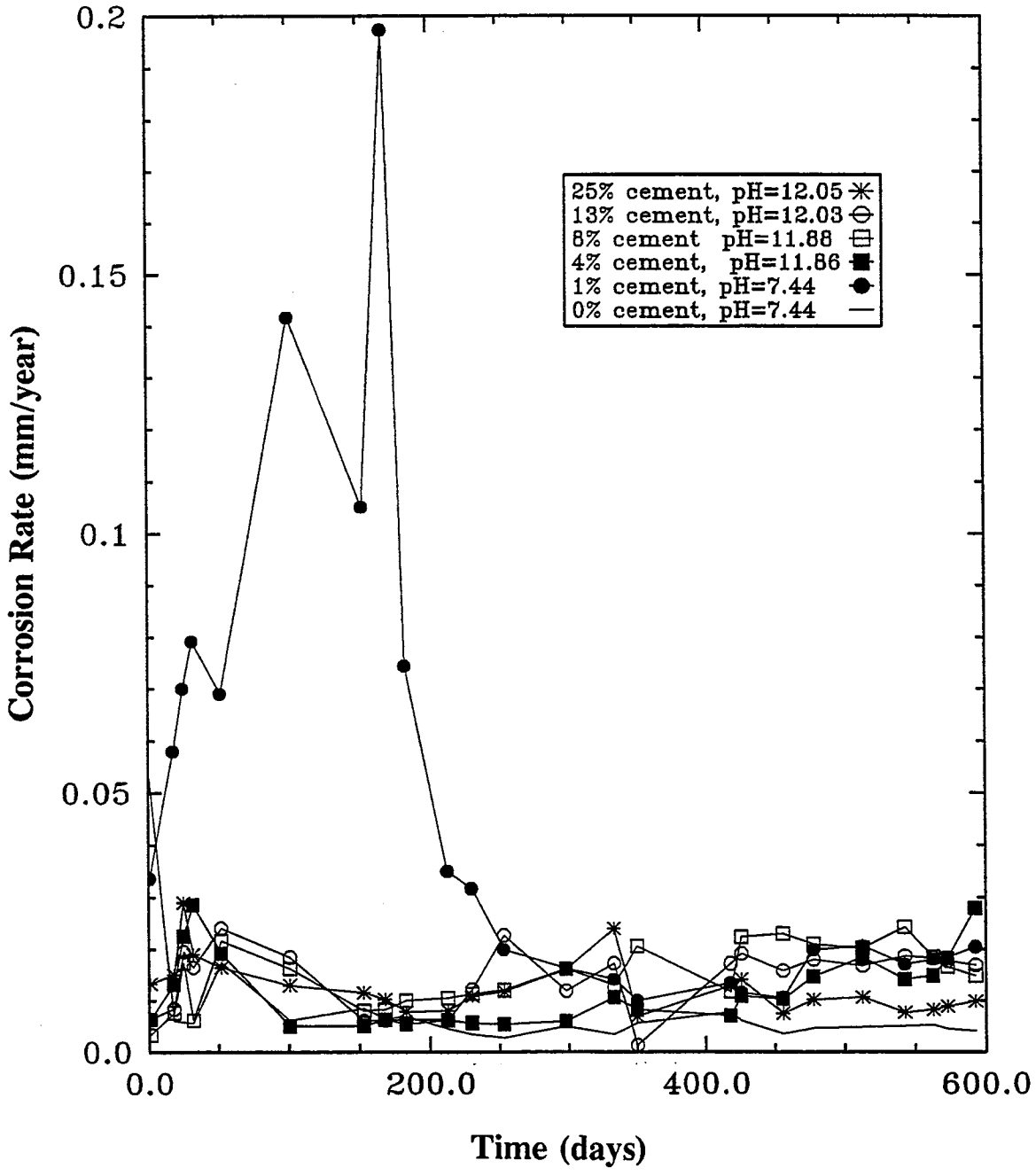

Variation of the Corrosion Rate of galvanized steel rods in different soil/water/cement compositions in water.

Fig. 6.6 - Corrosion Rates with Time (Galvanized Specimens, Natural pH)

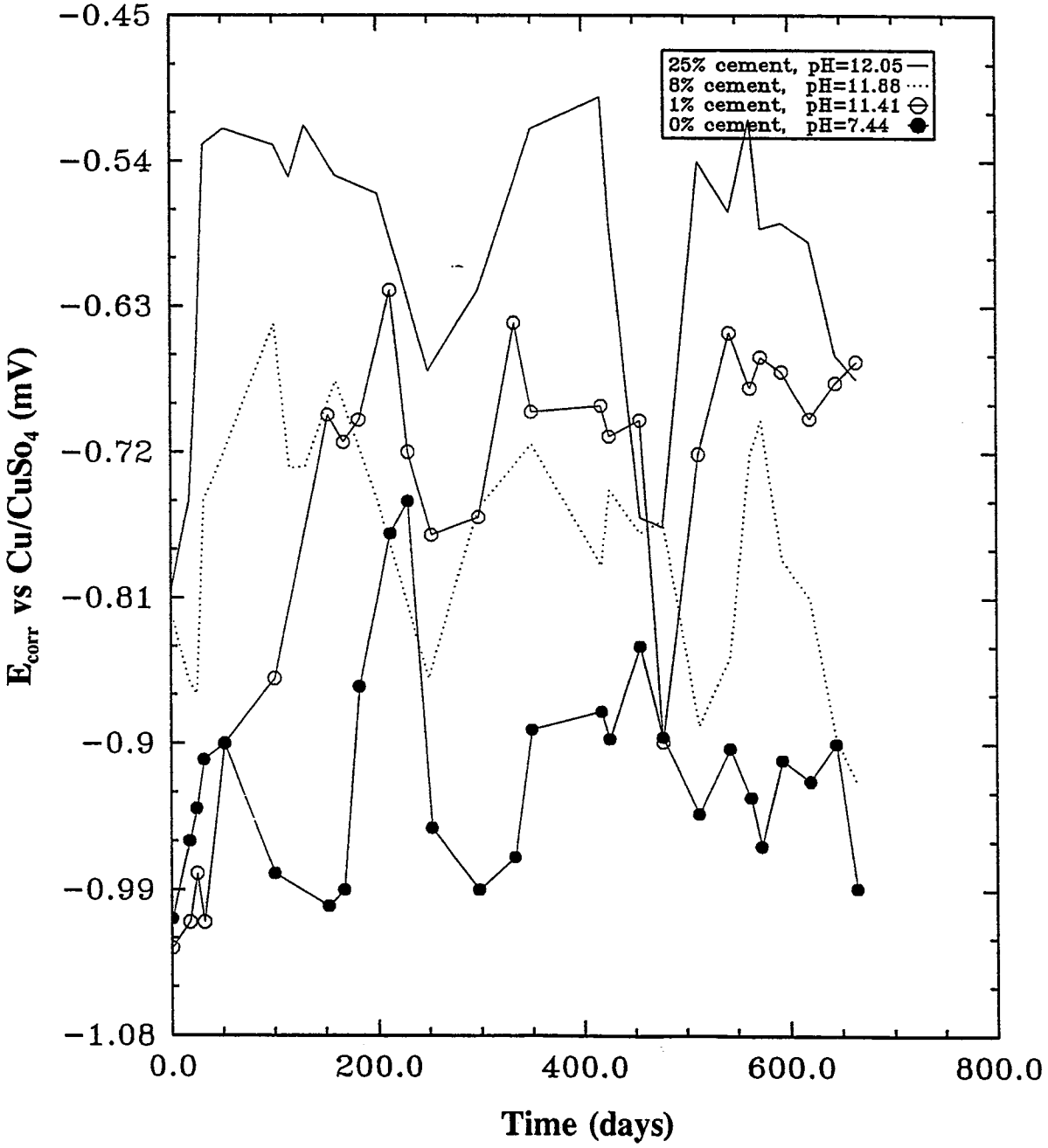

Variation of the Corrosion Potential of galvanized steel rods in different soil/water/cement compositions in water.

Fig. 6.7 - Corrosion Potentials with Time (Galvanized Specimens, Natural pH)

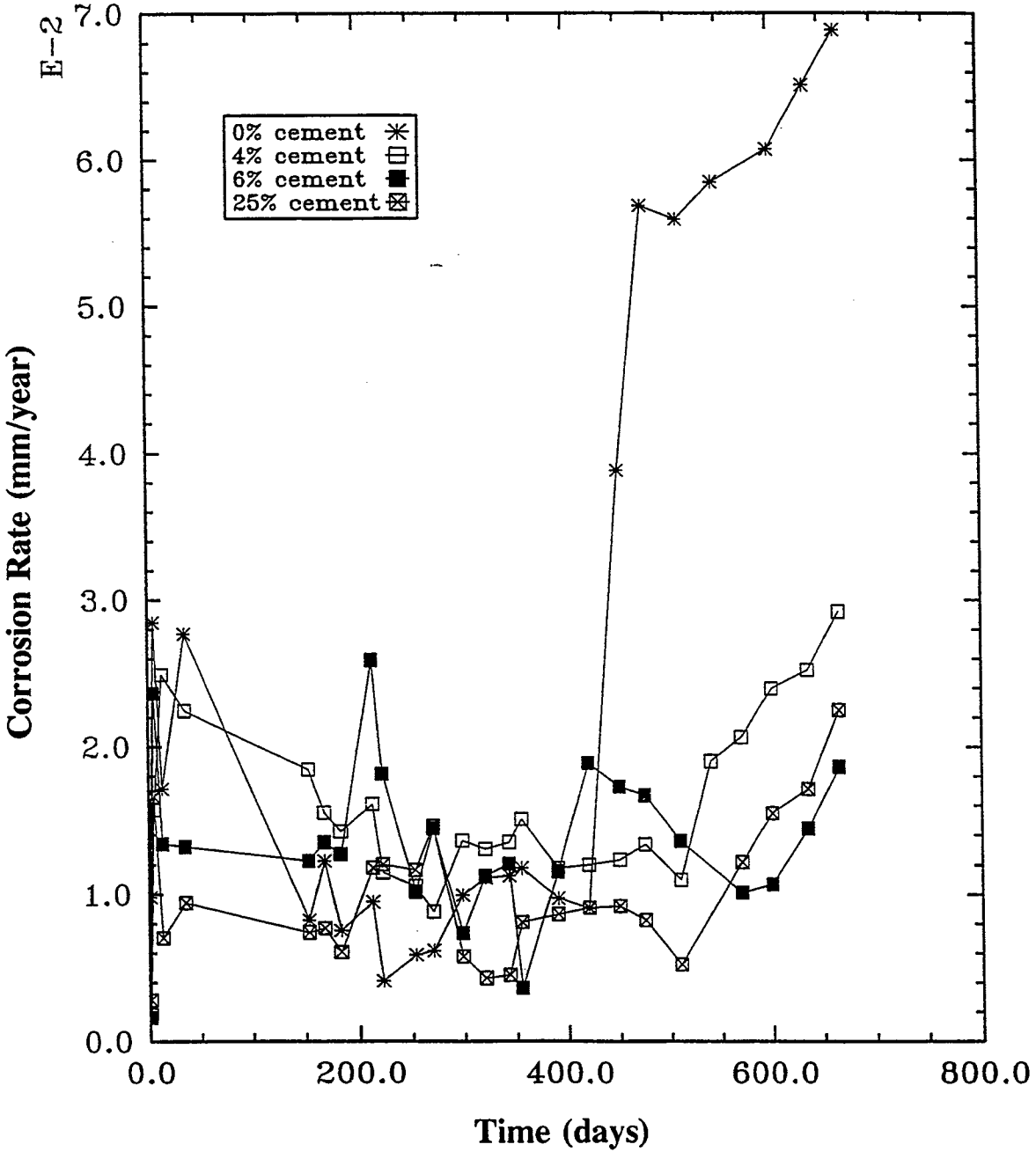

Variation of the Corrosion Rate of galvanized samples in different soil/water/cement compositions in water at pH = 12.

Fig. 6.8 - Corrosion Rates with Time (Galvanized Specimens, Controlled pH)

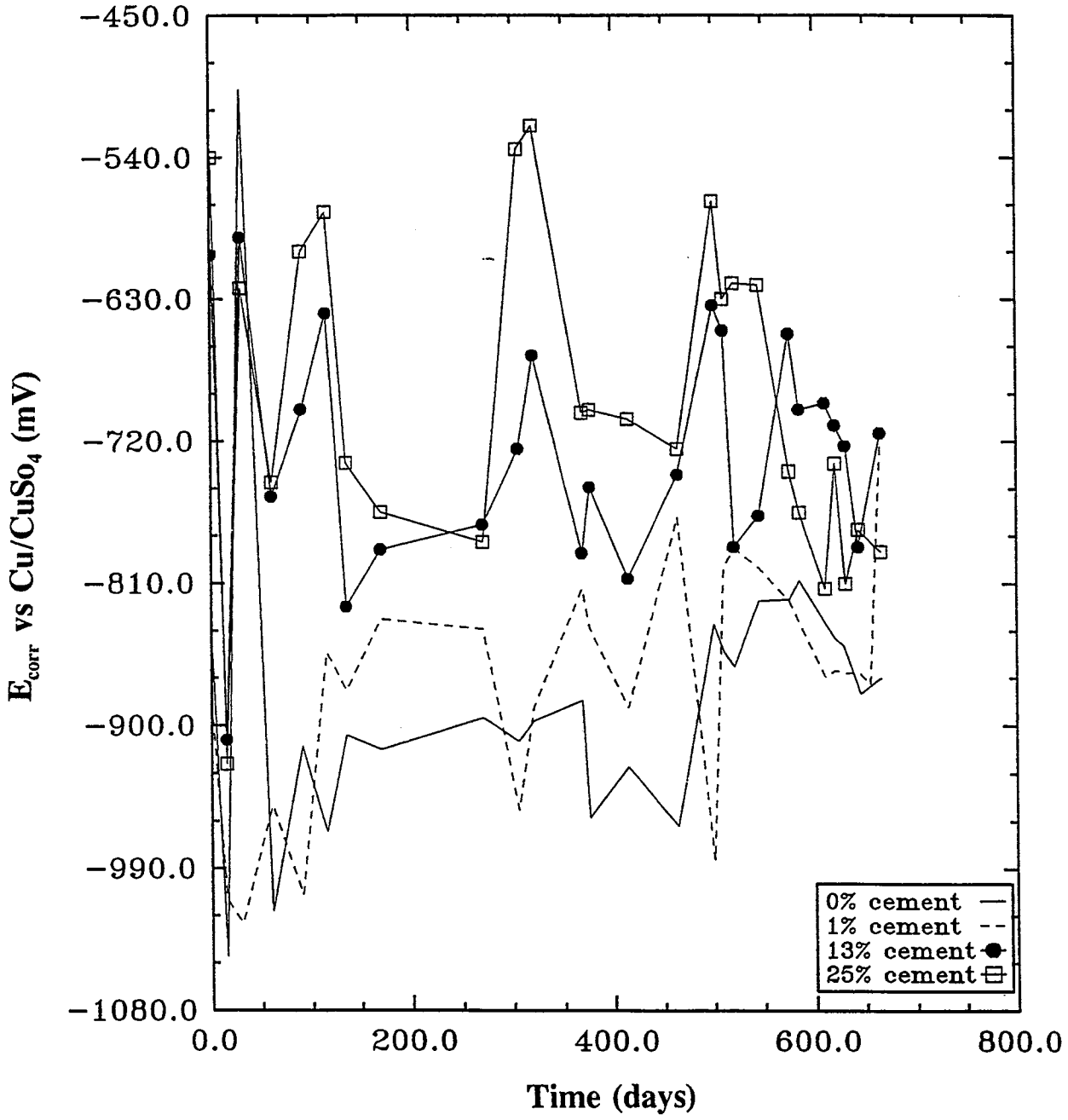

Variation of Corrosion Potential of galvanized steel rods in different soil/water/cement compositions in water at pH = 12.

Fig. 6.9 - Corrosion Potentials with Time (Galvanized Specimens, Controlled pH)

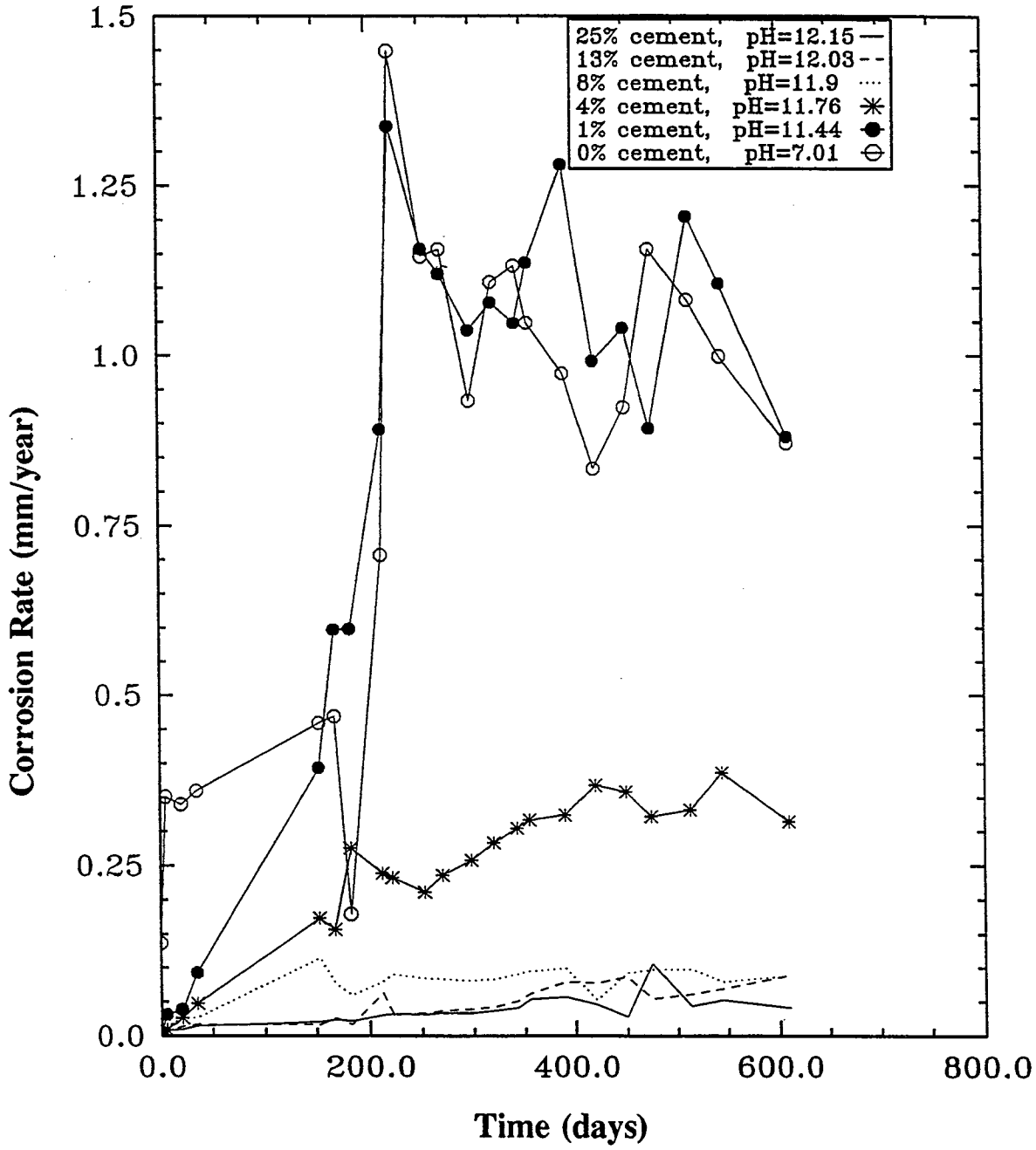

Variations of the Corrosion Rate of steel rods in different soil/water/cement compositions in NaCl solution.

Fig. 6.10 - Corrosion Rates (Steel Specimens, Natural pH, with Chlorides)

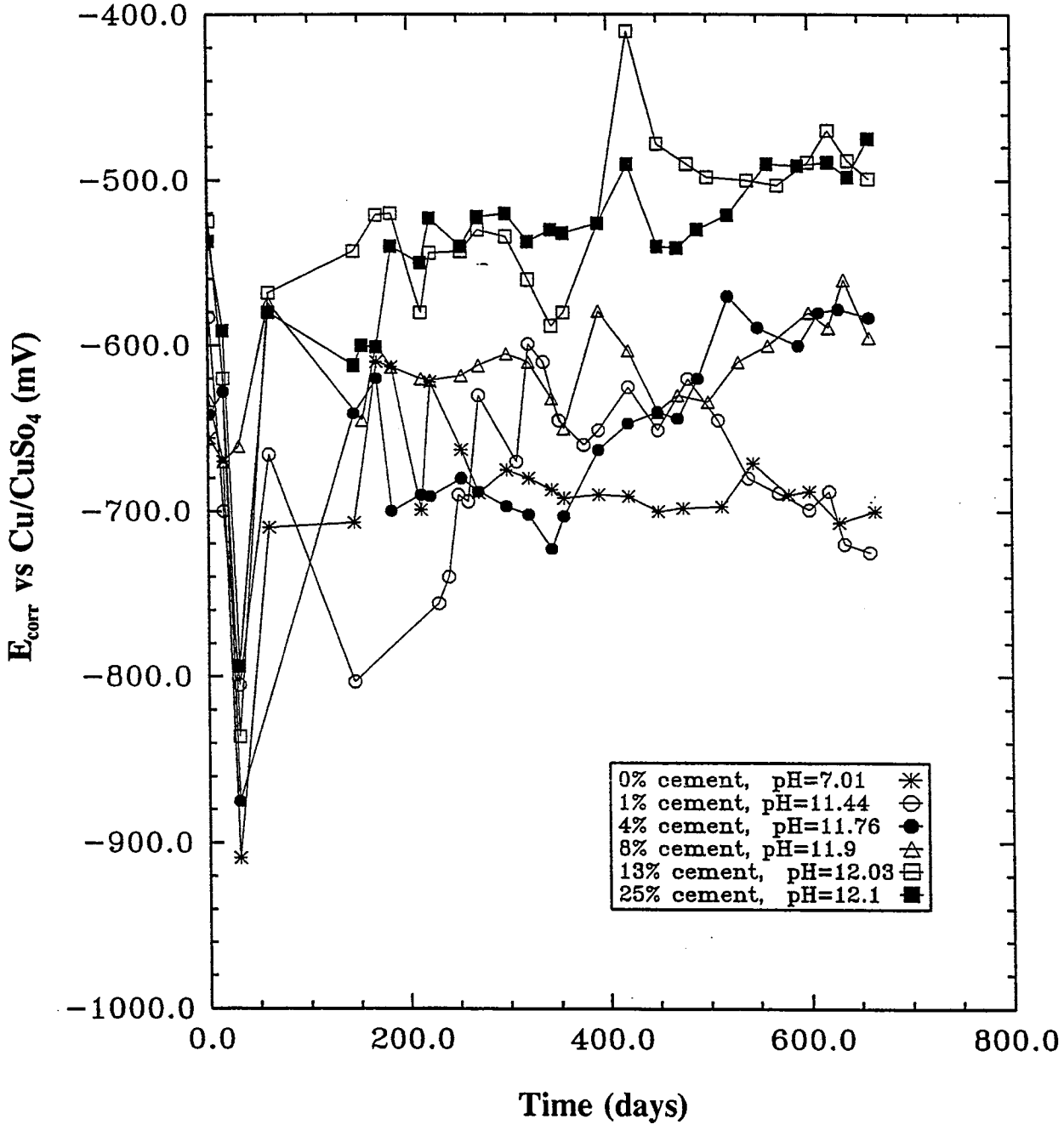

Variation of the Corrosion Potential of steel rods in different soil/water/cement compositions in 4% NaCl.

Fig. 6.11 - Corrosion Potentials (Steel Specimens, Natural pH, with Chlorides)

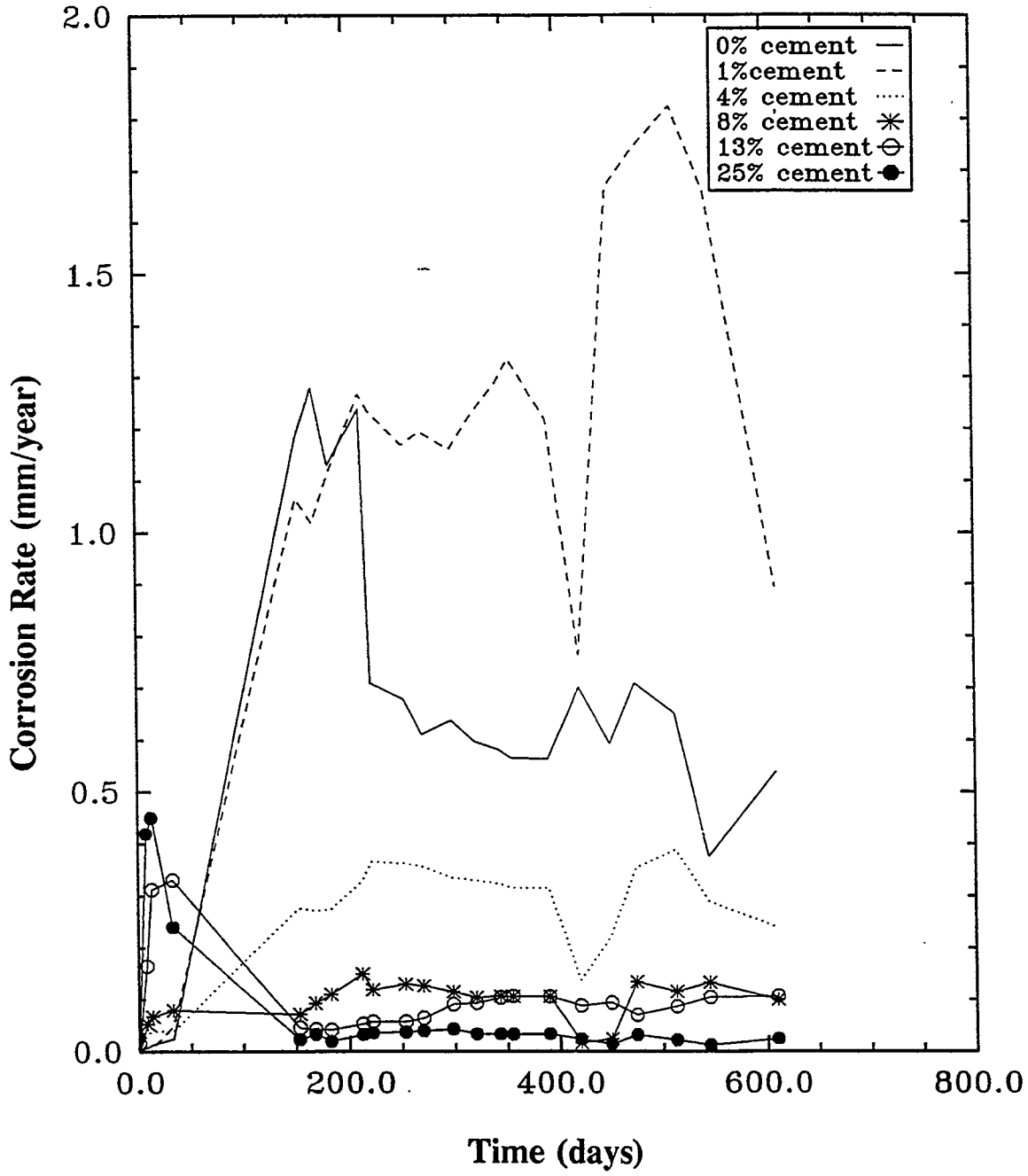

Variation of the Corrosion Rate of steel rods in different soil/water/cement compositions in NaCl solution at pH = 12.

Fig. 6.12 - Corrosion Rates (Steel Specimens, Controlled pH, with Chlorides)

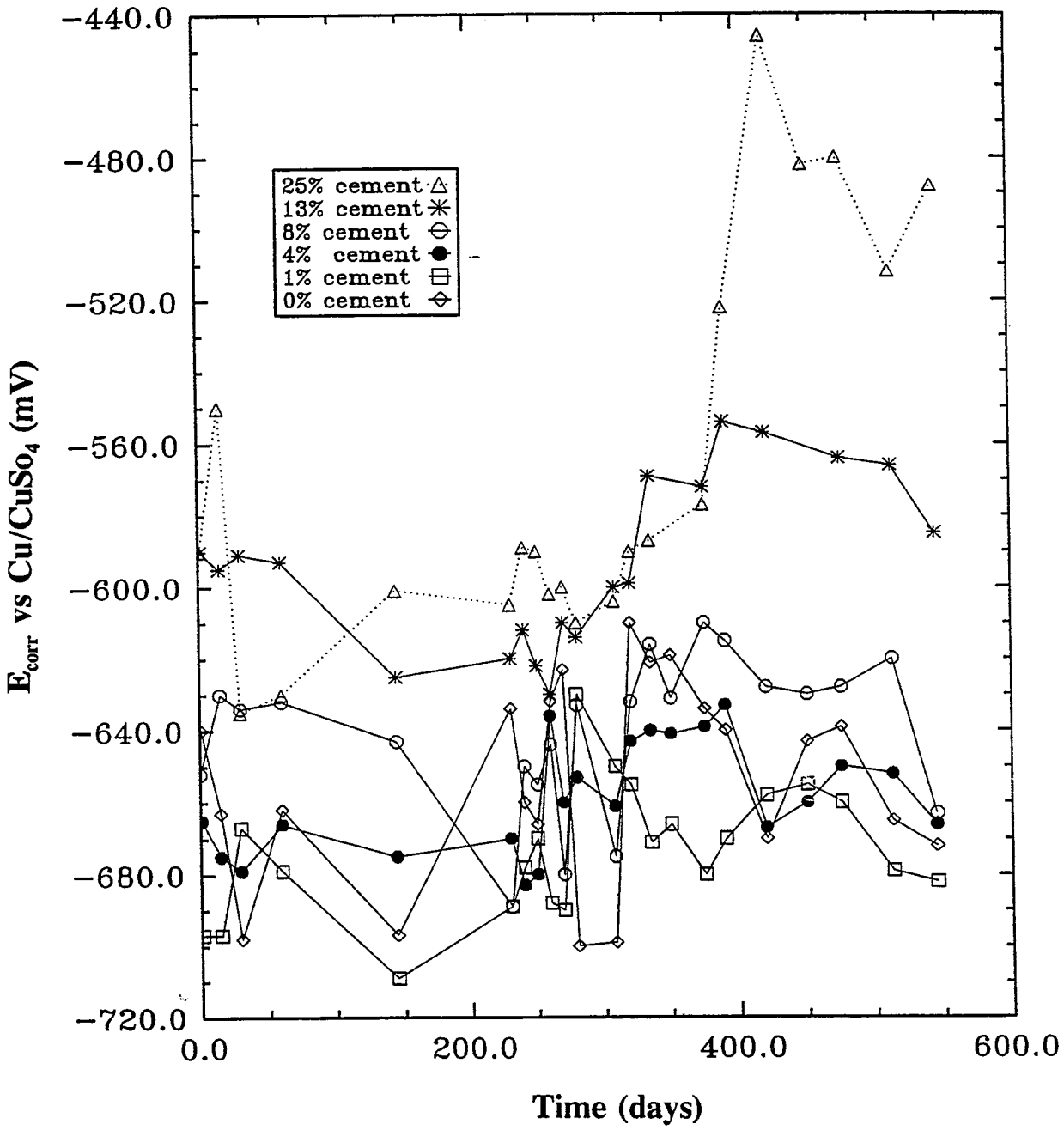

Variation of the Corrosion Potential of steel rods in different soil/water/cement compositions in NaCl at pH = 12.

Fig. 6.13 - Corrosion Potentials (Steel Specimens, Controlled pH, with Chlorides)

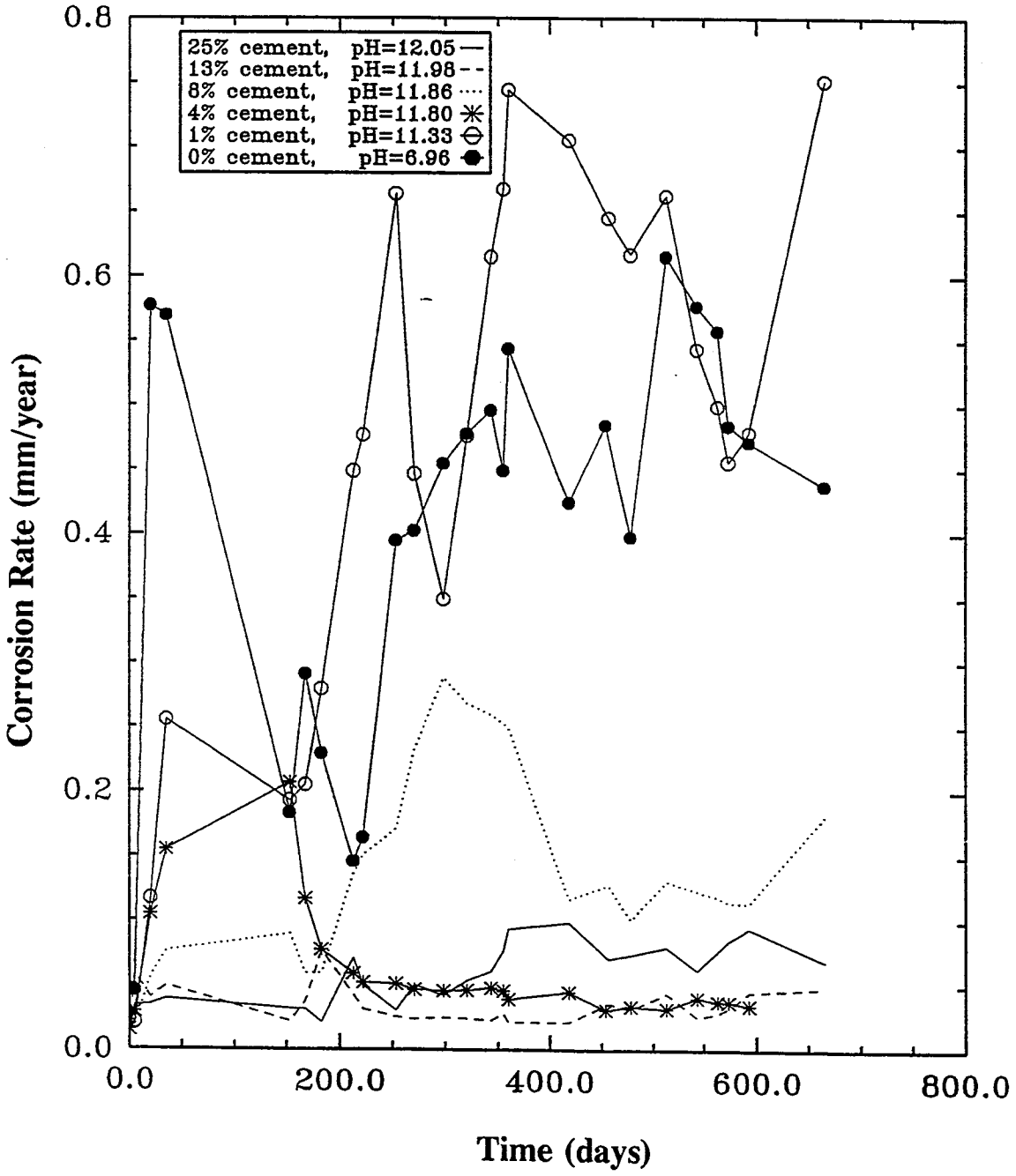

Variation of the Corrosion Rate of galvanized steel rods in different soil/water/cement compositions in NaCl.

Fig. 6.14 - Corrosion Rates (Galvanized Specimens, Natural pH, with Chlorides)

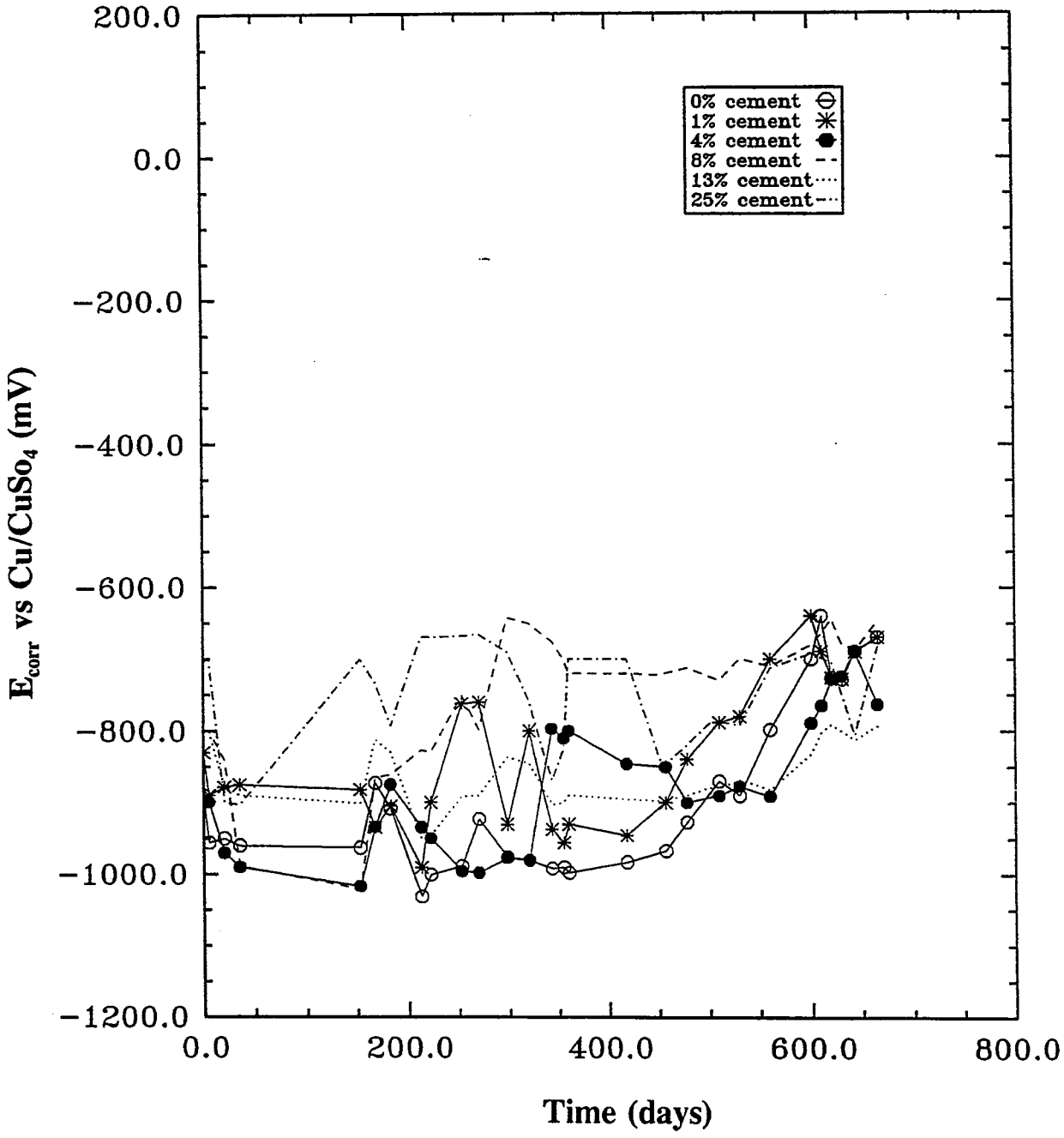

Variation of the Corrosion Potential of galvanized steel in different soil/water/cement compositions in 4% NaCl.

Fig. 6.15 - Corrosion Potentials (Galvanized Specimens, Natural pH, with Chlorides)

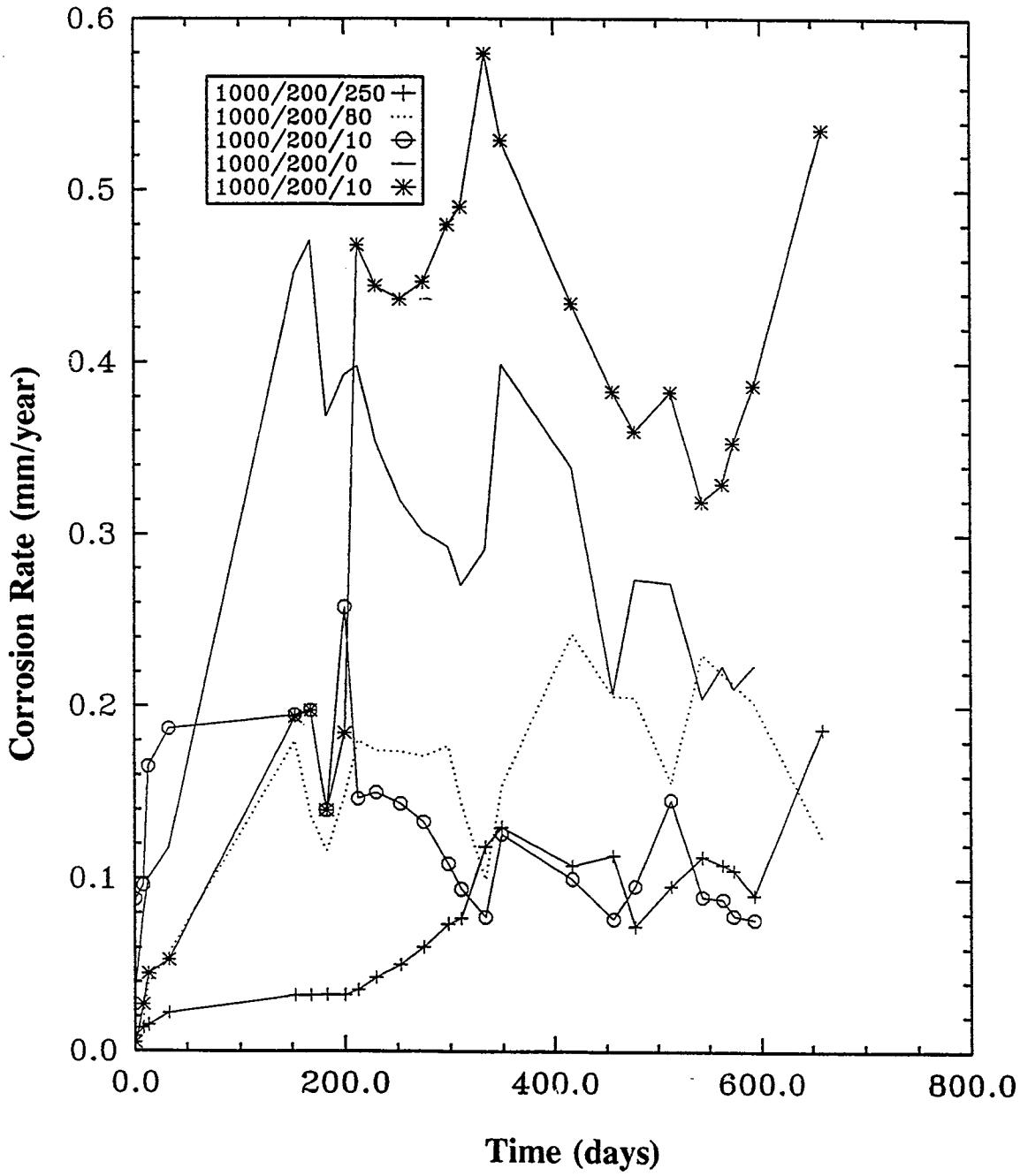

Variation of the Corrosion Rate of galvanized steel rods in different soil/water/cement compositions in NaCl at pH = 12.

Fig. 6.16 - Corrosion Rates (Galvanized Specimens, Controlled pH, with Chlorides)

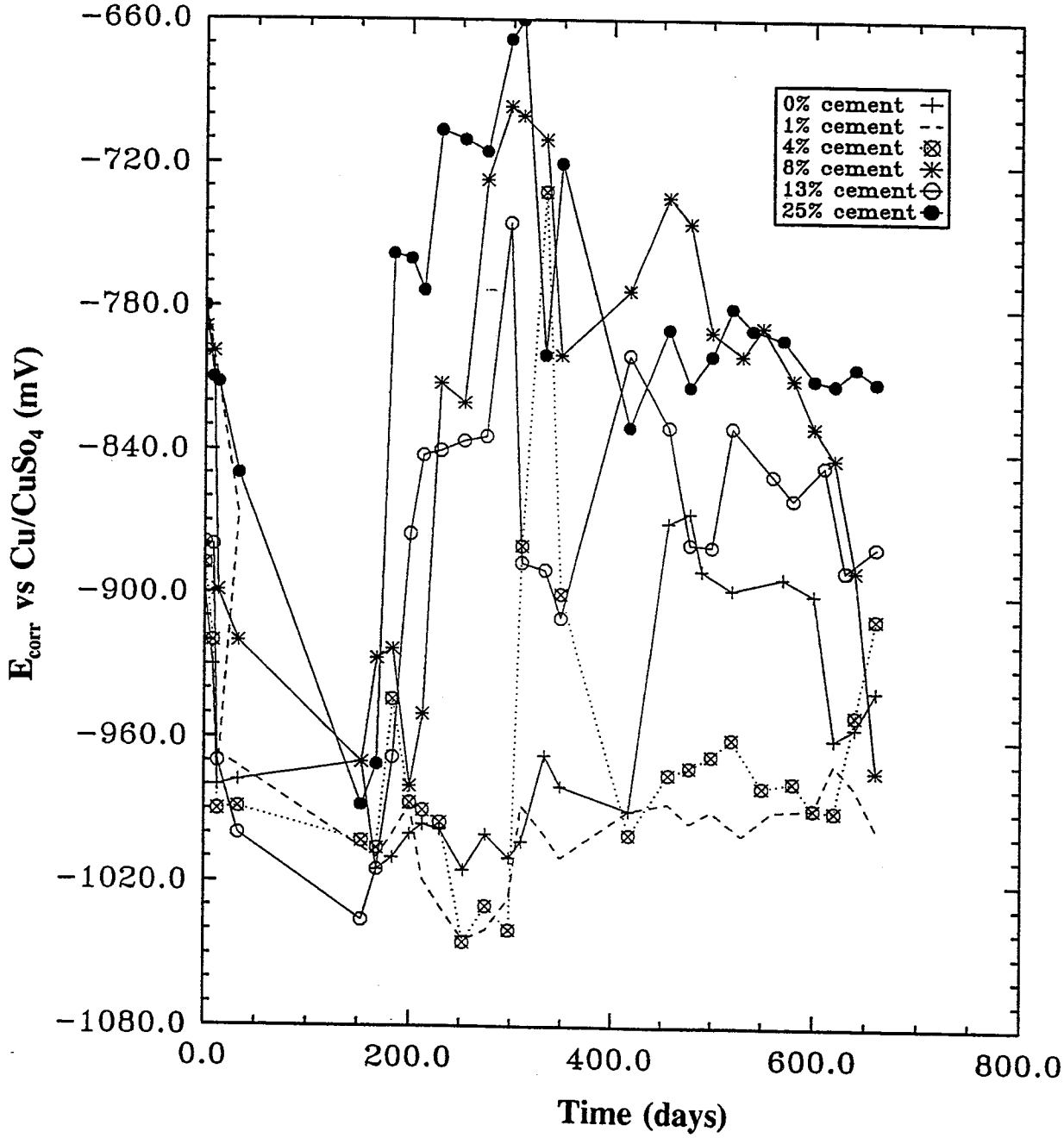

Variation of the Corrosion Potential of galvanized steel in different soil/water/cement compositions in NaCl at pH = 12.

Fig. 6.17 - Corrosion Potentials (Galvanized Specimens, Controlled pH, with Chlorides)

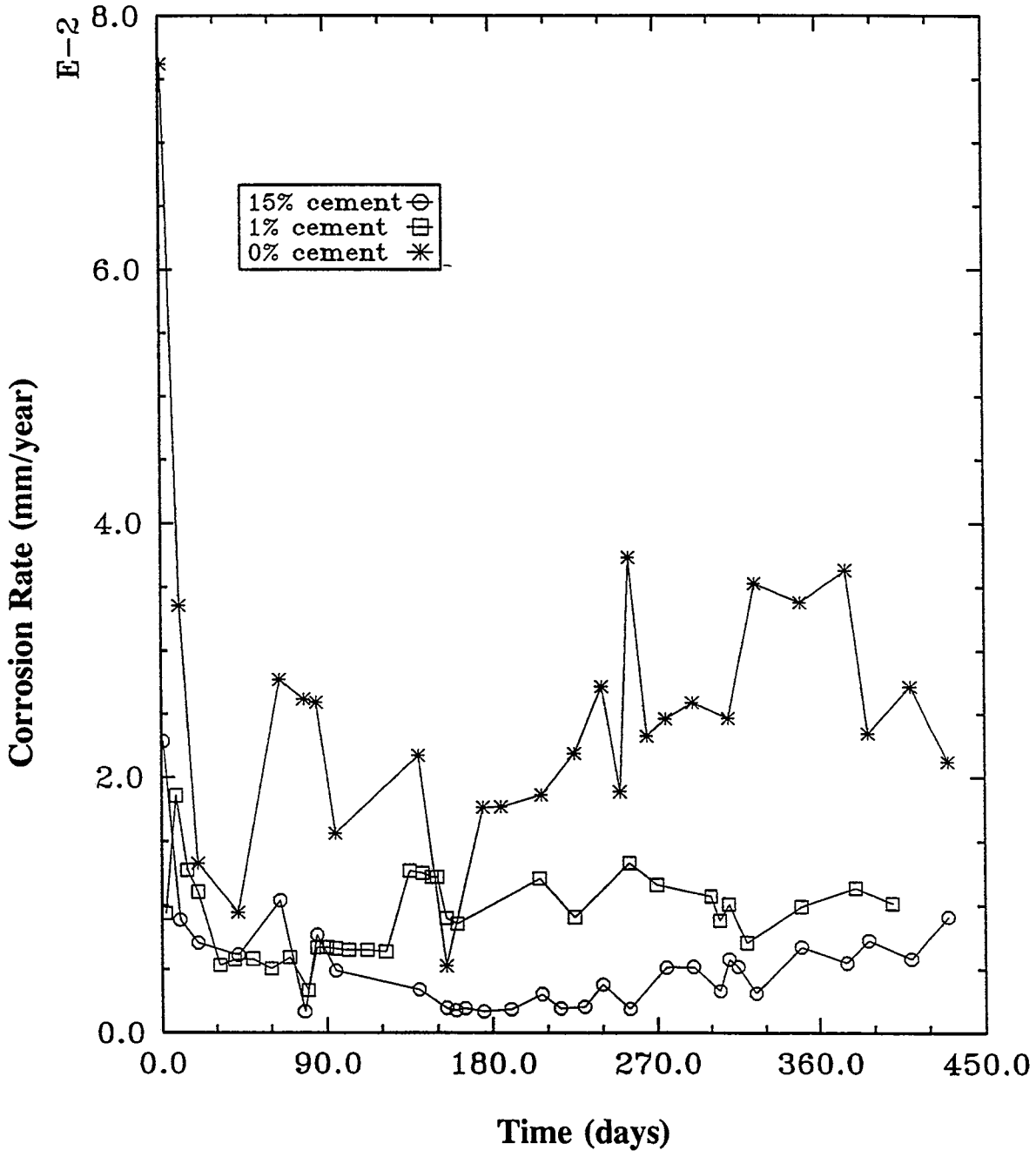

Corrosion Rate vs Time for cement stabilized sand samples in water.

Fig. 6.18 - Corrosion Rates, Extreme Cement Content (Galvanized Specimens, Natural pH)

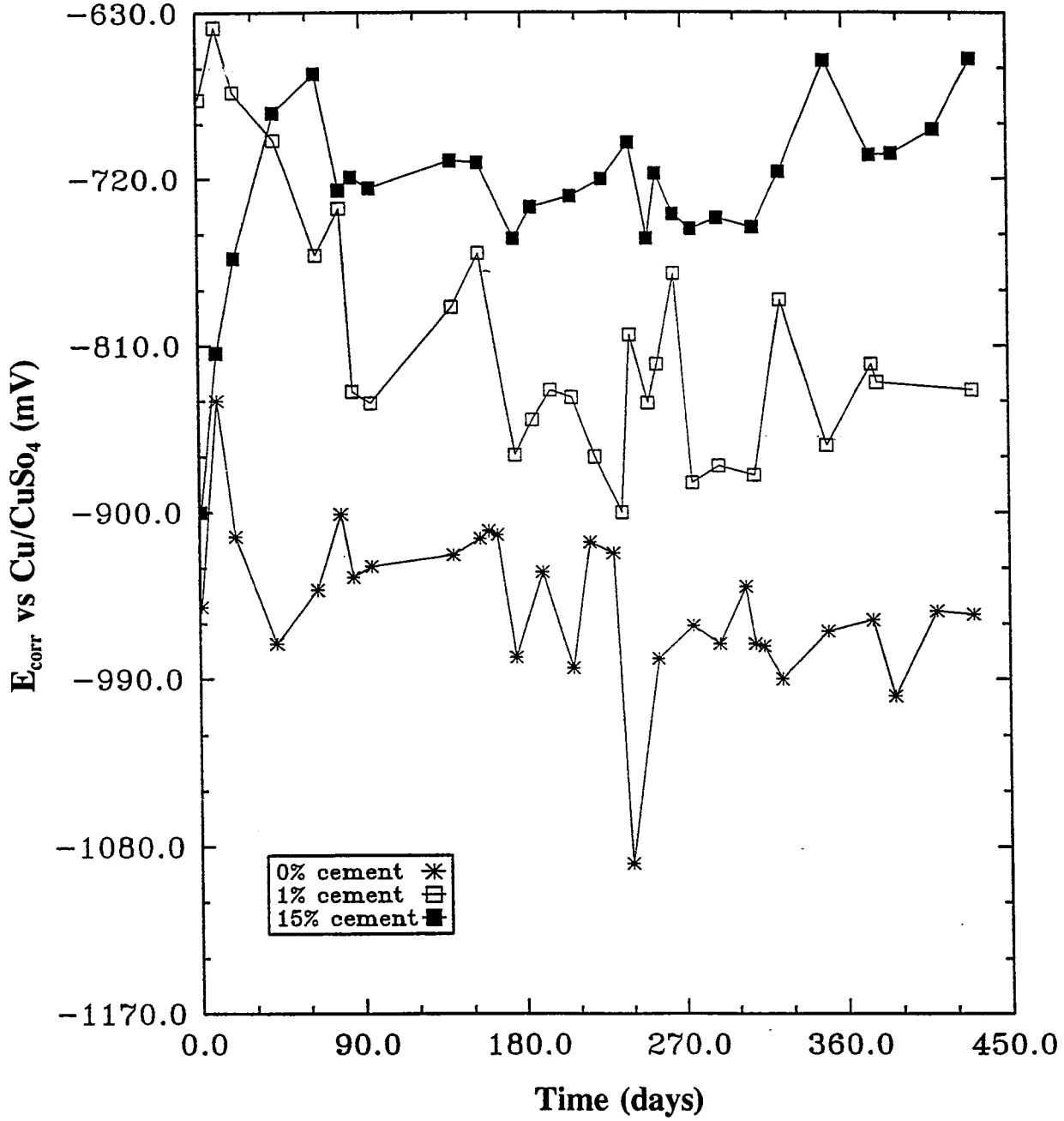

E_{corr} vs Time for cement stabilized sand samples in water.

Fig. 6.19 - Corrosion Potentials, Extreme Cement Content (Galvanized Specimens, Natural pH)

7. INVESTIGATION OF CRUSHED CONCRETE

7.1 INTRODUCTION

An additional consideration addressed at the request of the Bridge Division was to investigate the suitability of crushed concrete as an aggregate for fill behind such walls. This has become an issue because many contractors would like to dispose of surplus crushed concrete in this way. However, at the present time this material fails the standard specifications for such fill -- notably, the specifications for pH which are normally exceeded. Useful economies might be possible if it were feasible to utilize this fill more routinely.

The test program of this project was, therefore, extended to measure the corrosion behavior of crushed concrete, in the context of use as backfill material. This allowed the performance of this material to be compared with conventional fill.

7.2 TEST PROCEDURE

As an initial first step to evaluating this material, samples of crushed concrete were obtained in sampling bags from the District 12 laboratory, and conventional assessment of this material was made in terms of standard test methods Tex-128-E and Tex-129-E. This gave a pH value of 8.2 and a resistivity of 2201 ohm-cm. By comparison, the fill sand used in the preparation of the samples for the laboratory testing previously described had a pH of 7.1 and a resistivity of 22,011 ohm-cm.

Sets of cylindrical samples were then made up for laboratory testing of corrosion rate. As for the other tests, galvanized steel rod samples were embedded in sample mixtures together with water and also various percentages of cement to compare behavior with the normal fill. The potential corrosivity of these samples was then determined as before, by measuring the corrosion rate and corrosion potential in the following electrolytes: (i) distilled water at a natural pH resulting from the natural properties (including cement addition if present) of the mixture used; and (ii) in an environment made artificially aggressive by the addition of a 4% sodium chloride solution, and with a pH resulting from the composition of the mixture used. In this case, the use of a chemically buffered environment was not believed to be necessary.

Some of the samples were also sectioned after testing to check the visual appearance and to display any visible corrosion. Selected photographs of this are shown in the appendix and correspond to a maximum exposure time of up to 470 days. Corrosion was noticeable visually mainly on those samples in NaCl solution, but this is a qualitative indication only of very aggressive corrosion rates. The results of the laboratory measurements are discussed as follows.

7.3 RESULTS

7.3.1 General

Corrosion rates were determined using the methods described in Chapter 5. Variations of the corrosion rate of the test specimens for different cement ratios as a function of time are shown in Figures 7.1 and 7.2, and are discussed in turn in the following sections. Note that an exponent of E-2 is applicable to the vertical axis of Figure 7.1.

As mentioned in Chapter 5, when corrosion rate values are below about 1.1×10^{-3} mm/year, then the material is either assumed to be in the passive state, or the rate of attack is insignificant. Above this level, a certain amount of corrosion may be detected. For reference, maximum corrosion rates in uncracked concrete measured in very aggressive environments are usually found to be about 1.1×10^{1} mm/year.

7.3.2 Galvanized Specimens, Natural pH, Distilled Water

The variation of the corrosion rates of galvanized steel rods in different crushed concrete/cement ratios is shown in Figure 7.1 as a function of duration of storage. Only distilled water was added, so that the electrolyte was at natural pH, resulting only from the actual concentration of the materials used. As can be seen, the galvanized rod samples embedded in 4%, 6%, 8%, and 13% cement showed low corrosion rates up to the maximum exposure time of 470 days. The corrosion rates were in the range of 0.005 mm/year measured for 13% cement content, up to 0.02 mm/year measured for 4% cement content in the mixture. This is comparable with corrosion rate values measured for regular fill and discussed in Section 6.2.4, which had long-term corrosion rate values of 0.004 to 0.02 mm/year.

The galvanized rod samples with no cement content in the mixture showed somewhat higher corrosion rates than the others. The initial corrosion rate was approximately 0.018 mm/year, which is still relatively low. As the exposure time progressed, the samples presumably passivated somewhat, and the corrosion rate leveled off at an average corrosion rate value of 0.04 mm/year. After 275 days of exposure, the corrosion rate started to increase again to reach a corrosion rate of 0.07 mm/year after 470 days of exposure. This is somewhat higher than one would like, although it is not very different from the results shown in Figure 6.6. It is certainly less than the corrosion rate for 1% cement addition to normal fill.

7.3.3 Galvanized Specimens, Natural pH, with Chlorides

The effect of a more chemically aggressive environment was also investigated. Variations of the corrosion rate with time of galvanized steel rods embedded in different cement compositions in 4% NaCl solution are shown in Figure 7.2. The pH of the electrolyte shown in the figure was a function of the cement content in the samples. As can be seen, the highest corrosion rate was observed for galvanized steel rods embedded in mixtures with no cement content [pH=7.1] and 1% cement content [pH=9.3].

The most advanced corrosion was observed in the absence of cement in the mixture. The initial corrosion rate of this sample was 0.32 mm/year. After 460 days of exposure in 4% NaCl solution, the corrosion rate increased up to 0.58 mm/year. The galvanized sample embedded in the 1% cement mixture had an initial corrosion rate of 0.2 mm/year, which then reached a value of approximately 0.5 mm/year after 460 days of exposure. In both cases, the corrosion rate curve had a tendency to rise with time.

Although these are high values (as one would expect for an especially aggressive test environment), the important thing is that they can be compared with values for corrosion rates in regular fill, discussed in Section 6.3.4 and displayed in Figure 6.14, which averaged 0.5 mm/year and 0.72 mm/year for 0% and 1% cement, respectively. The values for normal fill are, therefore, somewhat worse than for crushed concrete fill.

Galvanized rod samples embedded in 4% cement at pH=10.1, in 6% cement at pH=11, in 8% cement at pH=11.5, and in 13% cement at pH=12, showed lower corrosion rates compared with those with zero and 1% cement content. For this set of samples, typical values of corrosion rates were in the range of 0.04 mm/year for 13% cement content and increased up to a value 0.15 mm/year for 4% cement content.

Again, this is actually marginally better than the corrosion rates for normal fill under comparable conditions, which were in the range of 0.04 to 0.07 mm/year for cement contents of 8% to 25%, and about 0.1% for 4% cement content.

The figures show that in both cases, corrosion rates measured initially and after 375 days showed a tendency to decrease with the increase of the cement content in the mixture, indicating that the pH at the substrate/metal/solution interface has a crucial role in the corrosion mechanism. As the exposure time advanced, the corrosion rate leveled off for all samples which contained more than 4% cement. This was the opposite of what was observed in the case of 0% and 1% cement content.

7.4 CONCLUSIONS

In general, corrosion rates of galvanized steel in crushed concrete were found to be comparable to, and possibly slightly better than, the samples exposed to sand fill. Average values were in the range of 0.005 mm/year up to 0.02 mm/year, which are in the range of the commonly accepted target of 0.01 mm/year, giving a design life of around 100 years. The results are almost identical with those obtained for corrosion rates of galvanized steel embedded in sand/cement mixtures.

As for conventional fill, the presence of anions in the form of 4% NaCl in the electrolyte greatly accelerated the rate of corrosion. Samples with little or no cement addition showed advanced corrosion rates of 0.5 and 0.58 mm/year, although again this was comparable with the results from regular sand fill. Samples with 4%, 6%, 8%, and 13% cement had lower corrosion rates under these conditions, in the range between 0.04 and 0.15 mm/year.

It was found that the addition of cement to specimens actually assisted in inhibiting corrosion rates. While it might be possible to make a case for advocating the addition of cement to crushed concrete to improve the corrosion performance, this is probably unnecessary in this instance, as the main purpose of this investigation was to check the suitability of crushed concrete.

The overall conclusion concerning this material, based on the results carried out over this time period, is that the use of crushed concrete in retaining wall backfill does not need to be discouraged from a corrosion point of view, even though the high natural pH levels had previously been assumed to render the material unacceptable. Its corrosivity appears to be no worse than conventional granular backfill. Should additional cement be present for additional stabilization, if desired, this is also acceptable, and, if anything, has a beneficial effect on the corrosion environment.

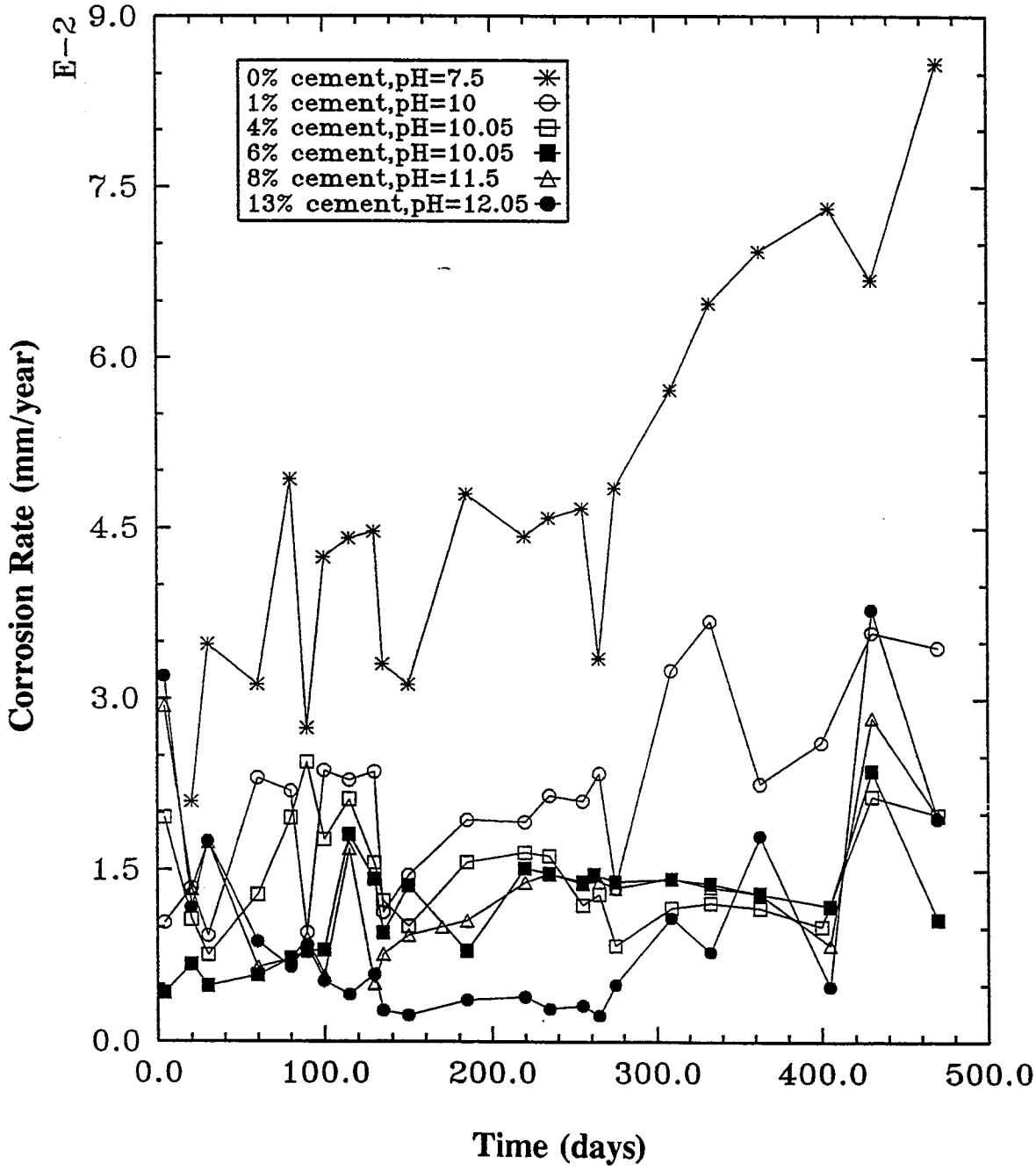

Corrosion Rate vs Time for crushed concrete samples in water.

Fig. 7.1 - Corrosion Rates, Crushed Concrete (Galvanized Specimens, Natural pH)

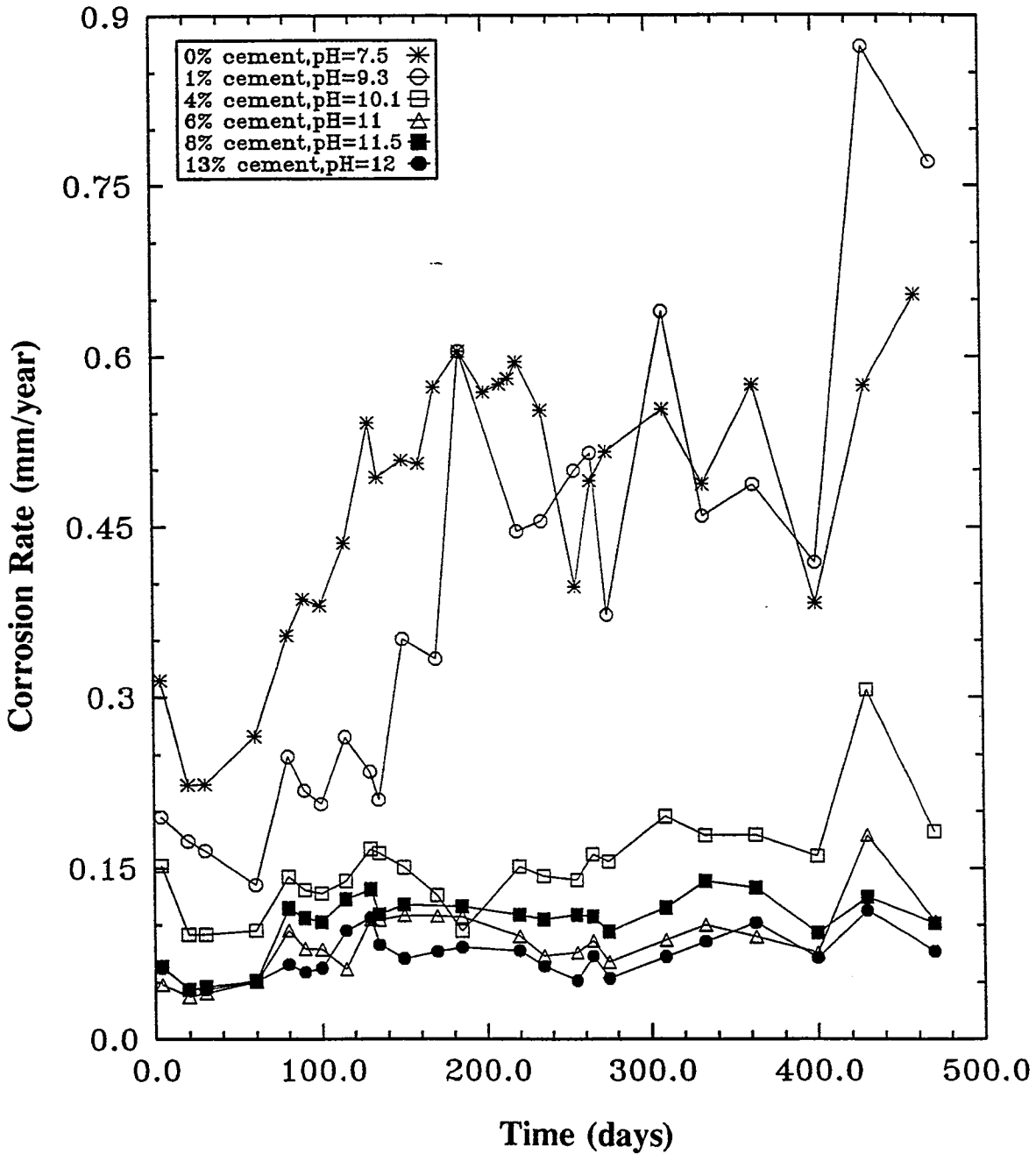

Corrosion Rate vs Time for crushed concrete samples in NaCl solution.

Fig. 7.2 - Corrosion Rates, Crushed Concrete (Galvanized Specimens, Natural pH, Chlorides)

8. CEMENT CONCENTRATION CELLS

8.1 GENERAL

Even though the laboratory tests previously described had been set up to measure the effect of cement addition, these tests involved samples that had been deliberately prepared to be homogeneous. An additional possible complication to the overall situation would occur if there were significant localized variations of properties within the fill. Such "corrosion cells" are known to have a major contributory effect to metallic corrosion of laboratory specimens under certain circumstances, as differential electro-chemical potentials will in principle occur between any two regions of variable concentration of the material in question (in this case, added cement).

In particular, major inhomogeneities of cement content with depth into the backfill might cause the existence of local concentration cells which would aggravate the natural corrosion environment and might be a primary cause of accelerated corrosion. Because significant variations in cement content had been measured in the fill behind the field retaining walls, as indicated in Chapter 4, it was necessary to investigate the possibility that this might be responsible for the accelerated corrosion at the problem site, particularily since the early results of the tests on uniform samples had not shown that the mere addition of cement by itself had caused much acceleration of corrosion.

Specific experiments were, therefore, devised to simulate the possible existence of concentration cells due to adjacent regions of differing cement content, consisting of laboratory cells set up between interconnected samples, as follows.

8.2 TEST PROCEDURE

In order to determine the effect of cement content distribution in the samples on creating a potential difference which may intensify the corrosion rate of galvanized reinforcing steel, special cement concentration cells were set up. These enabled the effect of differential cement distribution to be studied by measuring the corrosion potential and corrosion rate of short circuited samples prepared with different concentrations of cement. As already discussed, different cement contents present at the metal/concrete interface may cause different localized potentials to be established at the interface which may increase the corrosion rate of the sample.

The experiments were carried out by measuring the corrosion rates of galvanized reinforced steel embedded in two separate samples containing different cement contents, and the results were compared with the corrosion rates estimated when the same samples were short circuited. For example, in order to simulate the field conditions, a cylinder which contained 0% cement was short circuited with a cylinder which contained 13% cement; or a 1% cement cylinder with an 8% cement cylinder, etc. The corrosion rate of such short circuited samples was monitored as a function of time.

8.3 RESULTS

8.3.1 General

Figure 8.1 shows the corrosion rate determined between samples formed by galvanized steel strips embedded in unstabilized sand fill (i.e., 0% cement) and backfill with 15% cement, under natural pH conditions. This is superimposed on the concentration rates of the individual samples when tested separately. The overall corrosion rate is between the rates of each individual case and is relatively low, being of the order of 0.01 mm/year (note the exponent E-2 on the vertical axis).

In order to provide some additional supporting data on this effect, the following additional cement concentration cells were tested using distilled water as the electrolyte: 0% cement content connected to 13% cement content, and 1% cement content connected to 8% cement content. The particular samples used were those prepared initially using crushed concrete as backfill material because they were available at the time these tests were being planned. The main purpose of these initial tests was to see whether or not the effect of differential cement concentrations was significant, compared to the other factors that were liable to be causing corrosion. Had this been a major effect, then more experiments would have been performed on samples prepared using normal fill sand as the background matrix. However this was unnecessary in view of the conclusions of the tests reported below.

8.3.2 Galvanized Specimens, Distilled Water

In Figure 8.2, the corrosion rate of the concentration cell between cement contents of 0% and 13% is compared with the individual corrosion rates of the samples containing 0% cement and 13% cement separately. A corrosion rate of approximately 0.008 mm/year was observed for the galvanized rod samples embedded in 13% cement. This increased to about 0.015 mm/year when the sample with 13% cement content was short circuited with a sample containing 0% cement, but was still very much less than the value of approximately 0.05 mm/year exhibited by the sample containing 0% cement on its own.

The cell corrosion potential (shown in Figure 8.3 in addition to the separate corrosion potentials for each sample alone) was in between the corrosion potential values established for the individual samples. The data indicate that the different conditions and pH values at the interfaces do cause a difference in surface potentials to be established. This enhances to a limited extent the relatively low corrosion rate of the galvanized steel sample embedded in a higher cement content, but causes a substantial decrease of the much higher corrosion rate of the sample in the lower cement content. The net effect is to have a combined corrosion rate that is, in fact, intermediate between the corrosion rates of either sample independently.

Figure 8.4 shows the corrosion rate of the concentration cell between samples at 1% and 8% cement content. This gave an average corrosion rate value of 0.012 mm/year compared with a value of 0.008 mm/year measured with the sample containing 8% cement alone, and with a value of 0.02 mm/year of the sample containing 1% cement alone. Figure 8.5 gives the respective corrosion potentials, which again show that a potential difference is established between samples at different cement contents. As before, this contributes to an slight increase in the corrosion rate of the sample at higher cement content (and lower independent corrosion rate), representing a decrease in the corrosion rate relative to the sample at lower cement content (and higher initial corrosion rate).

8.3.3 Galvanized Specimens, with Chlorides

In order to check whether the same overall behavior would also be true in the presence of significant concentrations of anions, similar measurements were made for samples in contaminated electrolyte (simulated with 4% NaCl solution).

Figure 8.6 shows the corrosion rate of the cell established between samples of 0% and 13% cement content, which indicated an average corrosion rate value of 0.15 mm/year. This compared with a value of 0.07 mm/year measured for the sample which contained 13% cement and with a value of 0.5 mm/year for the sample which contained 0% cement. As shown in Figure 8.7, this can be explained by the potential difference established between the two environments, which increases the corrosion rate of one sample at the expense of the other. In all the experiments, the corrosion potential of the sample containing higher cement content shifted in the cathodic direction when short circuited with the sample containing lower cement content. The more negative potential at the interface enhanced the reduction of oxygen in this sample and, consequently, increased the rate of the anodic reaction (which in this case is zinc dissolution), while the reverse effect occurred with the other sample.

In Figure 8.8, the corrosion rate of the cell set up between samples at 1% and 8% cement is shown. This was estimated to result in an average corrosion rate of 0.16 mm/year, which was again intermediate between the value of 0.1 mm/year for the sample at 8% cement content, and the much higher value of 0.5 mm/year for the sample at only 1% cement content. Figure 8.9 shows the corrosion potentials for this situation, which display the same pattern as before.

8.4 CONCLUSIONS

In all tested samples, some kind of potential difference was indeed measured between different contents of cement in the mixture. Non-homogeneity of the cement content in the samples did cause a higher rate of corrosion to be observed than in some of the homogeneous samples, but less than others. This phenomena can be explained in terms of the corrosion potential of the sample containing more cement, which shifts in the cathodic (negative) direction when short circuited with the sample containing less cement. More negative potential at the interface enhances the reduction of oxygen and, consequently, increases the rate of the anodic reaction which, in this case, is zinc dissolution.

However, the general conclusion of this portion of the test program was that this effect was not significant. While a differential corrosion potential between regions at different cement concentrations could be measured, the net effect appeared simply to be that the resulting corrosion rates of galvanized steel specimens were intermediate between the corrosion rates for each cement content individually. While there was a certain amount of acceleration of corrosion for the specimen that had been corroding more slowly, the corrosion rate was less than that for the specimen that had otherwise been corroding more rapidly. The effect, although measurable, was not going to make a difference to the overall conclusions of the project since other factors clearly had a much greater effect on the overall behavior. As before, the presence of ionic contamination had by far the greatest effect, giving rise to greatly accelerated corrosion rate values.

At the same time, it is probably wise to discourage excessive variability in the backfill properties, as there is no doubt that major variations are, in general, undesirable. This would include not only cement contents (which undoubtedly did vary within the construction), but also compactive effort, particularily close to the face. It was noticeable in the course of the fieldwork that the intact strength of field samples close to the facing units was low. This was initially attributed to sub-standard cement content, but subsequent tests showed this not to be the case. Consequently, compaction densities close to the wall face were almost certainly low (as is the natural tendency of reinforced earth contractors), and this probably exacerbated the corrosion environment at the wall face by allowing easier penetration of surface water and atmospheric oxygen. It might be desirable to find some way of encouraging more effective compaction close to facing units in the future.

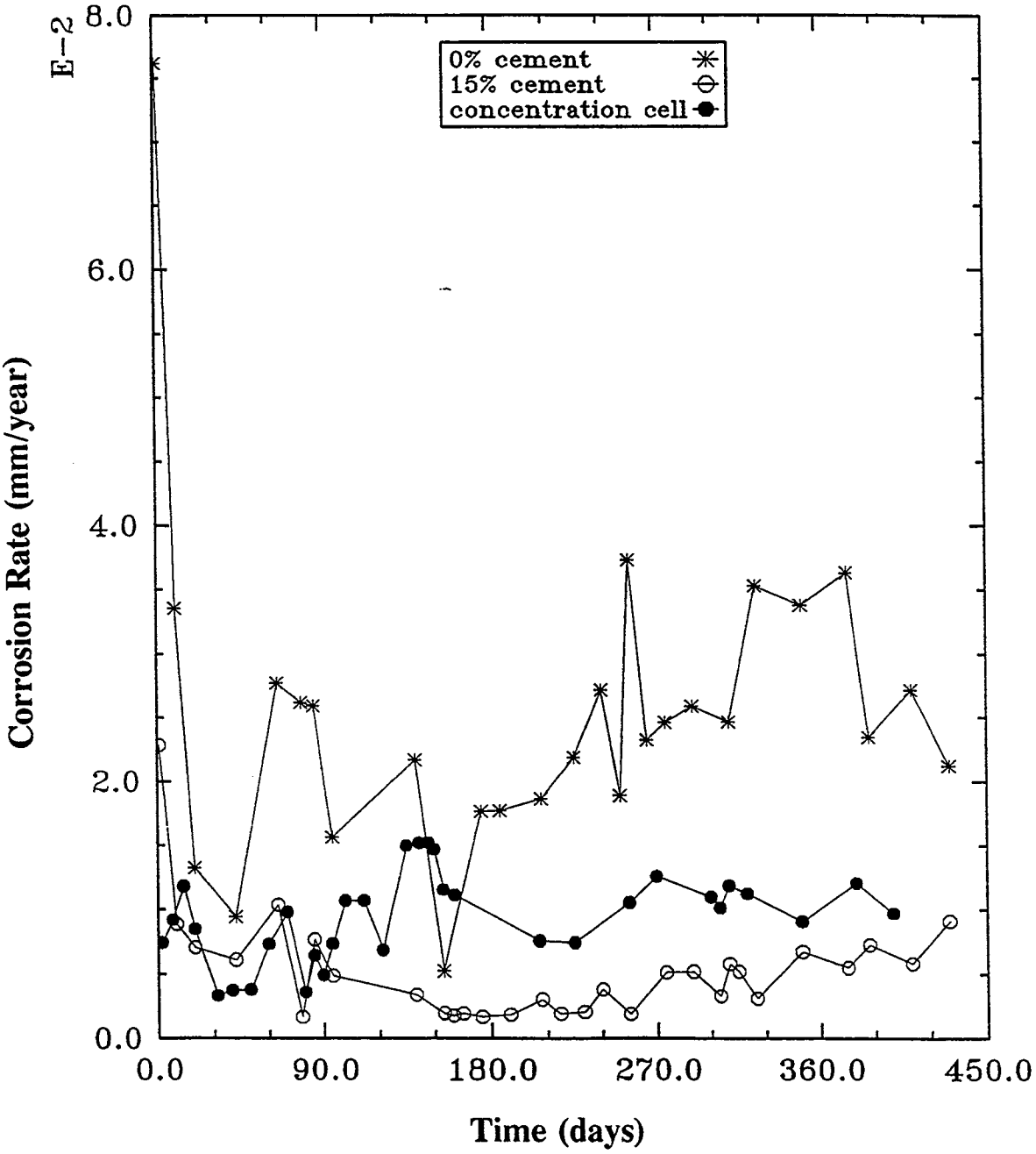

Concentration cell Corrosion Rate vs Time of cement stabilized sand samples in water.

Fig. 8.1 - Concentration Cell Rates, 0 to 15% Cement (Galvanized, Natural pH)

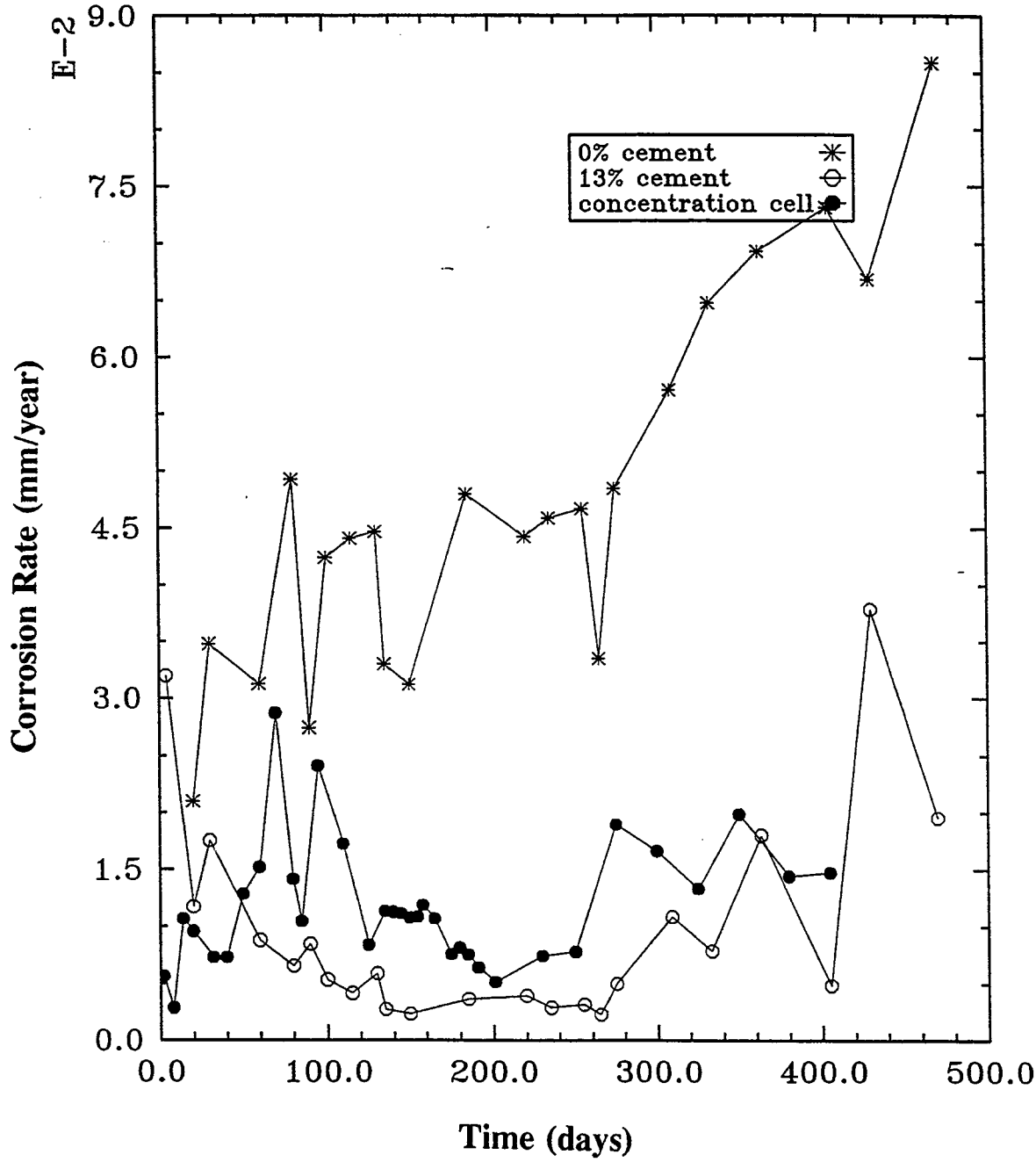

Concentration cell Corrosion Rate vs Time for crushed concrete samples in water.

Fig. 8.2 - Concentration Cell Rates, 0 to 13% Cement (Galvanized, Natural pH)

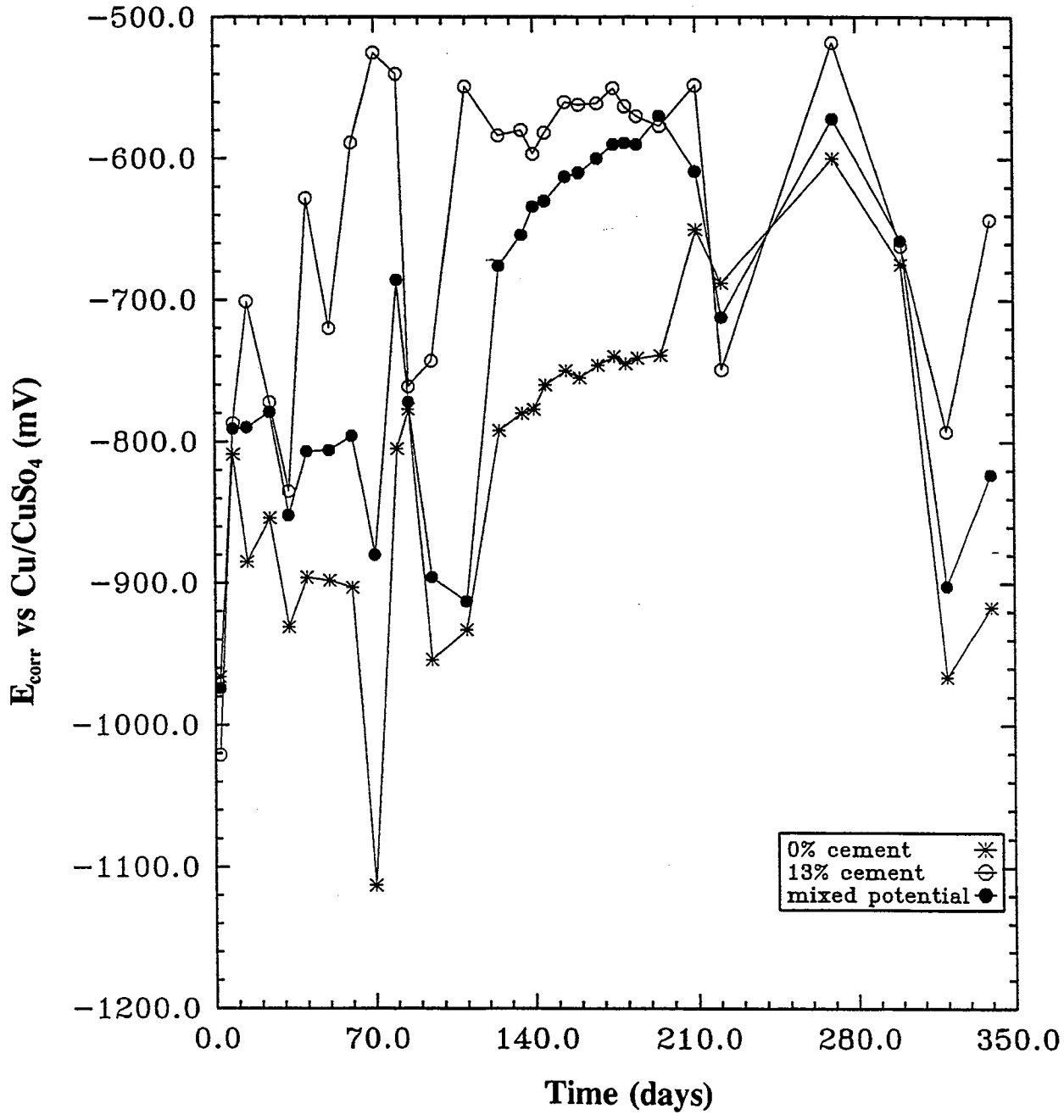

Concentration cell E_{corr} vs Time for crushed concrete samples in water.

Fig. 8.3 - Concentration Cell Potentials, 0 to 13% Cement (Galvanized, Natural pH)

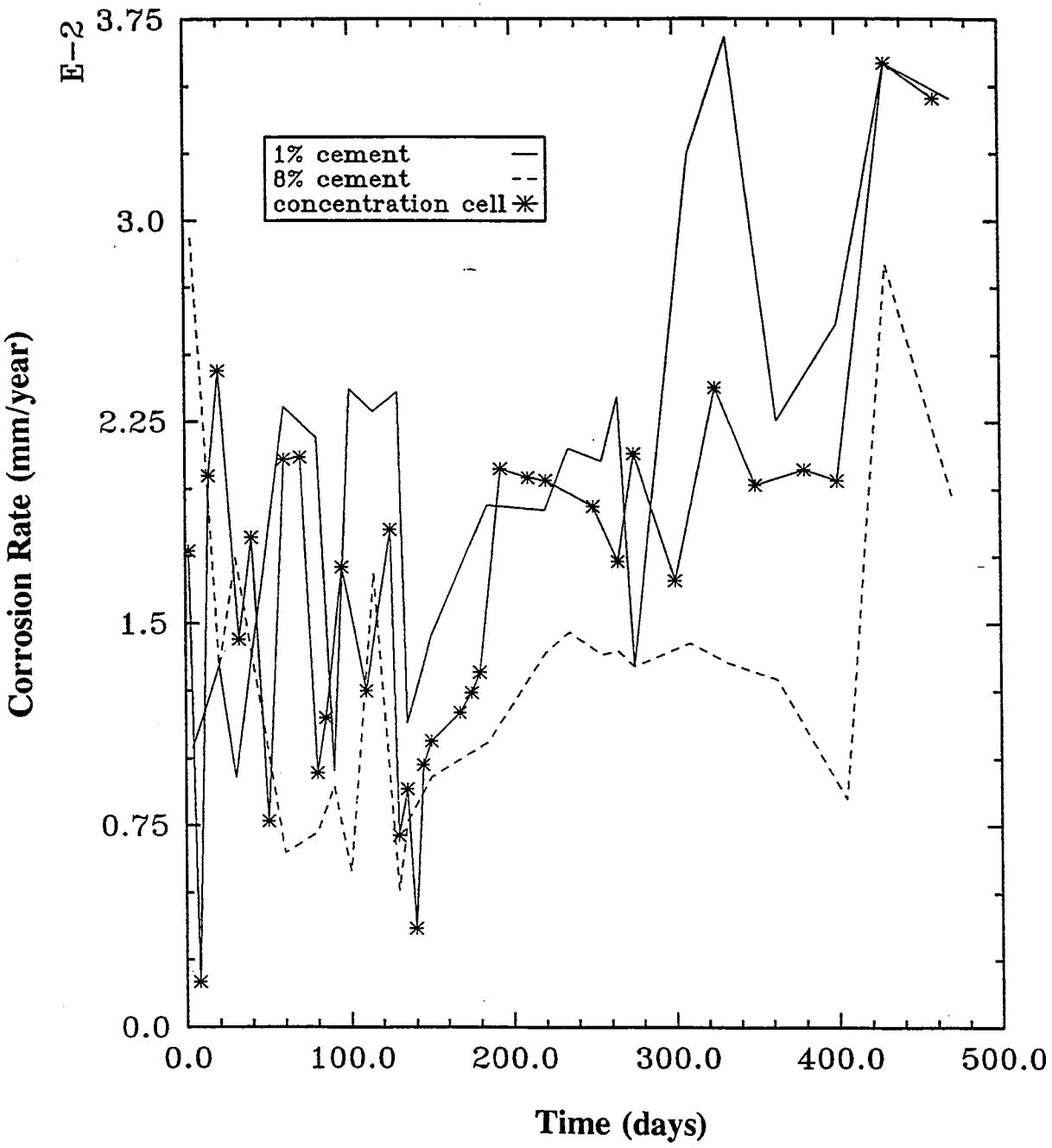

Concentration cell Corrosion Rate vs Time of crushed concrete samples in water.

Fig. 8.4 - Concentration Cell Rates, 1 to 8% Cement (Galvanized, Natural pH)

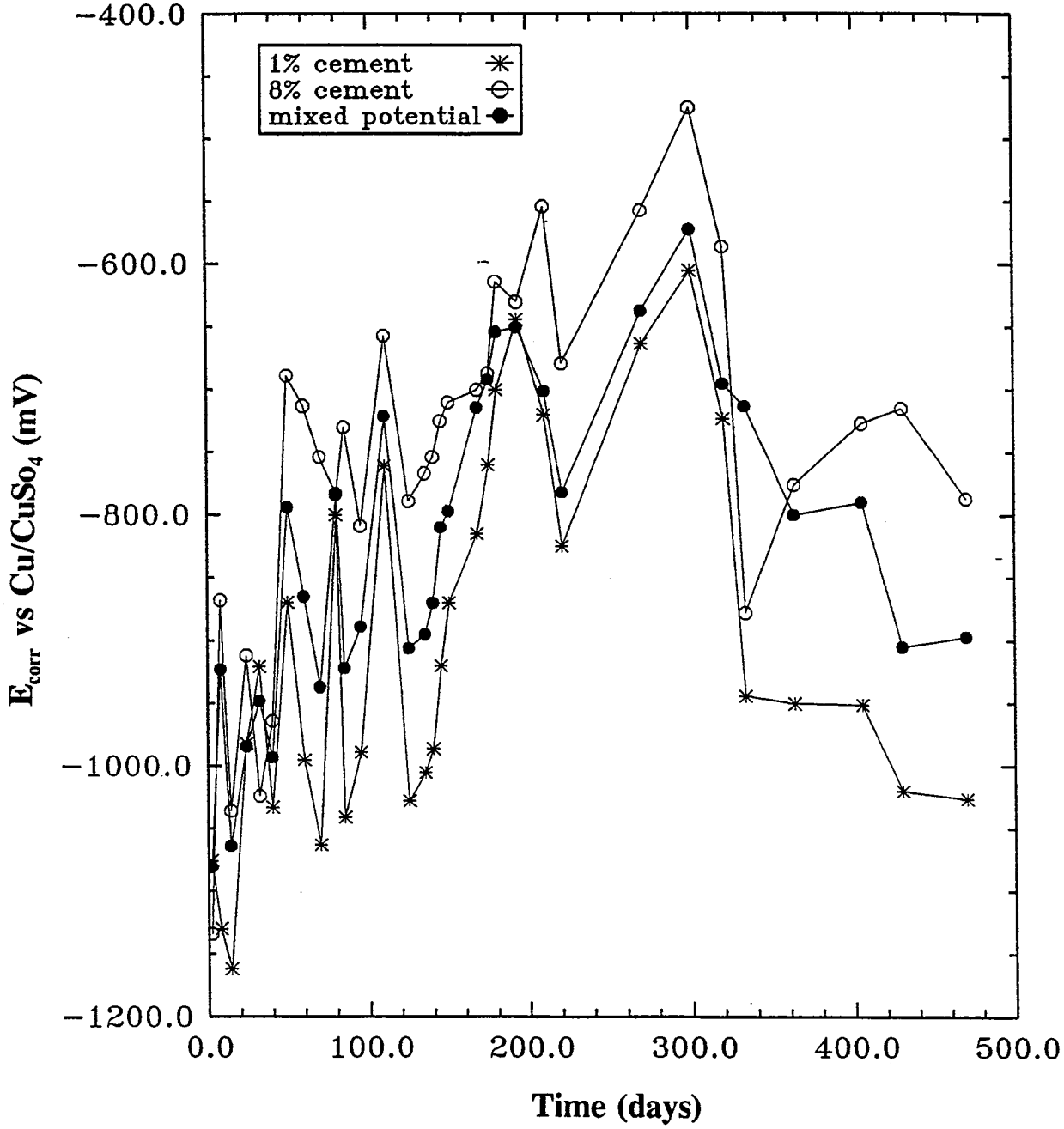

Concentration cell E_{corr} vs Time for crushed concrete samples in water.

Fig. 8.5 - Concentration Cell Potentials, 1 to 8% Cement (Galvanized, Natural pH)

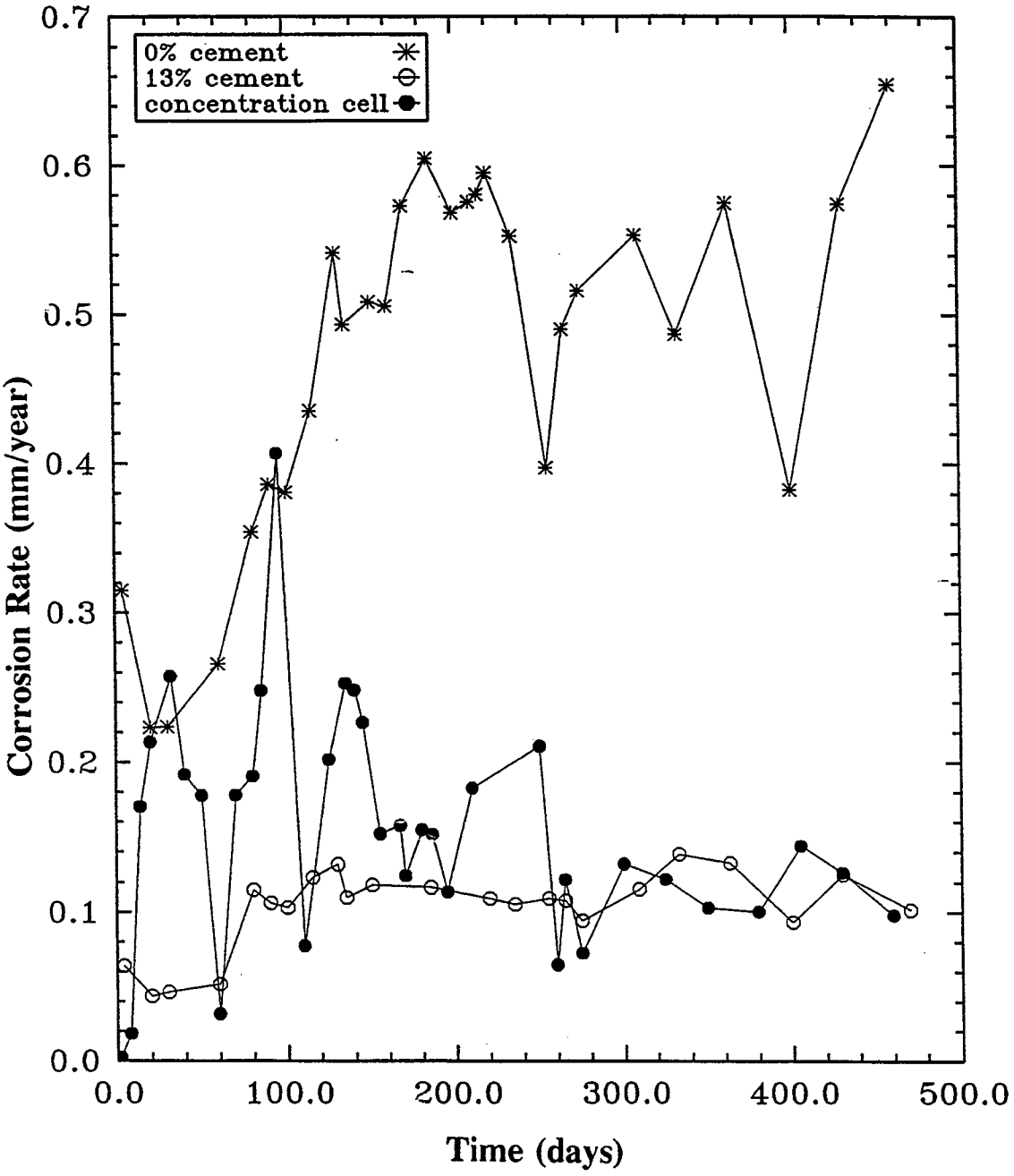

Concentration cell Corrosion Rate vs Time of crushed concrete samples in NaCl solution.

Fig. 8.6 - Rates for 0 to 13% Cement (Galvanized, Natural pH, Chlorides)

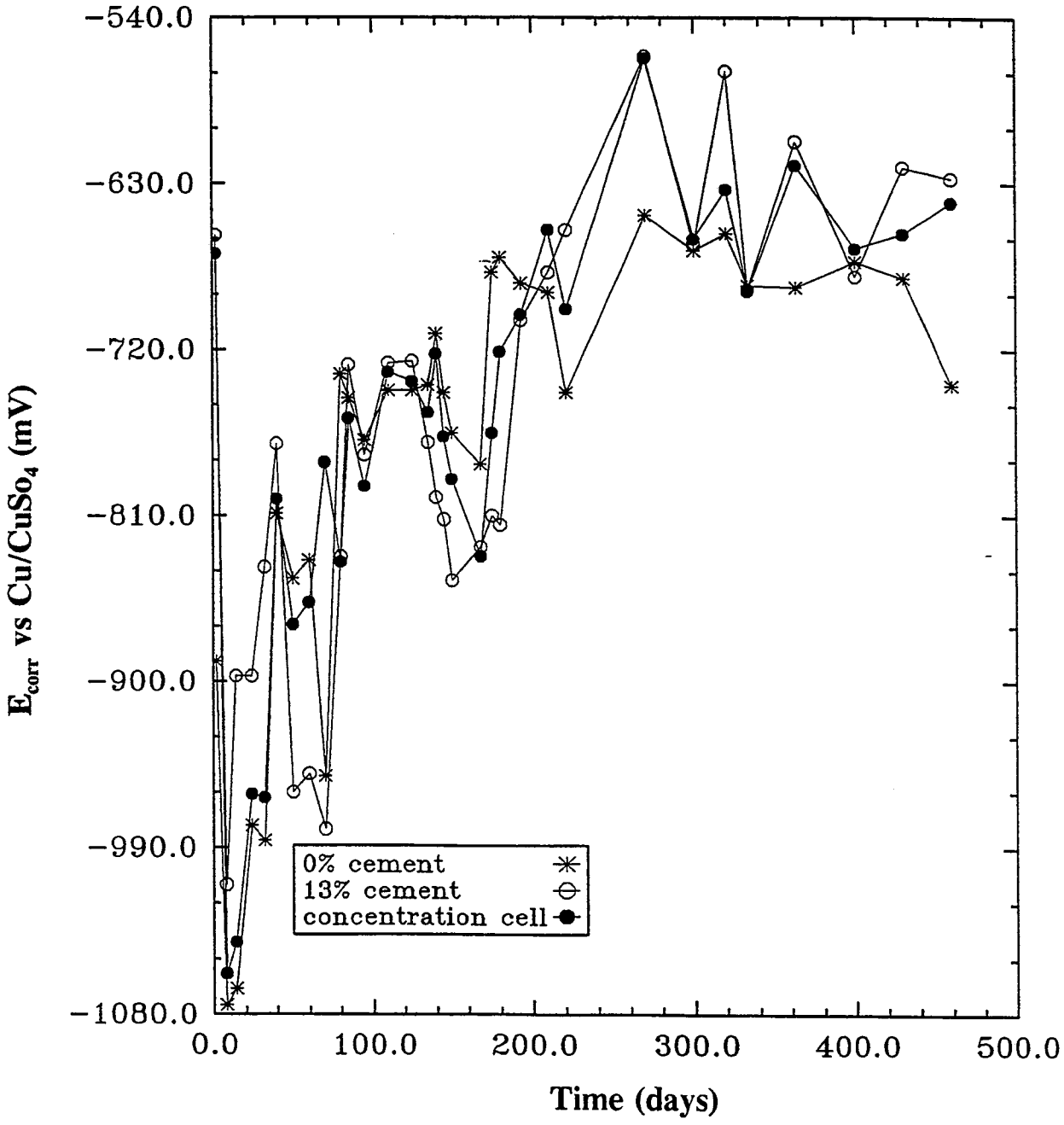

Concentration cell E_{corr} vs Time for crushed concrete samples in 4% NaCl solution.

Fig. 8.7 - Potentials for 0 to 13% Cement (Galvanized, Natural pH, Chloride)

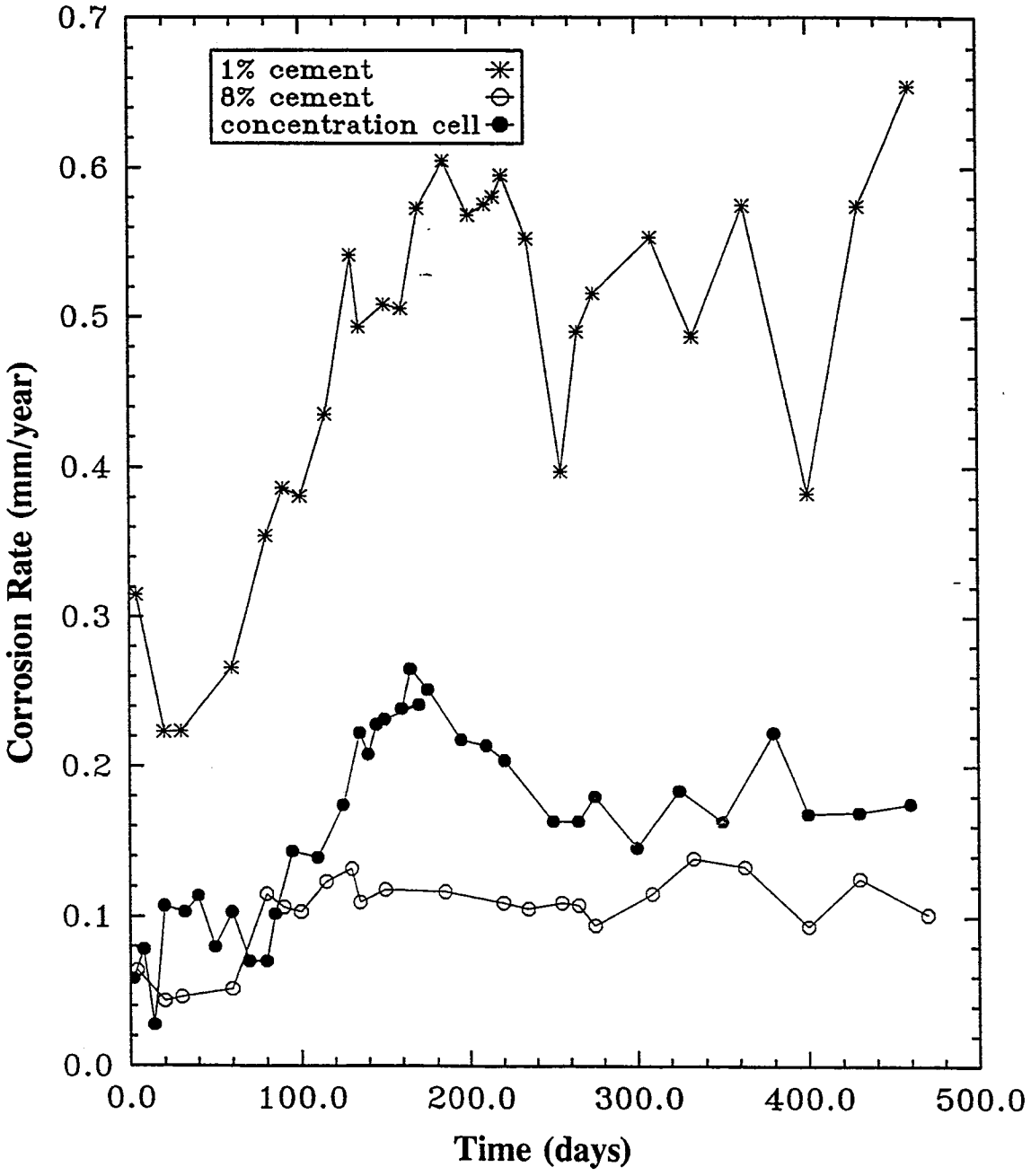

Concentration cell Corrosion Rate vs Time of crushed concrete samples in 4% NaCl solution.

Fig. 8.8 - Rates for 1 to 8% Cement (Galvanized, Natural pH, Chlorides)

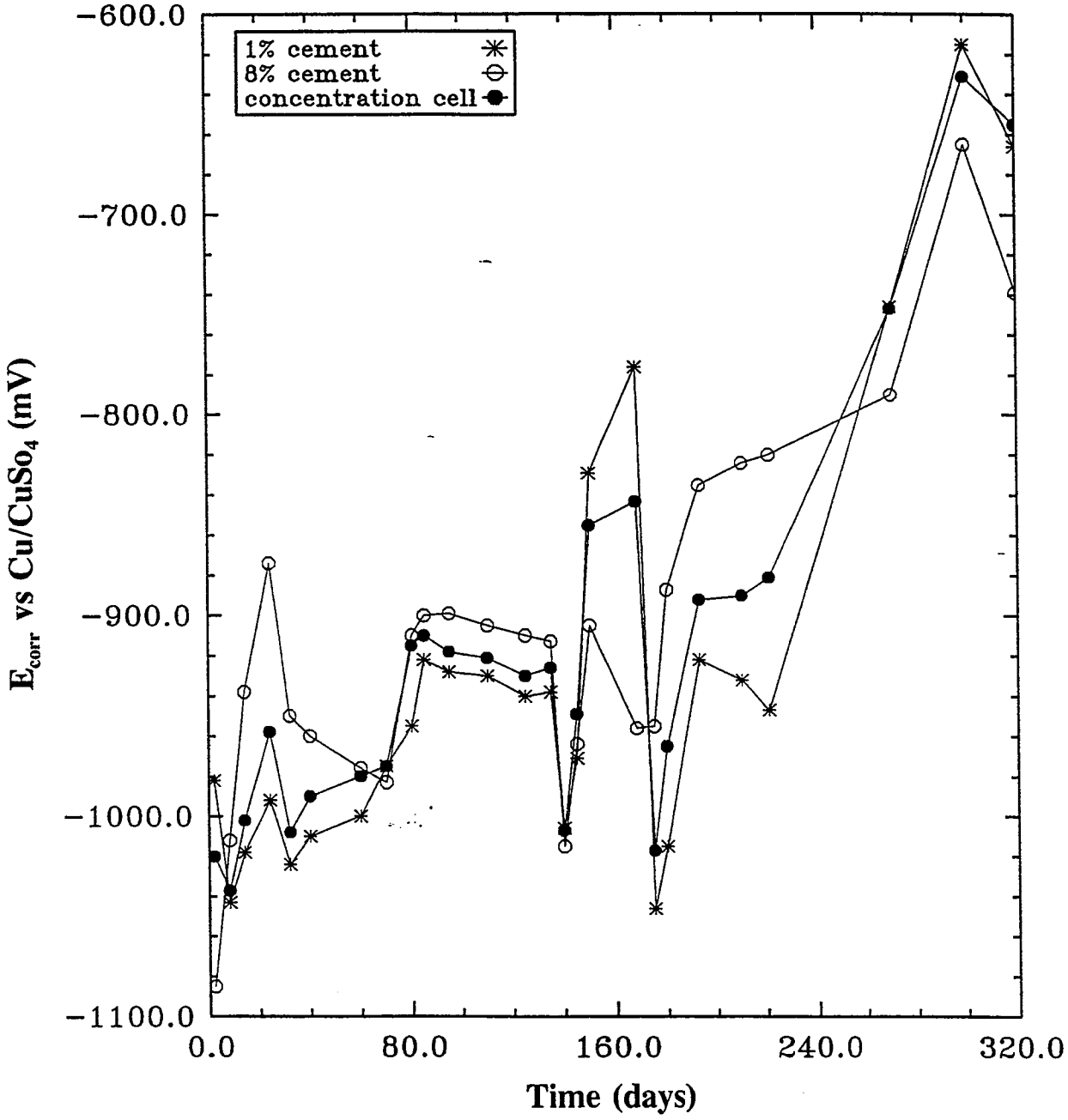

Concentration cell E_{corr} vs Time for crushed concrete samples in 4% NaCl solution.

Fig. 8.9 - Potentials for 1 to 8% Cement (Galvanized, Natural pH, Chlorides)

9. CHEMICAL ANALYSIS IN THE LABORATORY

9.1 GENERAL

During the course of the project, it became clear that the addition of cement alone could not realistically be blamed for the accelerated corrosion at the Deer Park retaining wall site. Attention then shifted to the possibility of unusual chemical constituents being present in the backfill. There had been some limited indication of this from the marginal resistivity results outlined in Chapter 4, although the resistivities measured were not in themselves unacceptable.

Chemical contamination is known to be one of the major contributors to corrosion in normal reinforcing steel. Even for galvanized steel, the immunity of the zinc coating can be destroyed by ions from external sources which can penetrate through the passive film and promote active corrosion, resulting eventually in severe structural damage. Other environmental agents are also known to disrupt normal chemical conditions, such as carbonation. Even in the protective presence of neat concrete, CO_2 from the atmosphere can cause a reduction in the pH to the extent that a passive oxide film is no longer stable and decomposes. Consequently, an increase in the corrosion rate of steel is observed. Along with condensation of water vapors, varying amounts of salts can also precipitate, resulting in additional mineralization not only from atmospheric fallout, but also from dew and fog. In industrial districts, active gases, such as SO_2, Cl_2, and H_2S can also increase the atmospheric corrosion rate (Tuuti, 1982).

Therefore, some initial surface chemistry tests were conducted on samples, to determine if there was anything anomalous. These used Electron Dispersion Spectroscopy (EDS) which permitted the chemical conditions on the surface of the fill particles to be measured, rather than the more general weighted value of chemical concentration given by conventional inorganic analysis on ground-up particles. It was initially supposed that common salt (chlorides) might be responsible for the accelerated corrosion, as this is the usual contaminant (Hutchison and Olson, 1967; Prior and Berthouex, 1967). In fact, initial analysis indicated that relatively low levels of chlorides were present (at least below usual problem levels). However, significant concentrations of sulfur ions (probably as sulfates) were initially measured, EDS measurements showing values of the order of 0.05% to 0.15% at the actual particle surfaces. As a result, a rigorous program of chemical testing was then initiated using several test methods, as follows.

9.2 X-RAY FLUORESCENCE ANALYSIS

X-ray fluorescence analysis (XRF) was also used to determine the chemical composition of the samples. A representative sample was ground to a fine powder and subsequently compressed into a pellet. The pellet was irradiated (for a short period of time) with X-rays generated in a high-intensity X-ray tube. The incident X-rays were absorbed by the samples according to Beer's law. Quantitative X-ray fluorescence analysis involves a quantitative comparison of the intensities of each X-ray with those of a standard of the same elemental makeup. Both peak and background intensities near the peak were counted in estimation of peak heights.

X-ray fluorescence analysis is a very sensitive and accurate method of determining trace elements in the ppm range because of the near-zero background. The fundamental results are shown in Figures 9.2 through 9.18, which also give the standard deviation values of RMS and Kf. Figure 9.1 lists the results of the XRF analyses of the various soil samples tested. The main constituents were found to be as follows: SiO_2 [50.67 to 58.6%]; TiO_2 [0.29 to 0.41%]; Al_2O_3 [5.93 to 7.36%]; Fe_2O_3 [1.13 to 2.75%]; MnO [0.022 to 0.031%]; MgO [0.73 to 1.25%]; CaO [10.16 to 15.49%]; Na_2O [0.24 to 0.56%]; K_2O [1.36 to 1.91%]; P_2O_5 [0.062 to 0.120%]; Cl [0.046% (460 ppm) to 2.28% (2288 ppm)]; SO_4^{-2} [0.39 (3912 ppm] to 0.83% (8297 ppm)]; Sr [80 to 135 ppm]; Rb [35 to 49 ppm]; Zn [0 to 63 ppm]; Cu [19 to 22 ppm]; and Ba [218 to 275 ppm].

9.3 SURFACE CHEMICAL PROPERTIES

The surface chemical composition of the samples were measured by using electron dispersion spectrometry (EDS) and the surface morphology by scanning electron microscopy (SEM) using a JEOL JSM-35 scanning electron microscope in conjunction with a Northern TN-200 X-Ray Analysis System on representative samples ground to pass a 0.1 mm sieve.

Typical EDS and SEM micrographs are shown in Figures 9.19 through 9.24, of samples from locations 1, 2, 3, and 6 (corresponding to the labeling system in Chapter 3), followed by additional combined EDS and SEM micrographs of other samples in Figures 9.25 through 9.33. The results of the EDS analyzes are summarized in Table 9.1, which gives a general relative indication of which major elements are present. The method is good at providing an overall picture of the chemical composition without giving precise measurements.

TABLE 9.1 - RELATIVE CHEMICAL COMPOSITION USING EDS

# 1	# 2	# 3	# 5	# 6	keV
O=	O=	O=	0=	O=	0.5
Na					0.95
Mg	Mg	Mg	Mg	Mg	1.25
Al	Al	Al	Al	Al	1.48
Si	Si	Si	Si	Si	1.73
S=	S=	S=	S=	S=	2.3
Cl	Cl		Cl	Cl	2.8
K	K	K	K	K	3.3
Ca	Ca	Ca	Ca	Ca	3.69+4.0
Ti					4.5
Fe	Fe	Fe	Fe	Fe	6.39+7.00

This indicates that the main constituents of the analyzed samples are: oxygen, magnesium, aluminum, silicon, potassium, and calcium. This would largely be expected for cement stabilized soil samples like this, as the main soil minerals will be magnesium and aluminum silicates, together with some calcium oxides and hydroxides from the added cement. Although it was supposed initially that contamination with chlorides might be the reason for the accelerated corrosion, only small amounts of chlorides were detected. However, significant amounts of sulfur ion were discovered in all samples, in the range of 0.05 to 0.15%, [500 ppm to 1500 ppm], and somewhat higher concentrations from locations 3 and 6. It seemed likely, therefore, that it was in fact sulfates, rather than chlorides, that were the problem anion.

These results corresponded, at least qualitatively, with the results of the X-Ray Fluorescence analysis which indicated significant quantities of sulfates present in concentrations of as high as 3912 to 8296 ppm (although these are liable to be something of an over-estimate), together with lesser values of chlorides.

9.4 INORGANIC TITRATION

In order to correlate the values of this wide spectrum chemical testing with more conventional and more widespread techniques, some traditional inorganic wet chemical titration was carried out on samples. This was initially done for chloride concentration according to the usual test standard for chloride contamination in concrete [AASHTO T-260 "Sampling and Testing for Total Chloride Ion in Concrete and Concrete Raw Materials", Test Method T 260-84, AASHTO, Washington, DC (1984)] using potentiometric titration and the standard acid-soluble test method. The acid soluble chloride ions were extracted by grinding the samples to pass a No. 1000 mesh screen and the powders were then boiled in nitric acid. The method involves a potentiometric titration of chloride ions with silver nitrate which is run from a burette in steps, and the potential difference between the silver electrode and the reference electrode recorded after each step. The potential difference between successive steps reaches a maximum at the point of equivalence. Then, ml of 0.02 normal $AgNO_3$ x 14.2 = mg/l or ppm of chloride ion.

The results obtained from this analysis are shown on the left hand side of Table 9.2.

TABLE 9.2 - CONVENTIONAL ANALYSIS OF CHLORIDE CONTENT

Sample	Chloride Content % [ppm] Test method AASHTO T-260	Sample	Chloride Content [ppm] Test method Tex-620-J
IC	0.071 [710]	NW 2-4	[236]
2C	0.095 [950]		
3C	0.090 [900]		
5C	0.103 [1030]		
6C	0.085 [850]	SE 0-2	[626]
3D	0.087 [870]	SW 4-6	[248]
5D	0.096 [960]	NE 0-2	[224]
6D	0.115 [1150]		

In addition, in order to tie all this chemical analysis back to the standards commonly used by TxDOT, wet chemical analysis was carried out according to test method Tex-620-J which requires large samples of soil. In view of the fact that both XRF and EDS had indicated that sulfur (or sulfates) was more prevalent than chlorides, this analysis was performed for both chlorides and sulphates, and the results are shown in Table 9.3.

TABLE 9.3 - CHLORIDE & SULFATE CONTENT ACCORDING TO TEX 620-J

Sample	Chloride Content ppm	Sulfate Content ppm
NW 2'-4'	236	1248
SW 4'-6'	248	1797
SE 0'-2'	626	1523
NE 0'-2'	224	2126

This showed very high sulfate levels, varying from 1248 ppm to 2126 ppm (well above the current maximum allowable value of 200 ppm), and quite high chlorides (224 to 626 ppm - quite a bit above the current maximum allowable value of 100 ppm).

For comparison, the chloride values are also listed in table 9.2, and it can be seen that the results from the TEX test are similar to, but somewhat lower than, the values obtained by the AASHTO method. The EDS, XRF, and wet analyses all indicate significant concentrations of sulfates present, together with smaller amounts of chlorides. Although these were not subject to test at the time the wall was constructed, the concentrations are significantly above the current maximum allowable of 200 ppm and 100 ppm for sulphate and chlorides, respectively, and were presumably at least in part responsible for the marginal resistivity values originally measured during first construction.

9.5 CONCLUSIONS

A suite of chemical analyses have been performed on samples of the backfill from the Deer Park retaining wall, including wide analyses for a range of trace elements in case there was any hitherto undetected contaminant present. The results indicate no especially exotic contaminant present, but a certain amount of chlorides present and (especially) high concentrations of sulfur present in the form of sulphates. This was detected by all the measuring techniques used, and the values as correlated to standard potentiometric wet chemical analyses were significantly above the current maximum allowable of 200 ppm and 100 ppm for sulphate and chlorides, respectively.

Previous laboratory work reported in the earlier chapters has shown that the presence of anions has a major effect on the acceleration of corrosion, and that the accelerated corrosion observed in the field cannot be explained by the presence or addition of cement, as originally thought. It is concluded, therefore, that it is the presence of large amounts of sulfur ions (and to a secondary extent possibly also chlorides) in the fill soil that is the main cause for the observed severe corrosion of the galvanized reinforcement in Deer Park retaining wall.

It is likely that these sulfur ions were originally present in the fill as a contaminant, or alternatively may have resulted from the penetration of sulfur ions from the environment. Acid rains are a possible source of sulfur and sulfate contaminations. In any case, it would appear that the sulfur ion plays the major role in the observed corrosion of the galvanized steel reinforcement in the Deer Park retaining wall and is the prime cause of the accelerated corrosion at this site. In this respect, the project will almost certainly encourage and amplify the recent changes to backfill corrosivity specifications to specifically measure ionic concentrations, rather than just using backflll resistivity as a general overall measure as has been the tendency in the past.

Summary of the XRF analyses of soil samples drilled from Deer Park retaining wall.

	Sample#	1	2	C	D	4	B	5	3	A
	WEIGHT	N.E(2'-3.5')	SW(10'-12')	SN4-6	NE)-2	S.W(u'-6')	NW2-4	N.E(5'-7')	S.E(4'-6')	SE0-2
SiO2	%	58.60	54.28	51.94	53.72	53.91	50.67	58.80	52.39	52.02
TiO2	%	0.29	0.40	0.37	0.29	0.40	0.39	0.30	0.41	0.31
Al2O3	%	5.93	7.33	6.92	6.26	7.48	7.13	6.70	7.36	7.00
Fe2O3	%	2.75	1.98	1.93	1.88	2.02	1.99	1.13	2.64	1.92
MnO	%	0.03	0.03	0.04	0.02	0.04	0.03	0.02	0.03	0.03
MgO	%	0.73	1.18	1.12	0.85	1.25	1.24	0.80	1.21	1.18
CaO	%	10.16	12.79	13.23	12.52	12.93	14.37	10.54	15.49	16.46
Na2O	%	0.48	0.29	0.56	0.20	0.28	0.24	0.34	0.54	0.24
K2O	%	1.61	1.71	1.82	1.36	1.69	1.71	1.62	1.91	1.38
P2O5	%	0.06	0.11	0.11	0.07	0.11	0.12	0.07	0.10	0.10
Sr	ppm	84	101	104	80	104	106	81	118	135
Rb	ppm	35	44	45	35	45	45	39	49	47
Zn	ppm	58	56	54	63	55	55	53	25	0
Cu	ppm	22	19	19	18	17	15	14	17	9
Ba	ppm	227	275	278	218	258	244	262	251	252
Cl	ppm	9470	511	22883	16941	456	12119	540	12633	472
S	ppm	7796	4485	8297	6923	4387	4163	5562	6776	3912
SUM	%	82.40	80.66	81.20	79.61	80.65	79.57	80.98	84.05	81.11

Fig. 9.1 - Summary of X-Ray Fluorescence Analysis

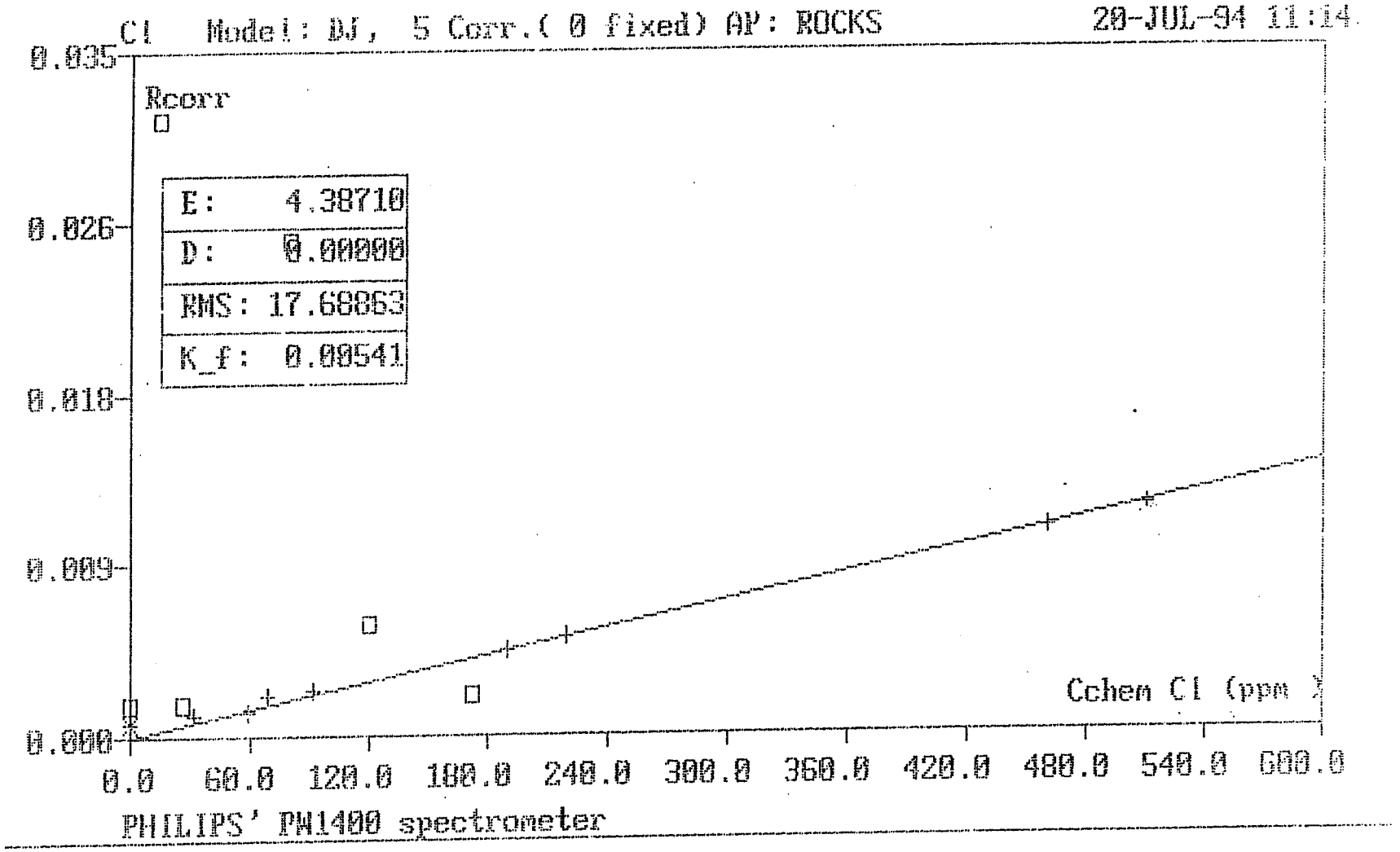

Fig. 9.2 - XRF Standardization Curves for Cl

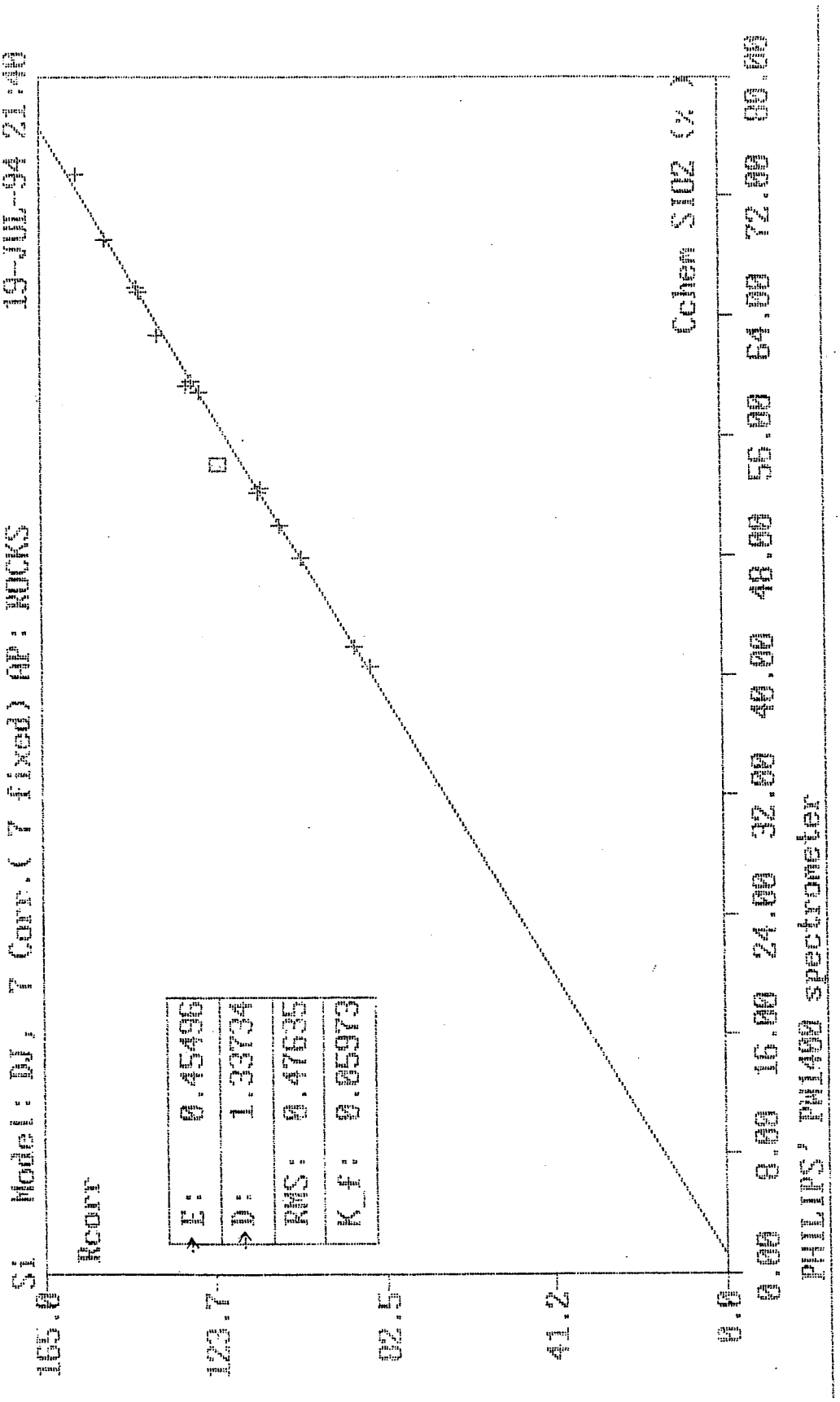

Fig. 9.3 - XRF Standardization Curves for SiO_2

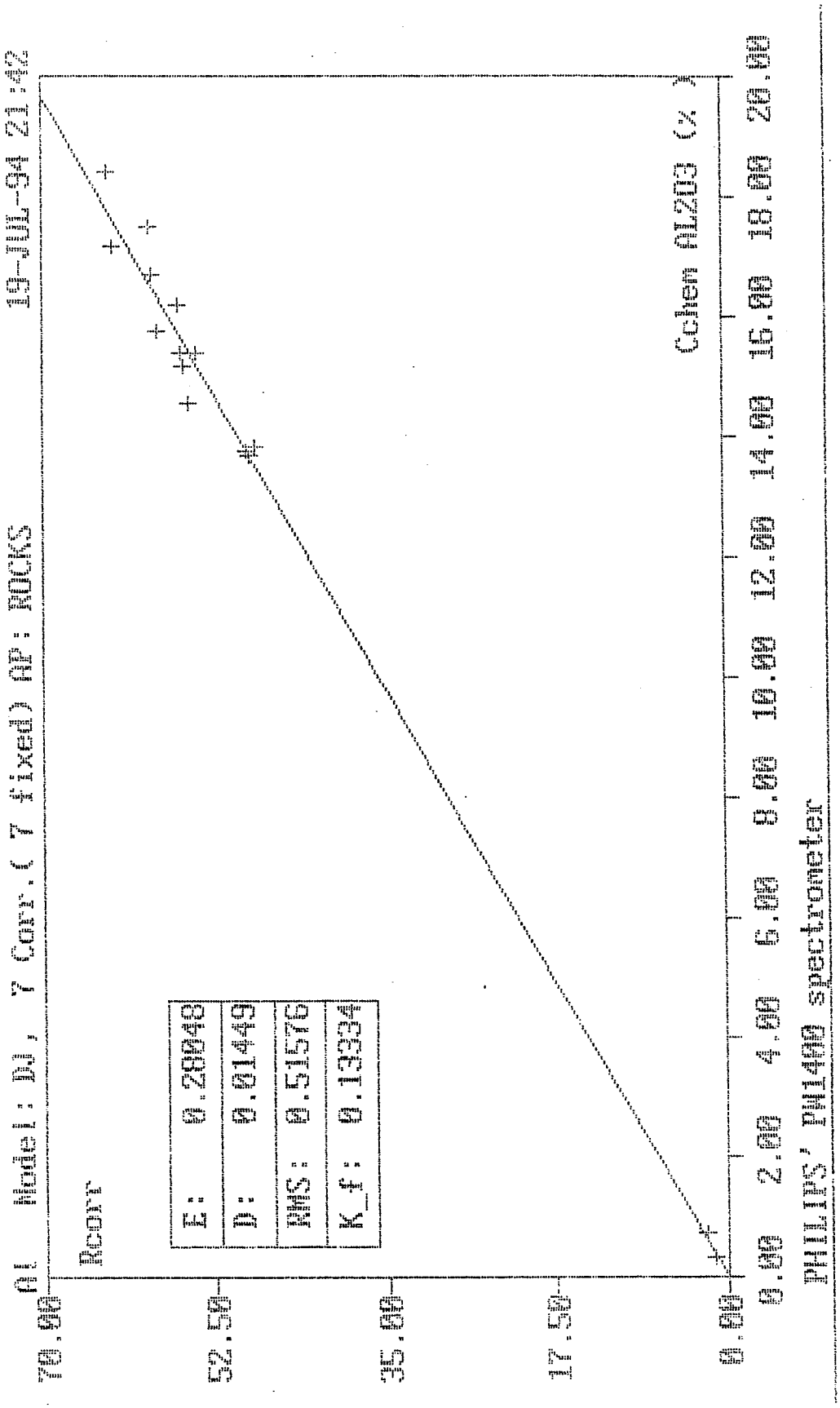

Fig. 9.4 - XRF Standardization Curves for Al_2O_3

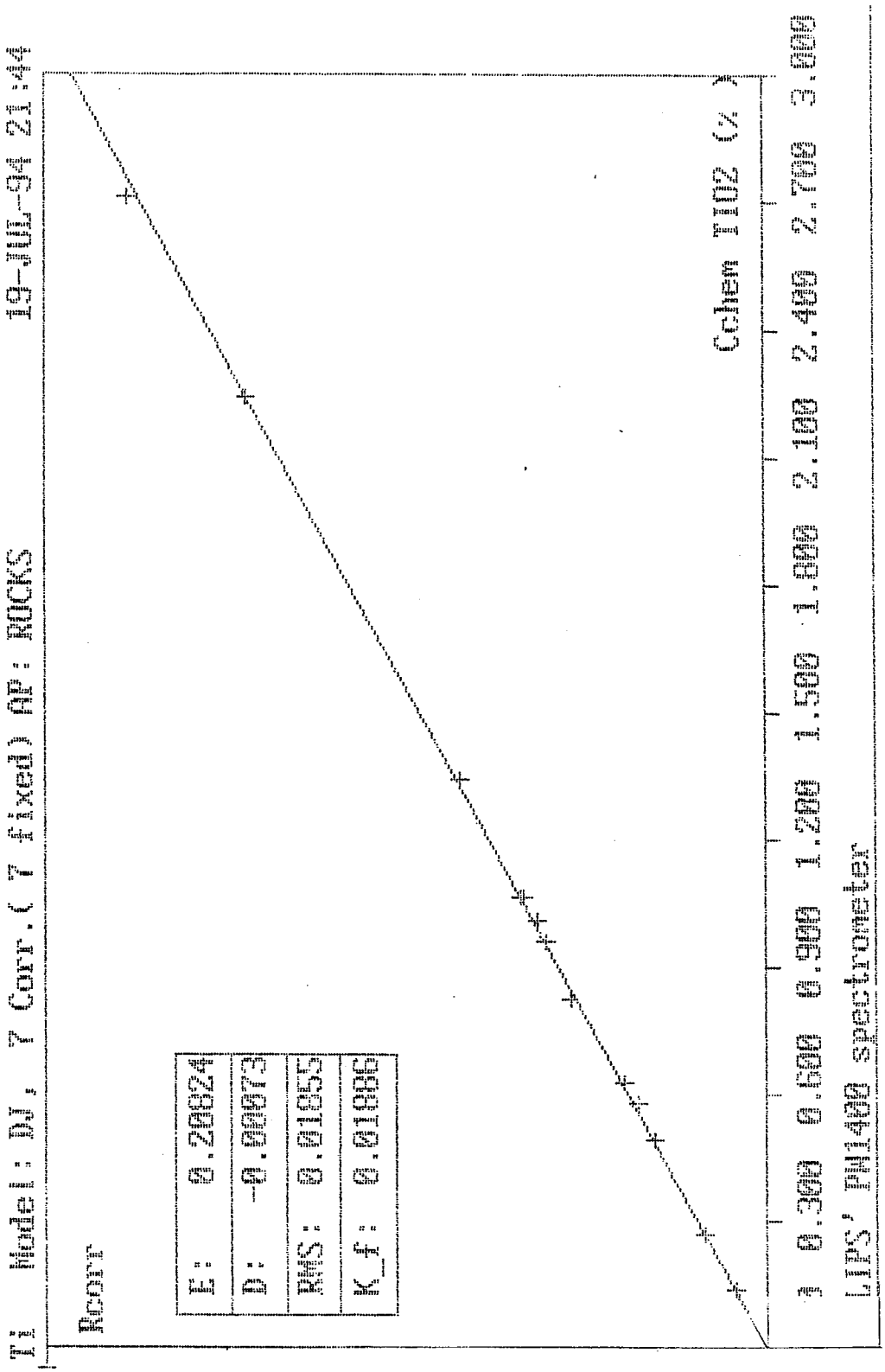

Fig. 9.5 - XRF Standardization Curves for TiO_2

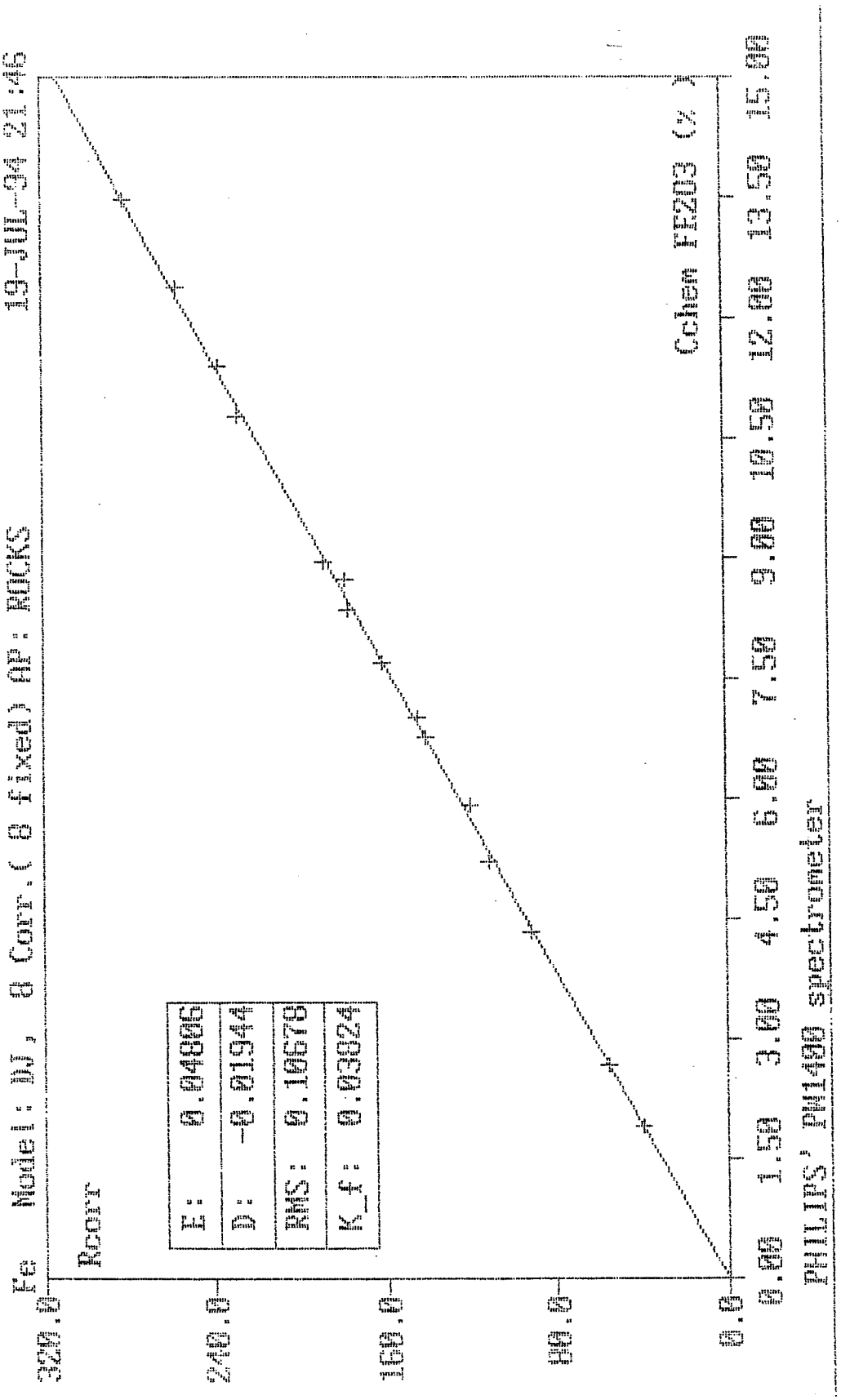

Fig. 9.6 - XRF Standardization Curves for Fe_2O_3

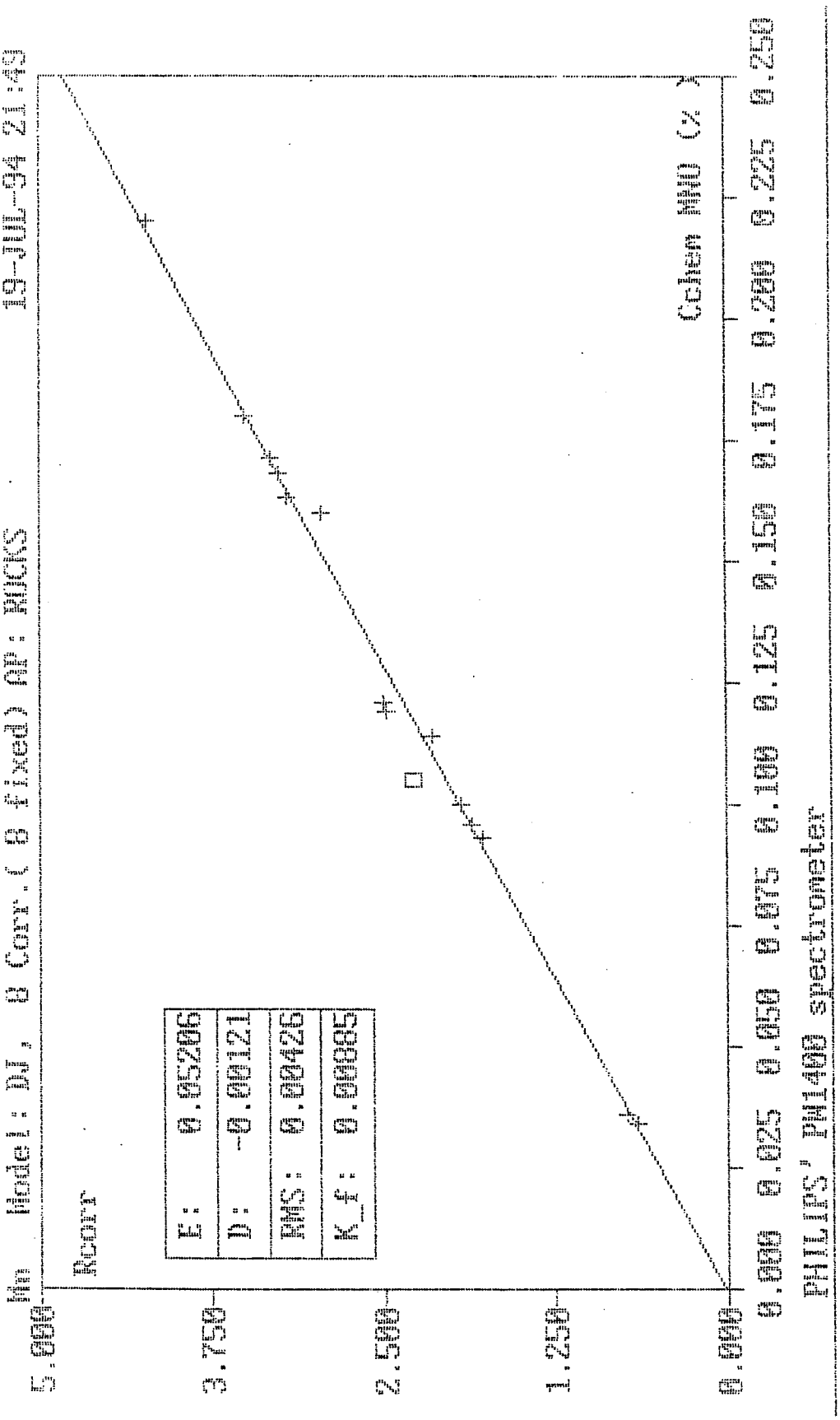

Fig. 9.7 - XRF Standardization Curves for MnO

Fig. 9.8 - XRF Standardization Curves for MgO

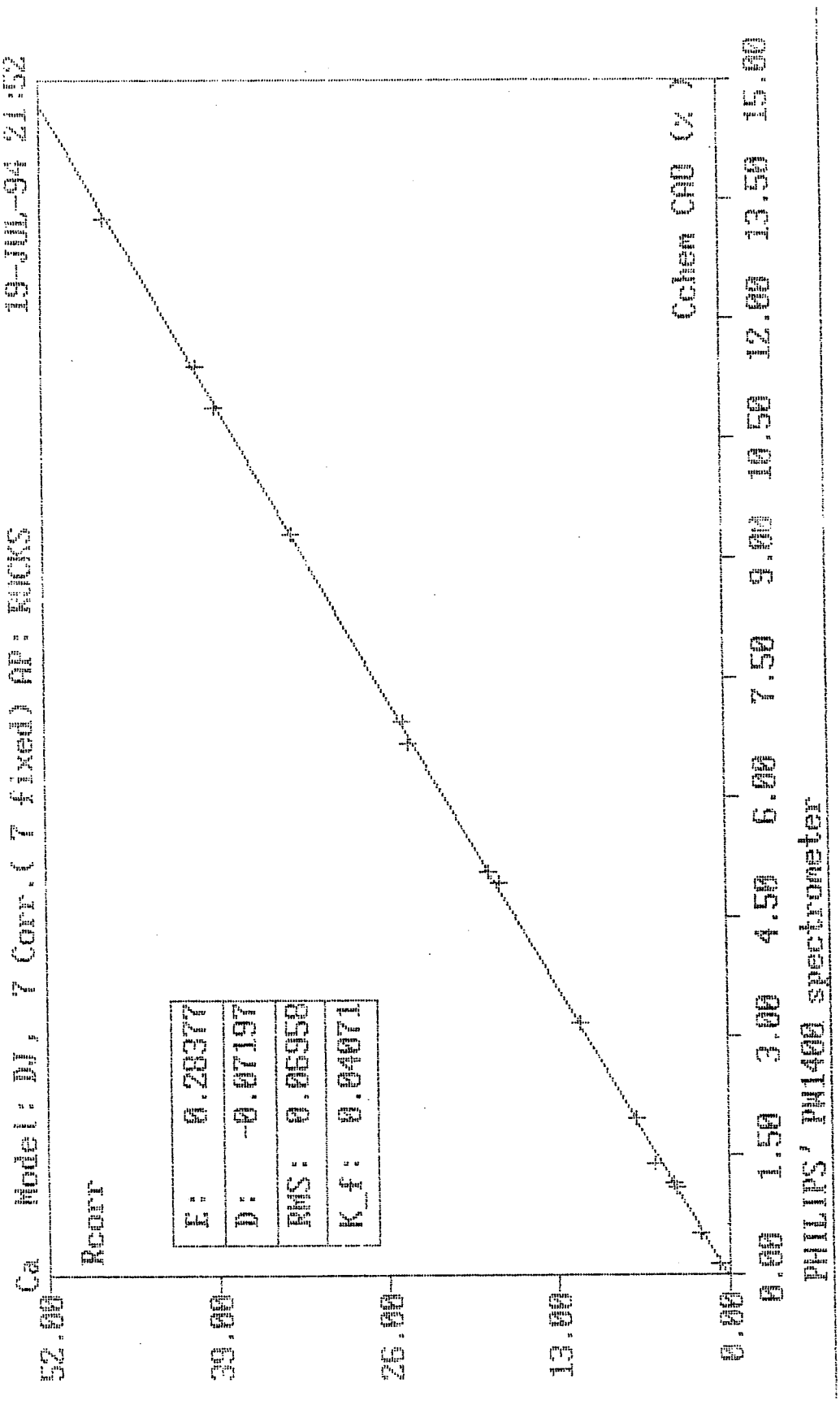

Fig. 9.9 - XRF Standardization Curves for CaO

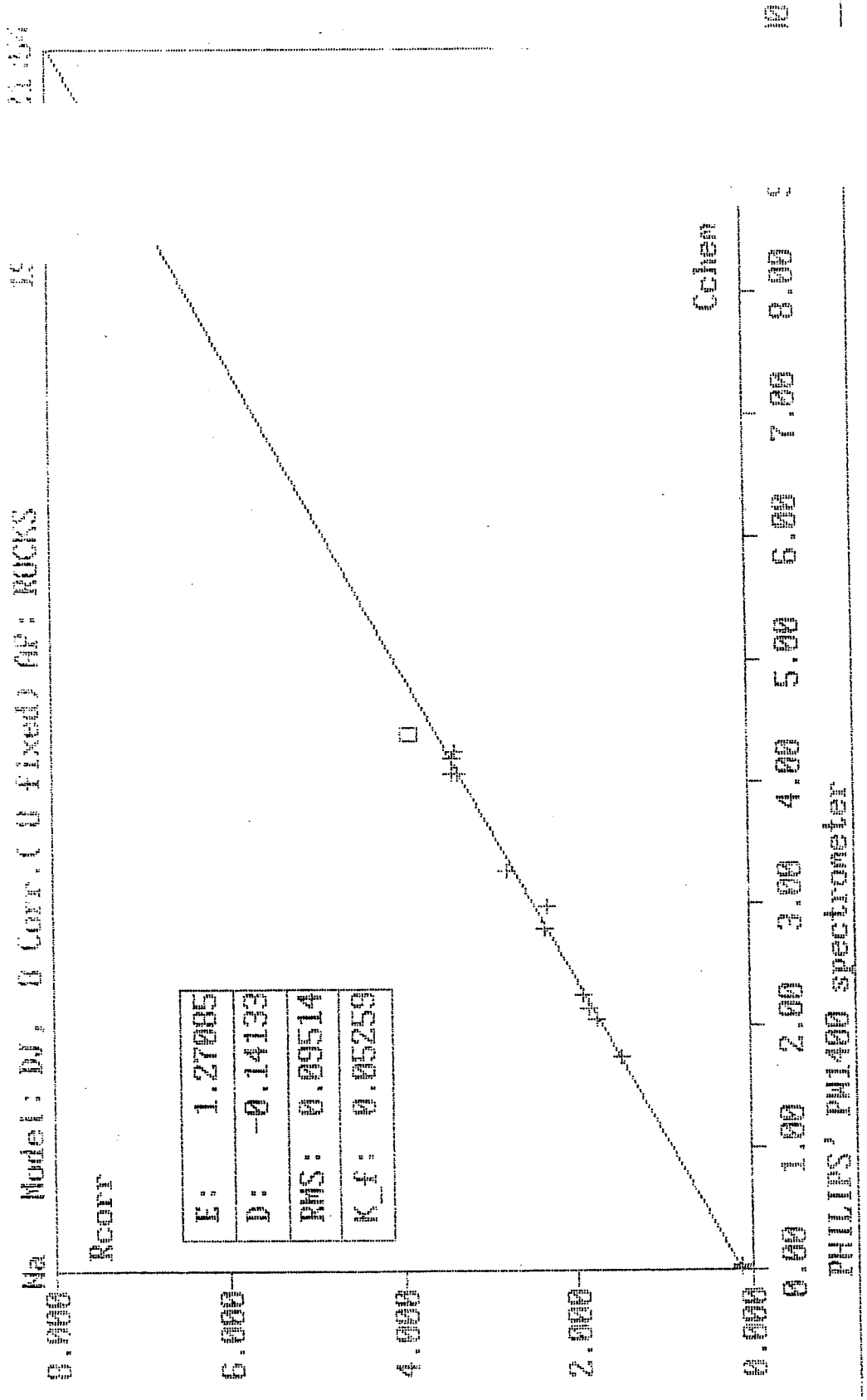

Fig. 9.10 - XRF Standardization Curves for Na_2O

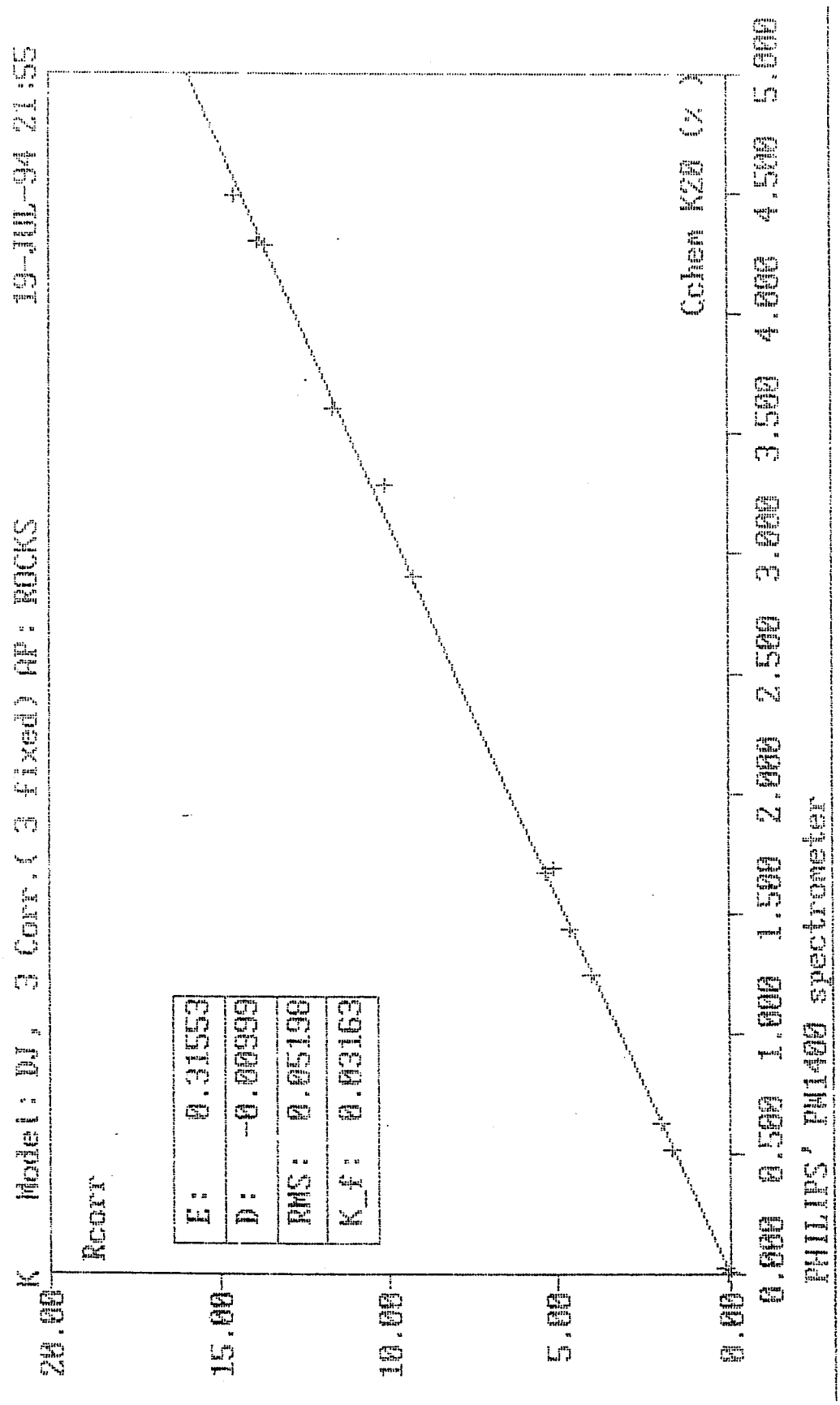

Fig. 9.11 - XRF Standardization Curves for K_2O

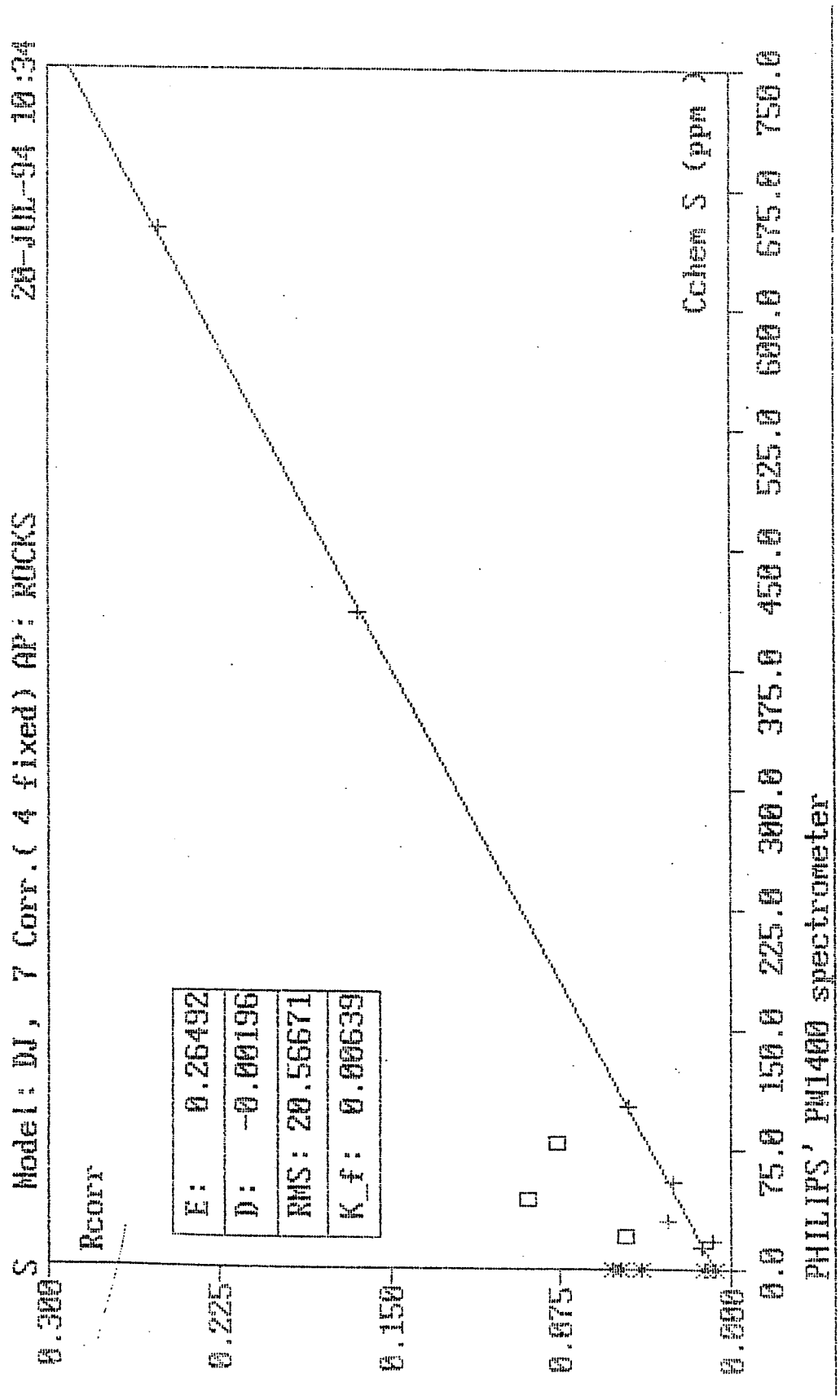

Fig. 9.12 - XRF Standardization Curves for S

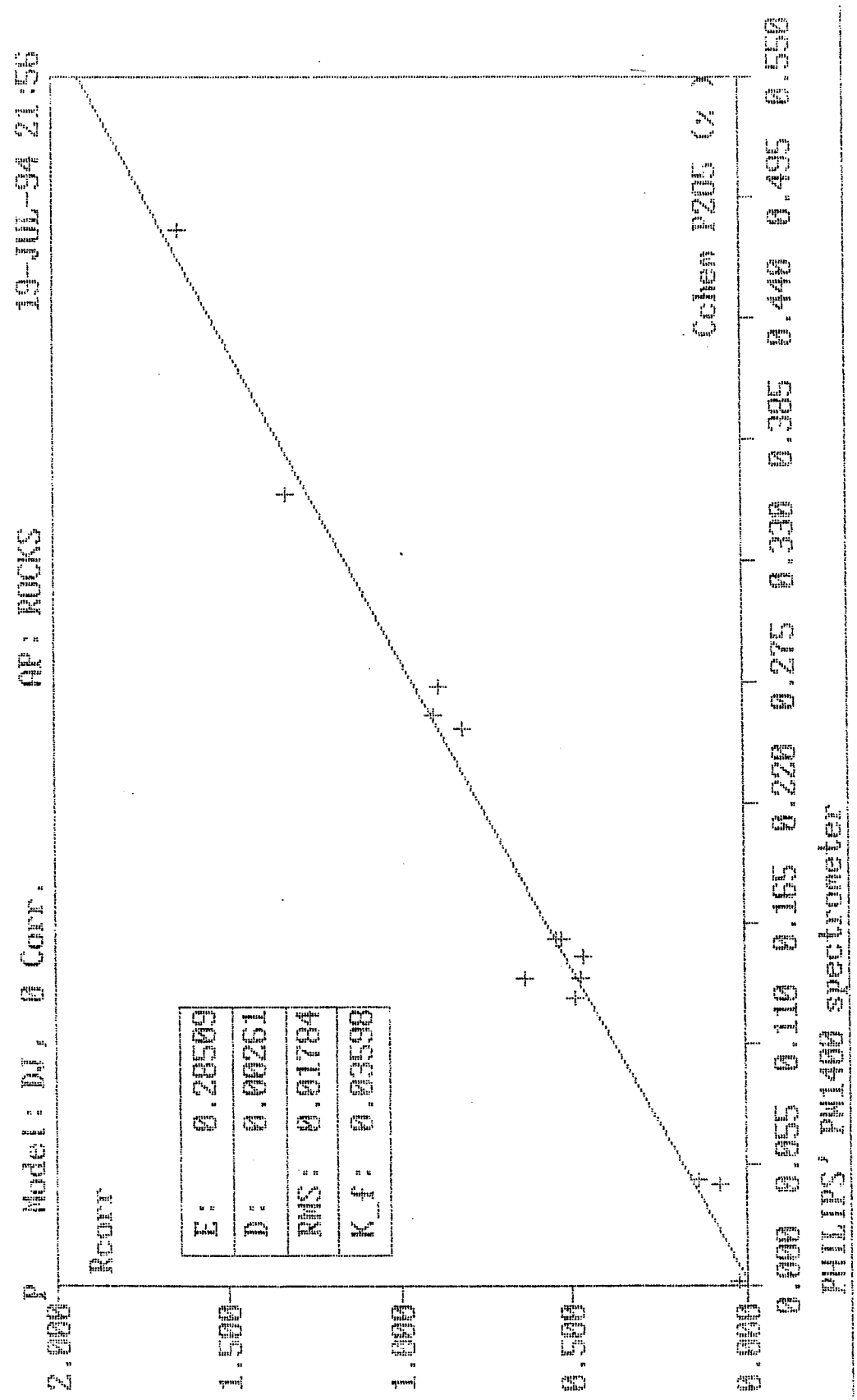

Fig. 9.13 - XRF Standardization Curves for P_2O_5

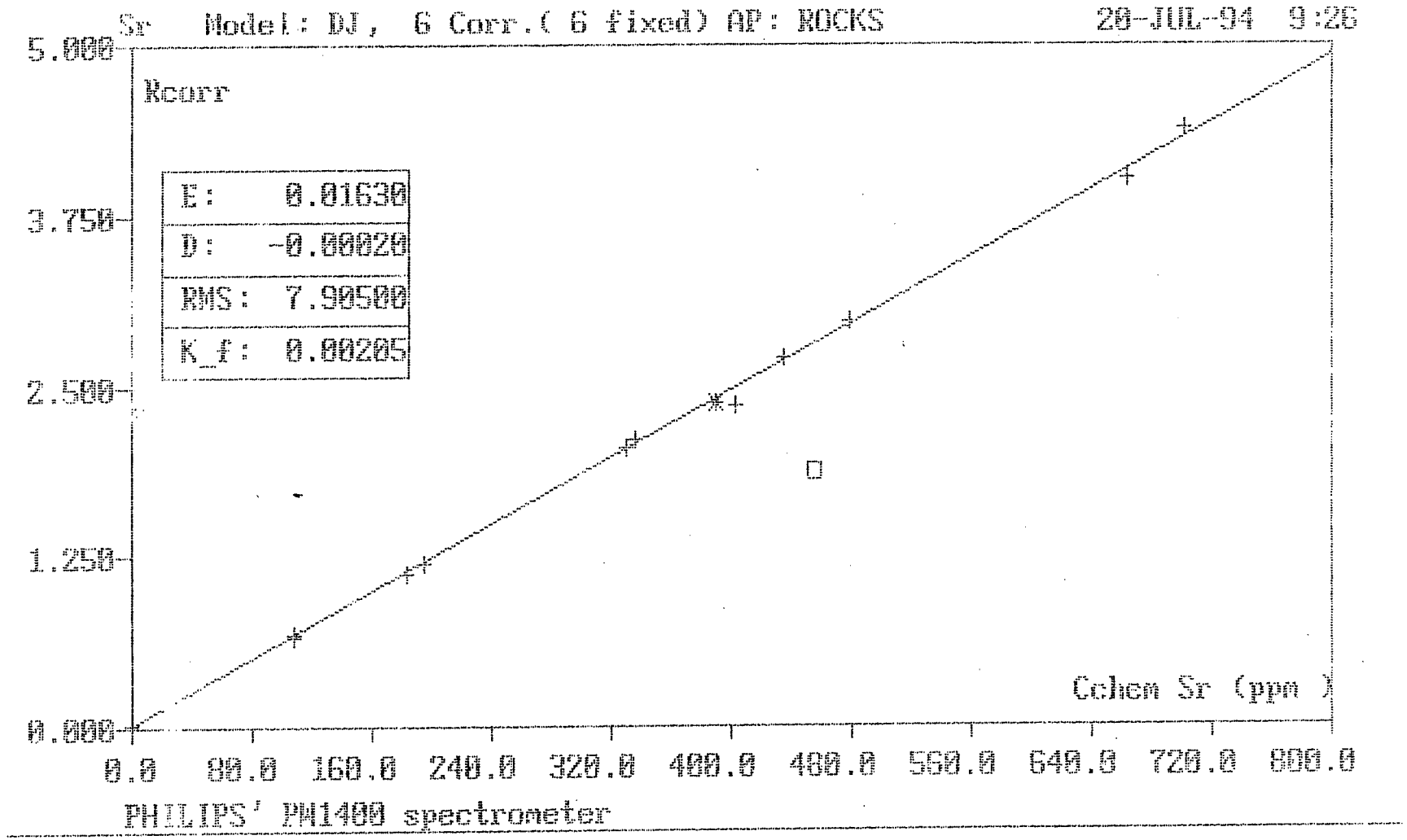

Fig. 9.14 - XRF Standardization Curves for Sr

Fig. 9.15 - XRF Standardization Curves for Rb

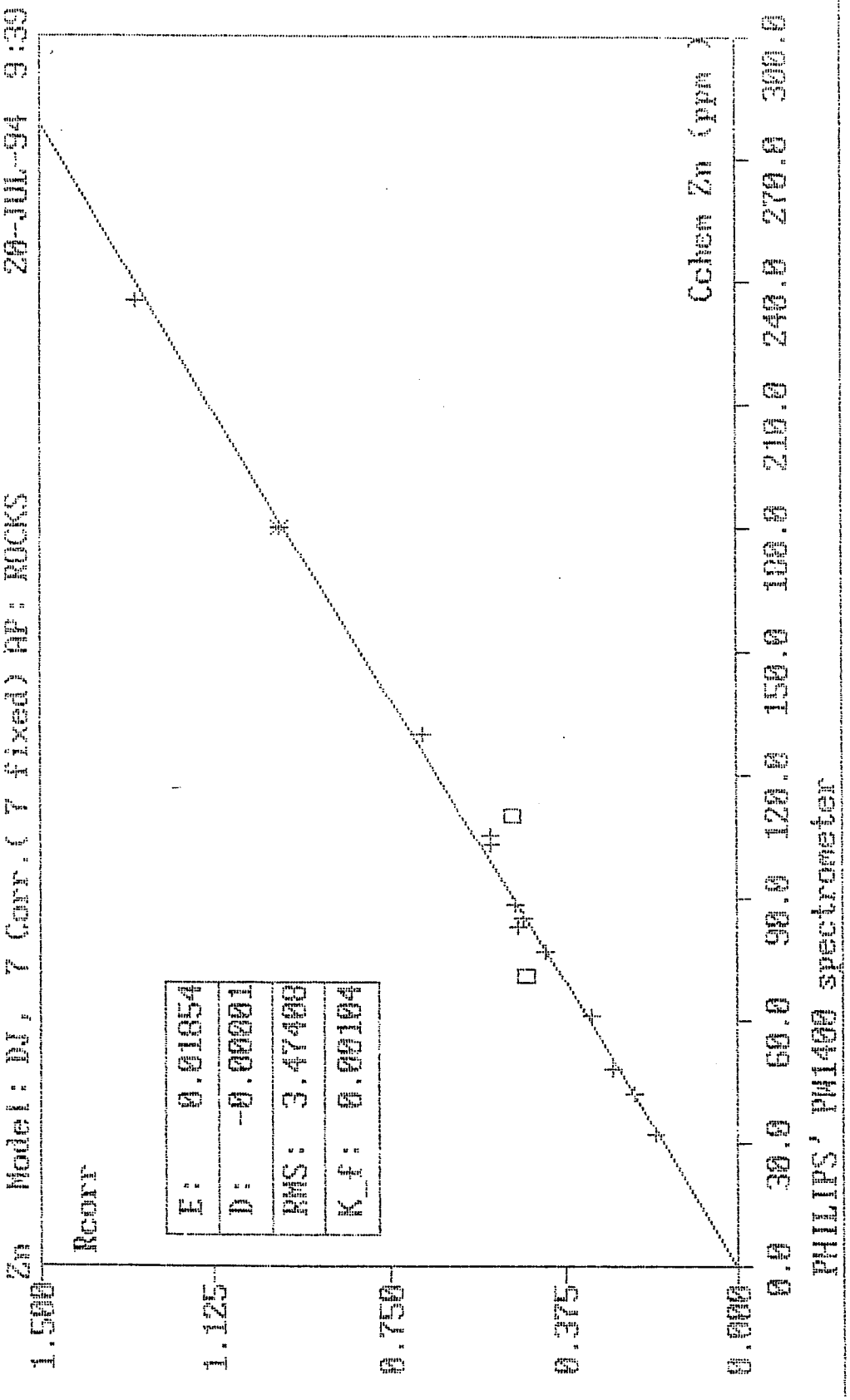

Fig. 9.16 - XRF Standardization Curves for Zn

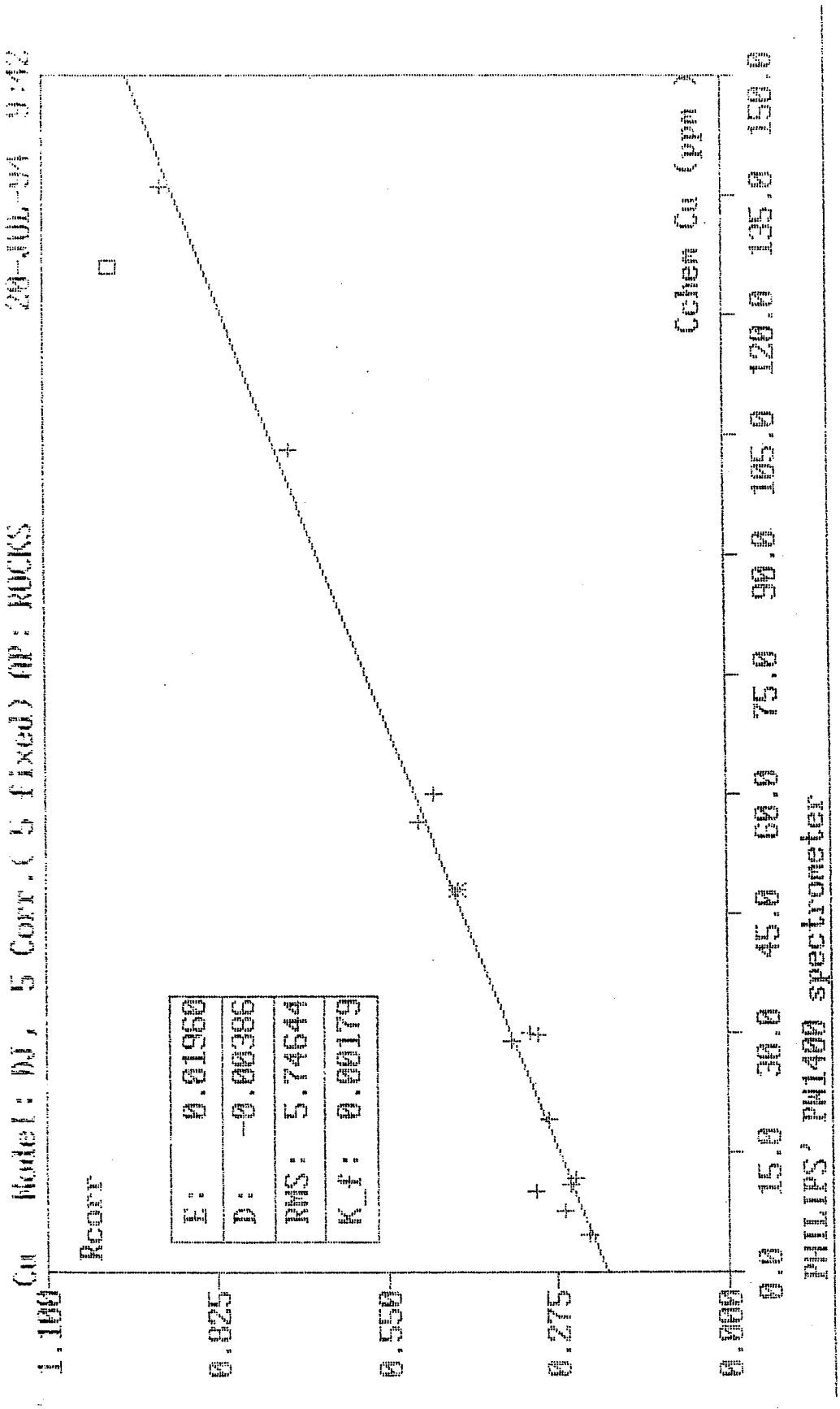

Fig. 9.17 - XRF Standardization Curves for Cu

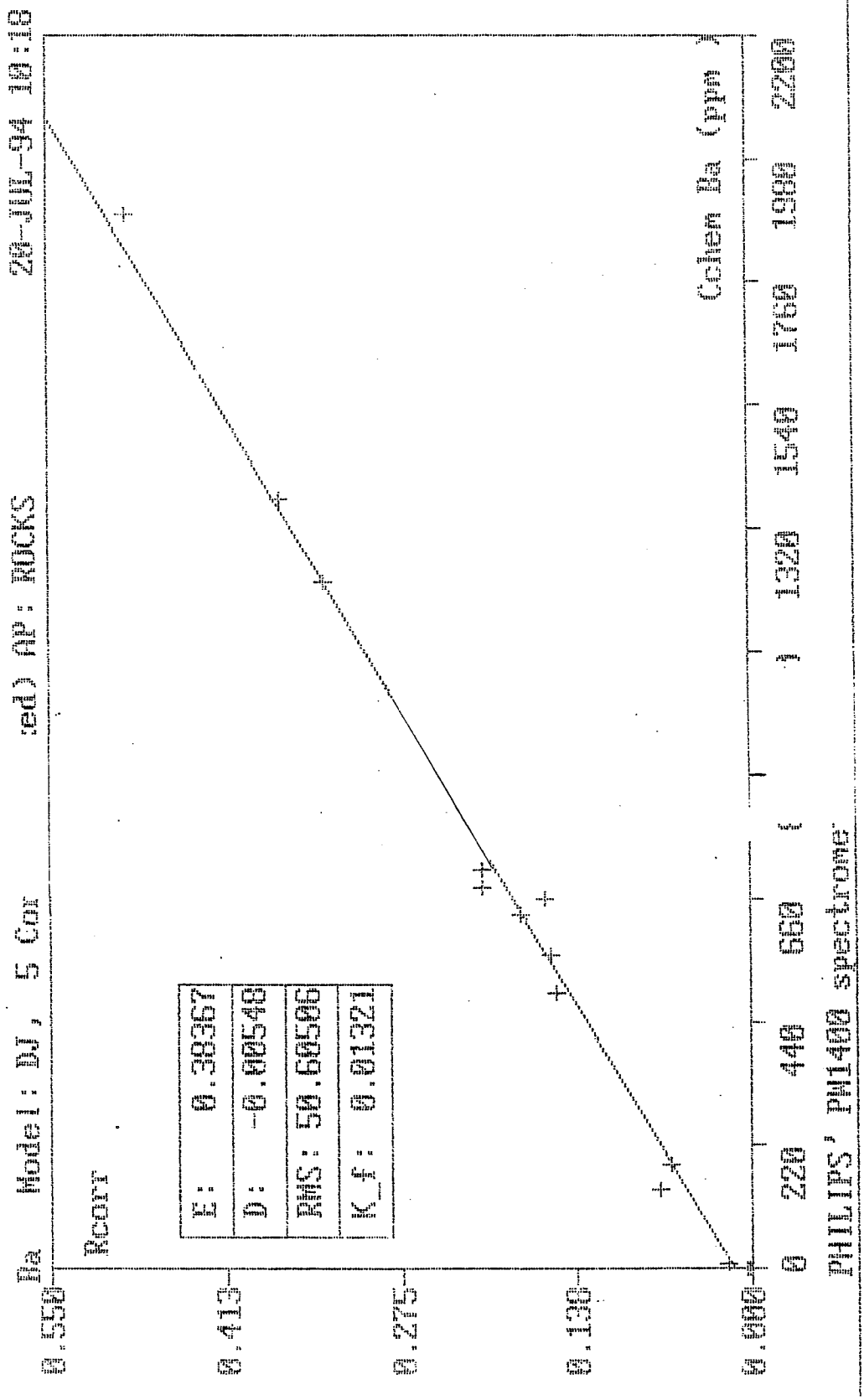

Fig. 9.18 - XRF Standardization Curves for Ba

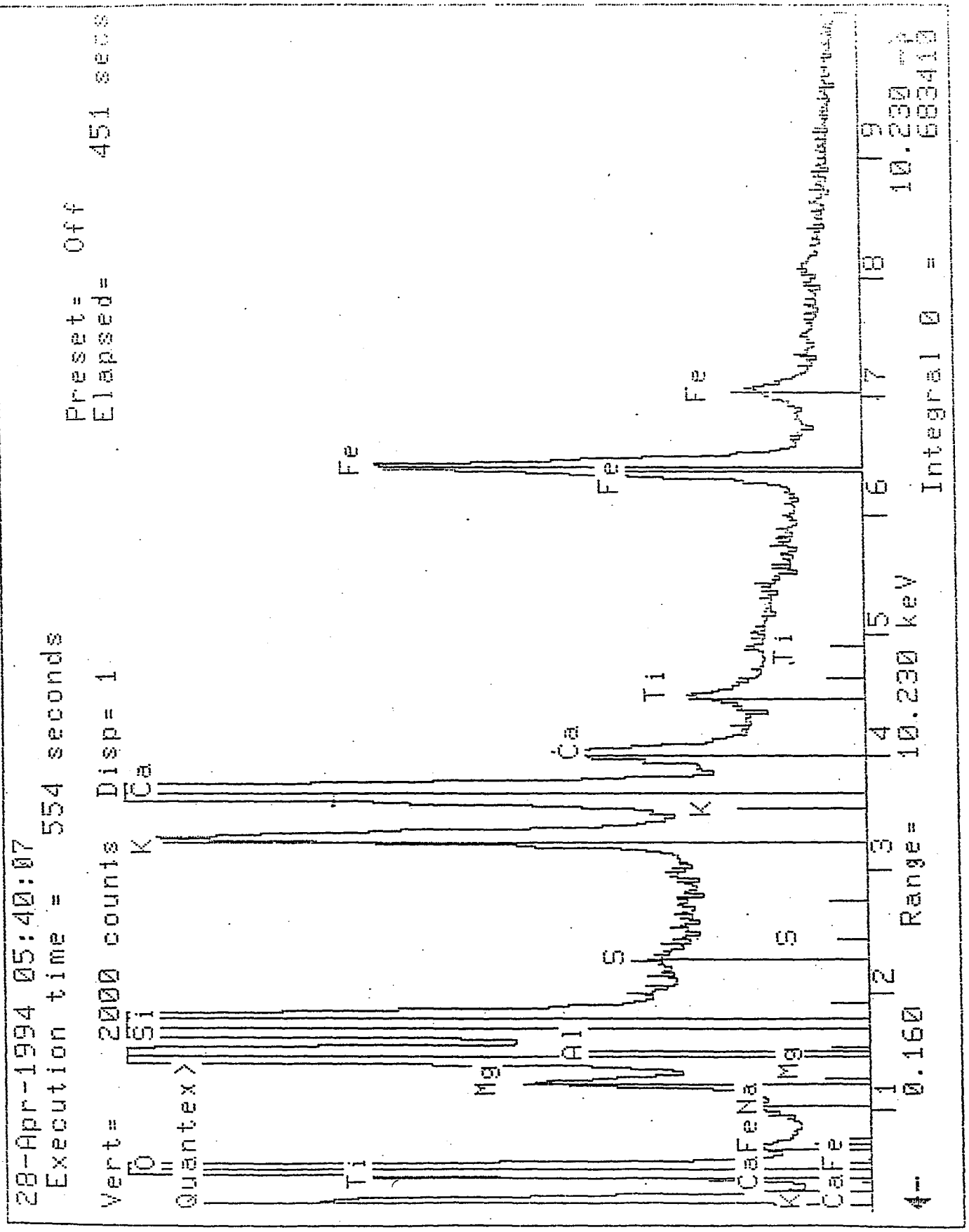

EDS spectrum of sample 1c

Fig. 9.19 - EDS Spectrum of Sample 1C

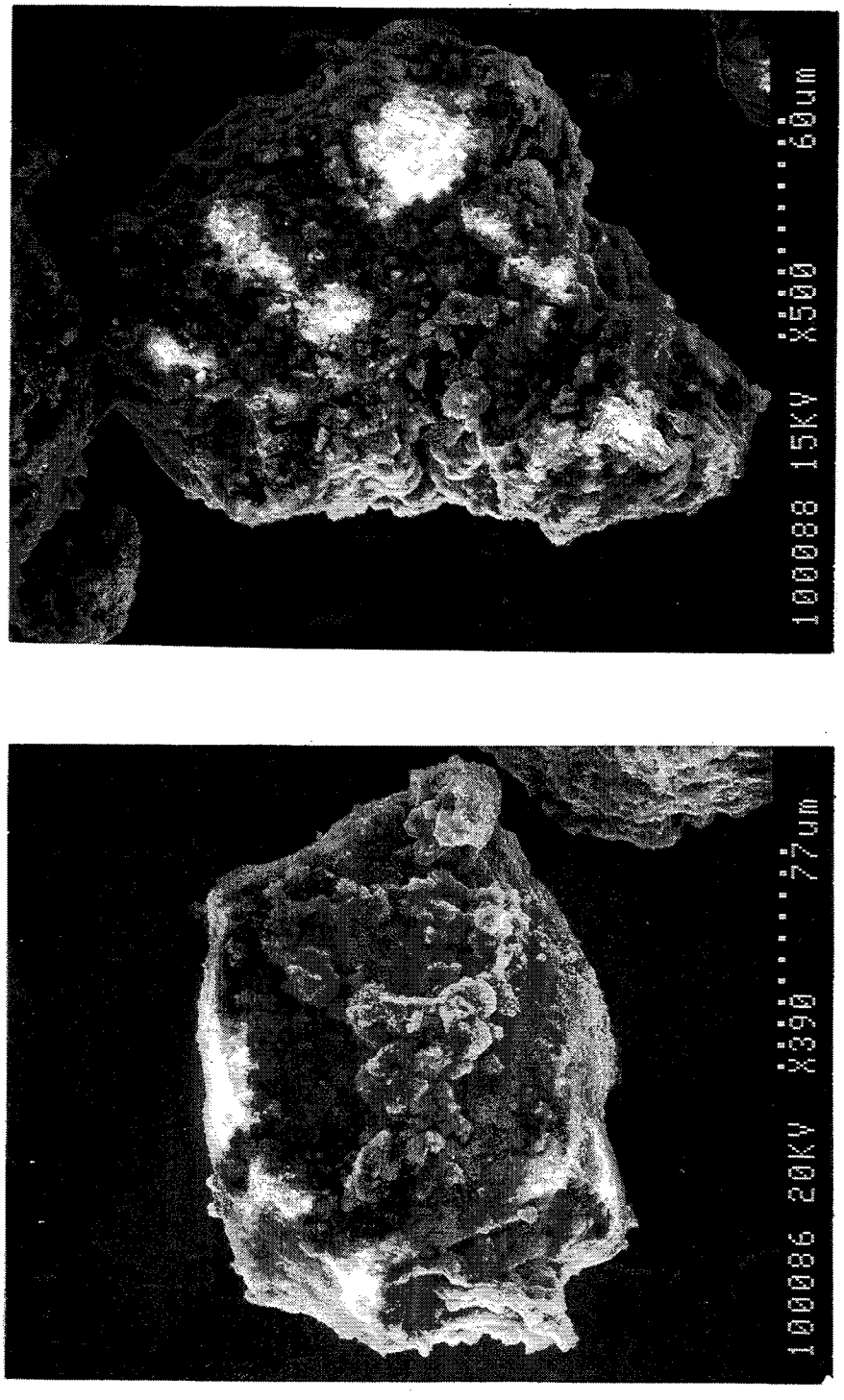

SEM micrograph -Sample 1c

Fig. 9.20 - SEM Micrograph of Sample 1C

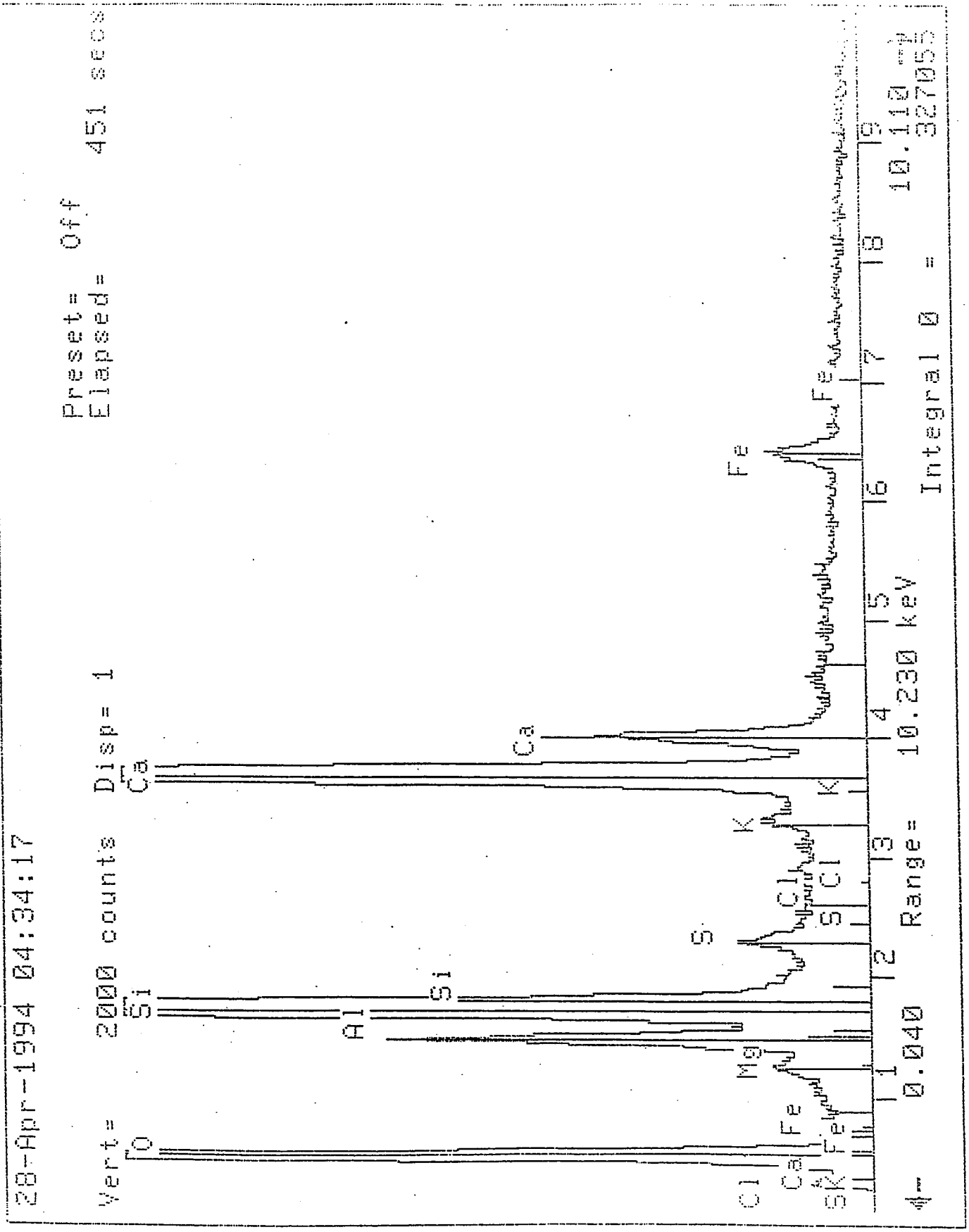

EDS spectrum of sample 2c

Fig. 9.21 - EDS Spectrum of Sample 2C

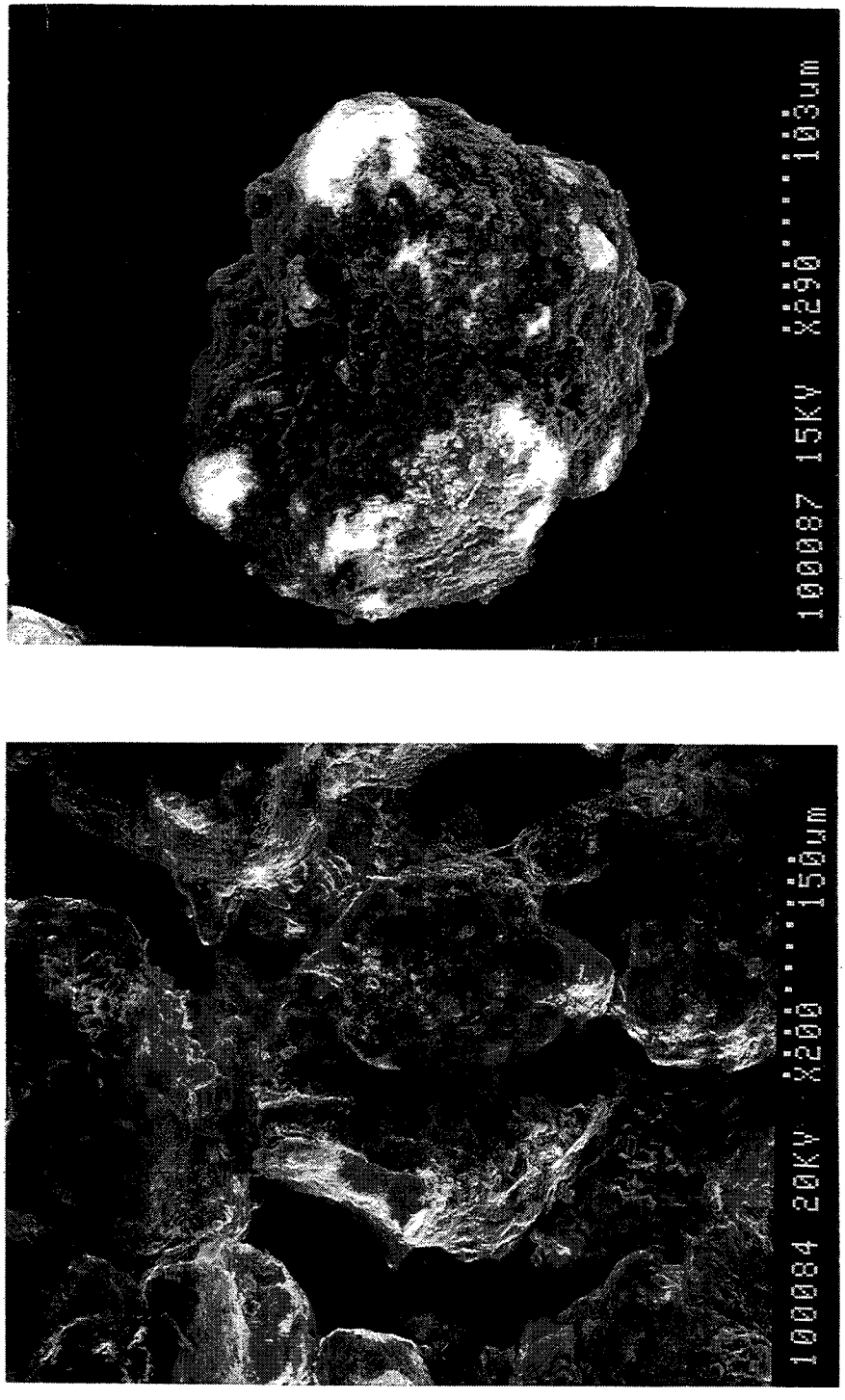

SEM micrograph -Sample 2c

Fig. 9.22 - SEM Micrograph of Sample 2C

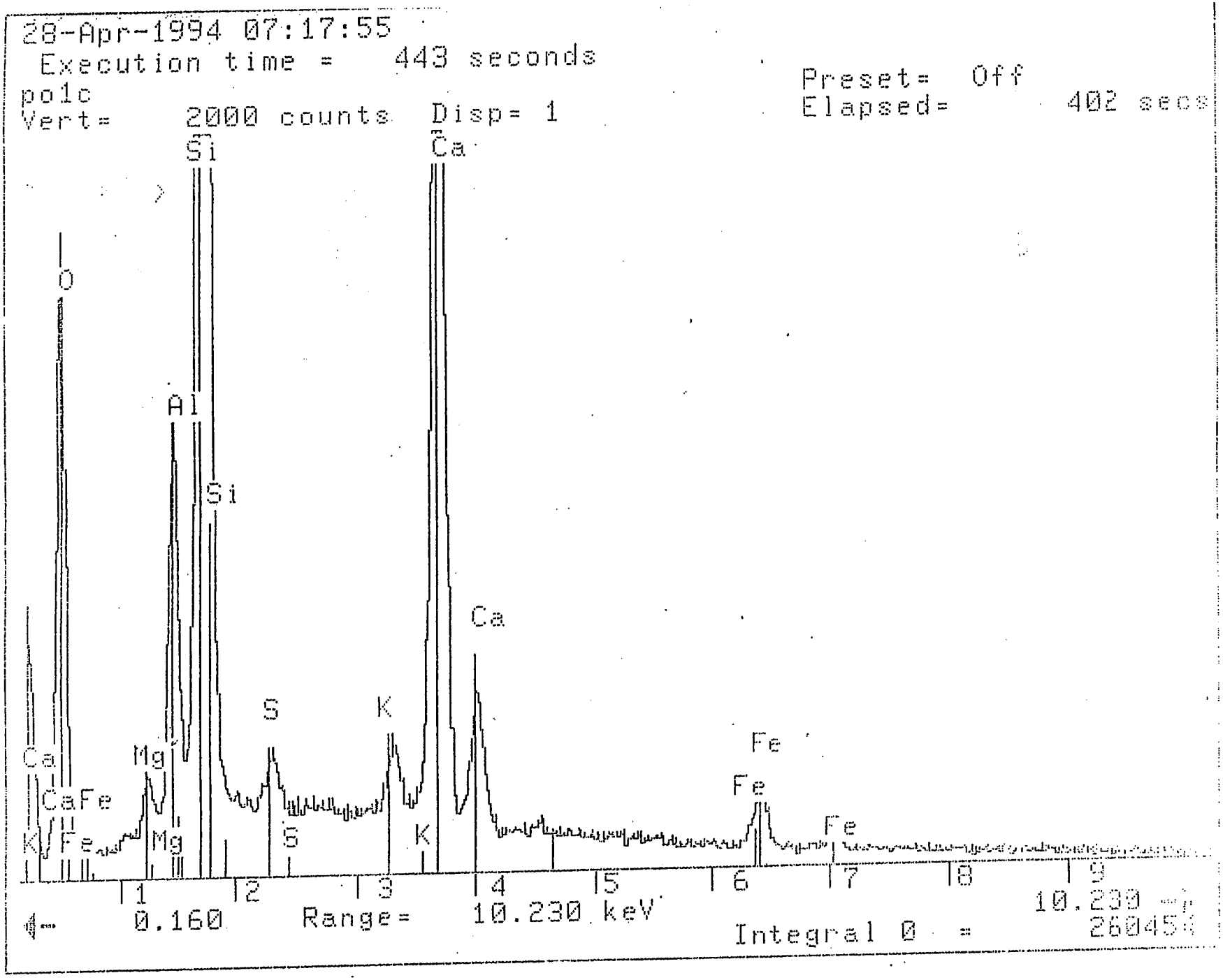

Fig. 9.23 - EDS Spectrum of Sample 3C

EDS spectrum of sample 3c

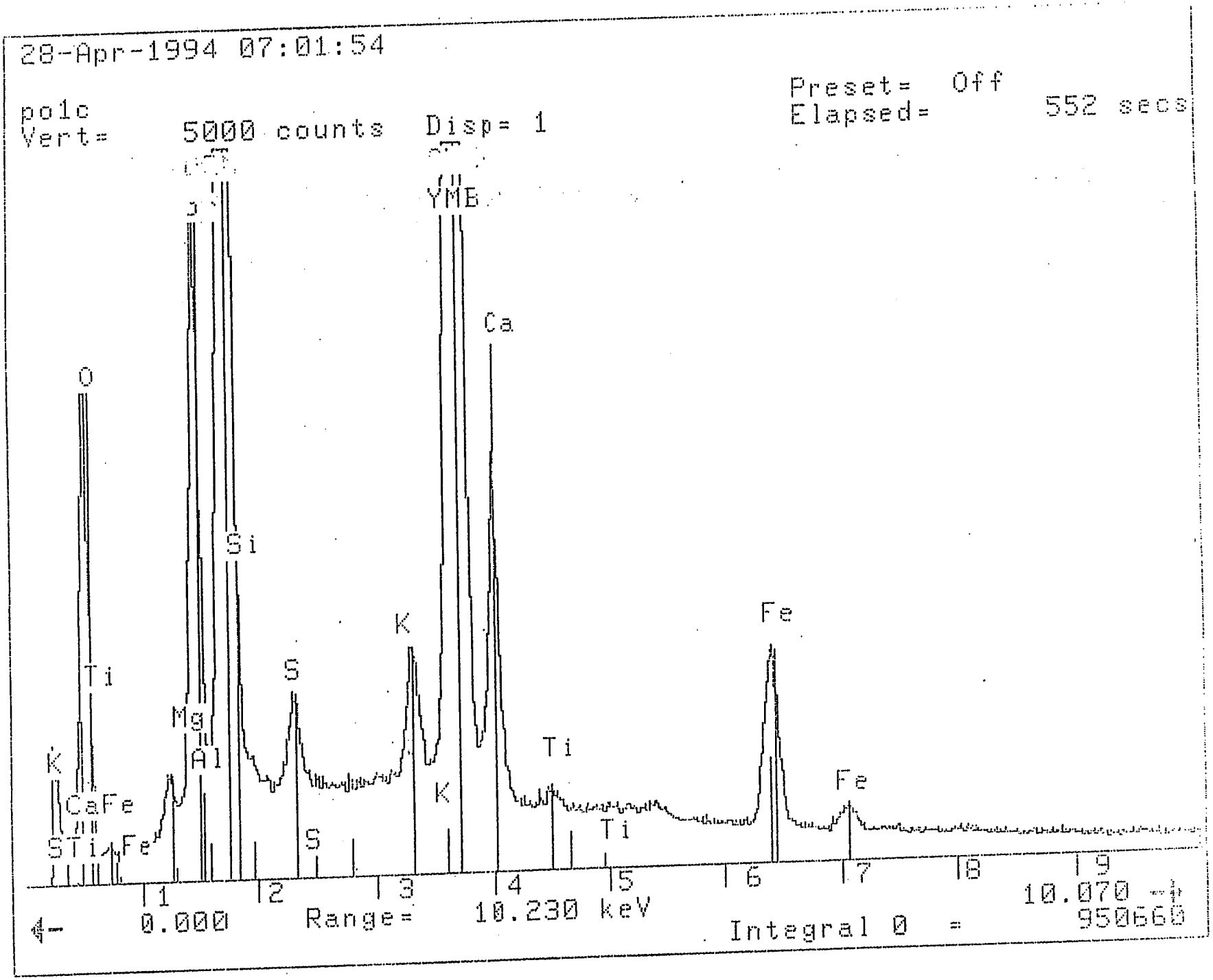

EDS spectrum of sample 6c

Fig. 9.24 - EDS Spectrum of Sample 6C

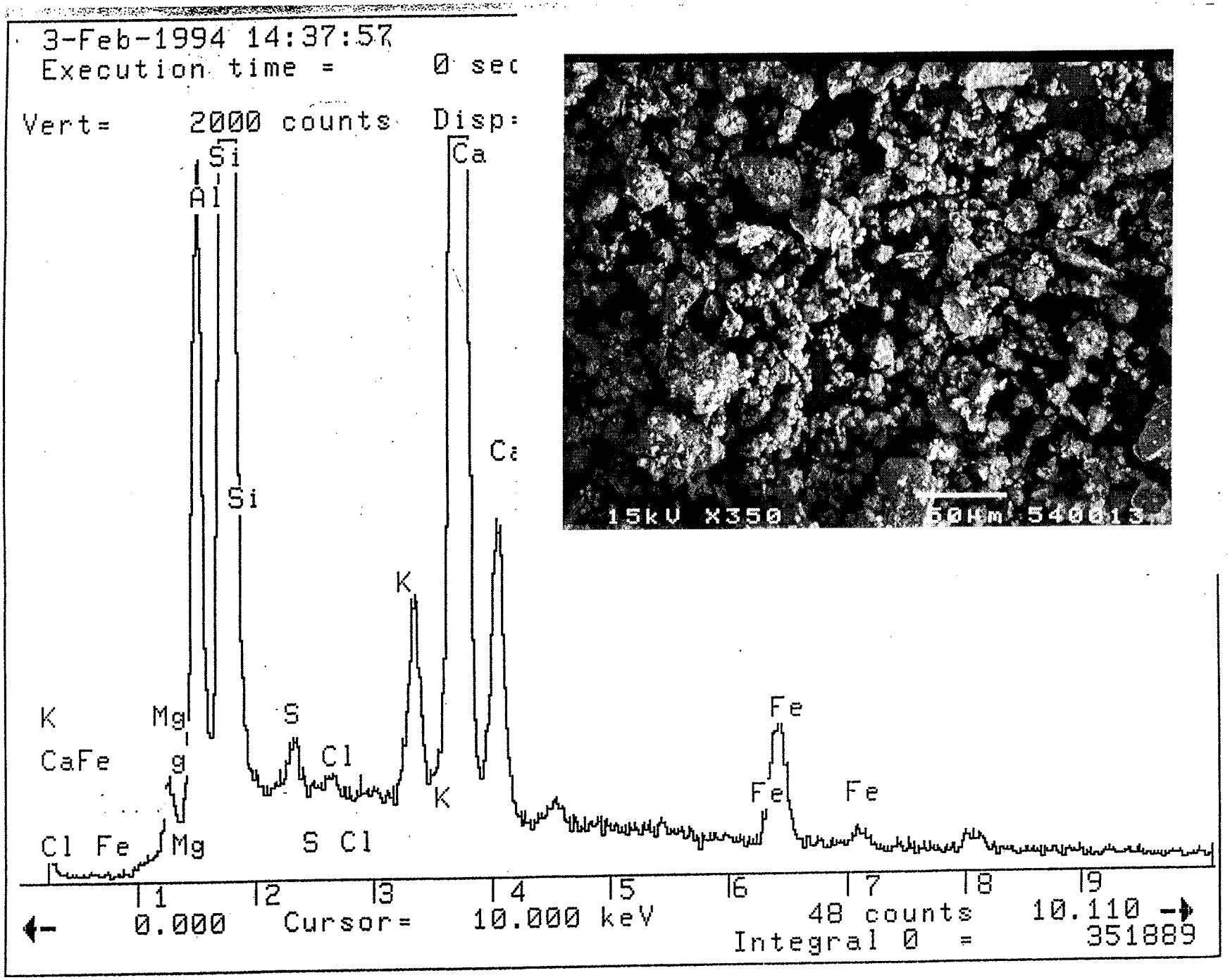

Fig. 9.25 - EDS Spectrum and SEM Micrograph of Sample NE 2'-3.5'

Typical EDS and SEM micrograph
of sample N.E.(2'–3.5')

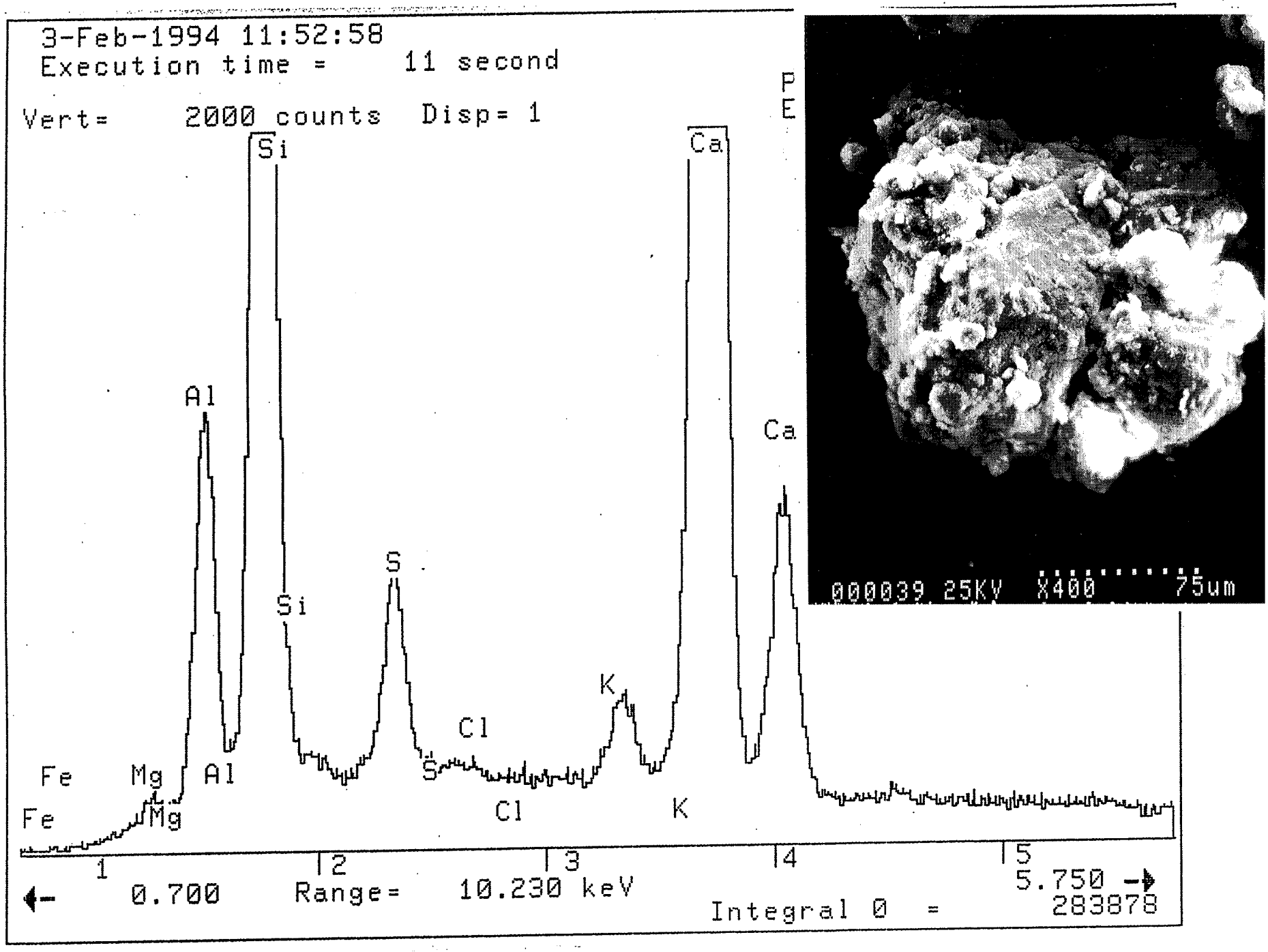

Fig. 9.26 - EDS Spectrum and SEM Micrograph of Sample SW 10'-12'

Typical EDS and SEM micrograph
of sample SW (10'–12')

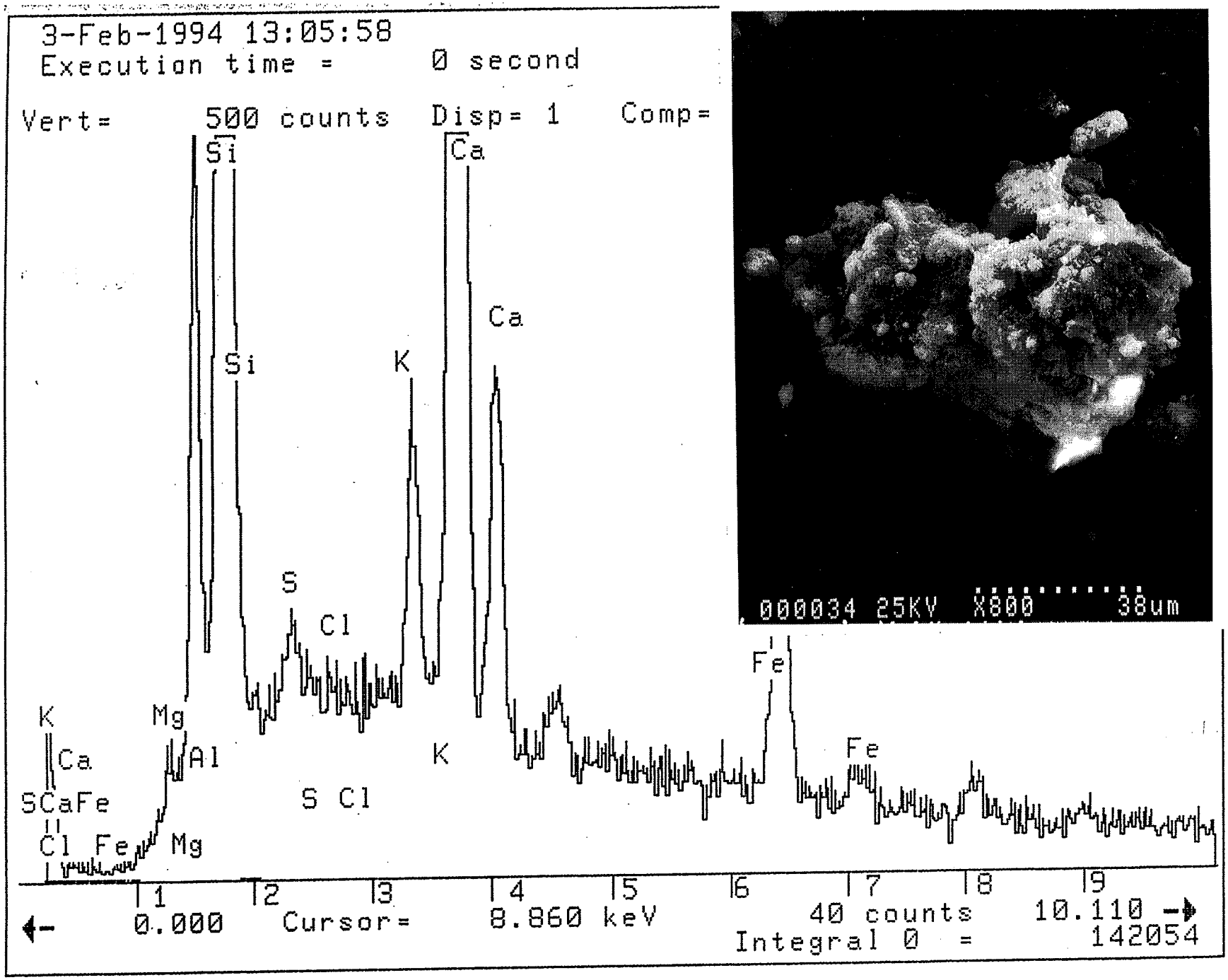

Fig. 9.27 - EDS Spectrum and SEM Micrograph of Sample SE 4'-6'

Typical EDS and SEM micrograph of sample SE (4'–6')

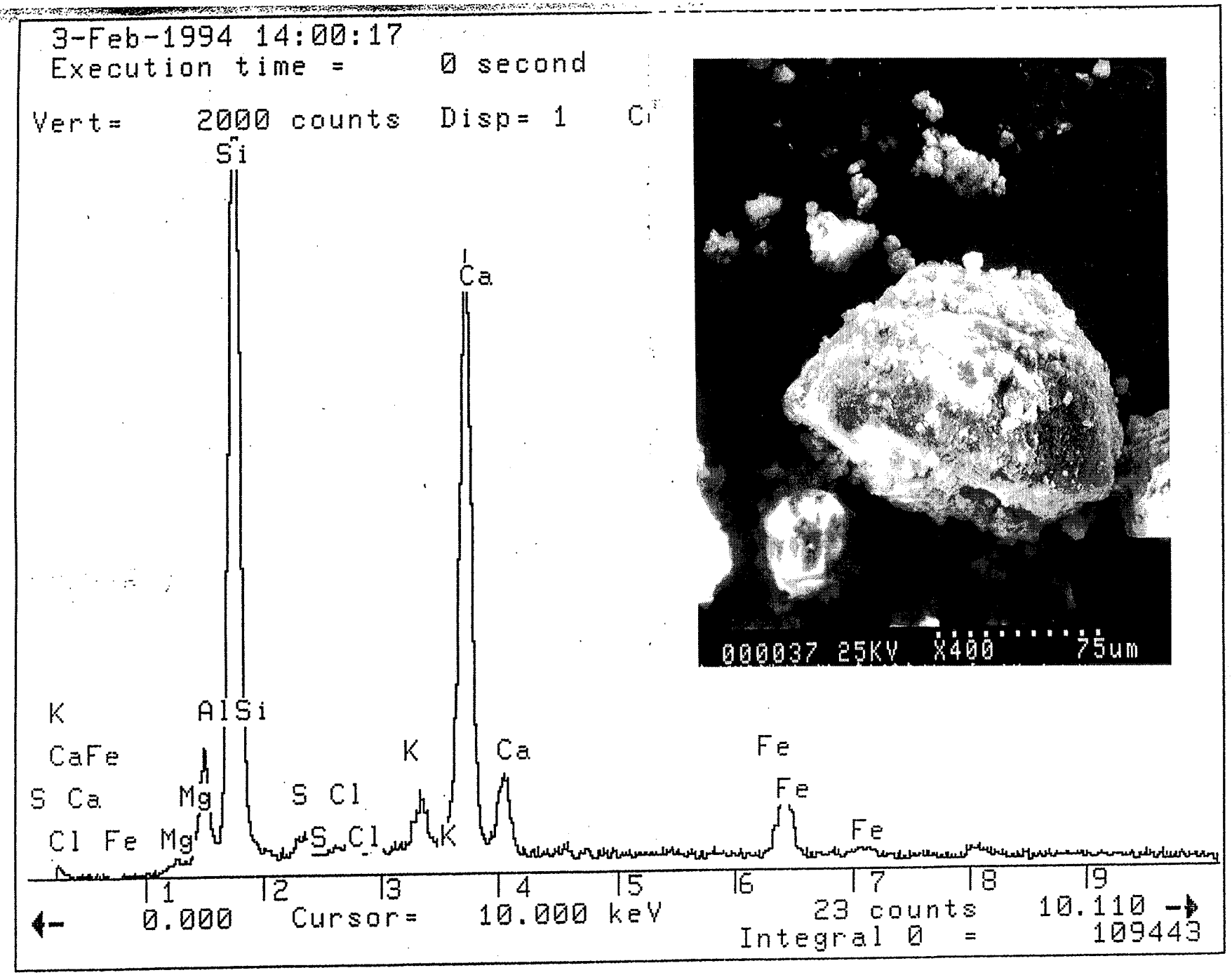

Fig. 9.28 - EDS Spectrum and SEM Micrograph of Sample SW 4'-6'

Typical EDS and SEM micrograph
of sample S.W (4'–6')

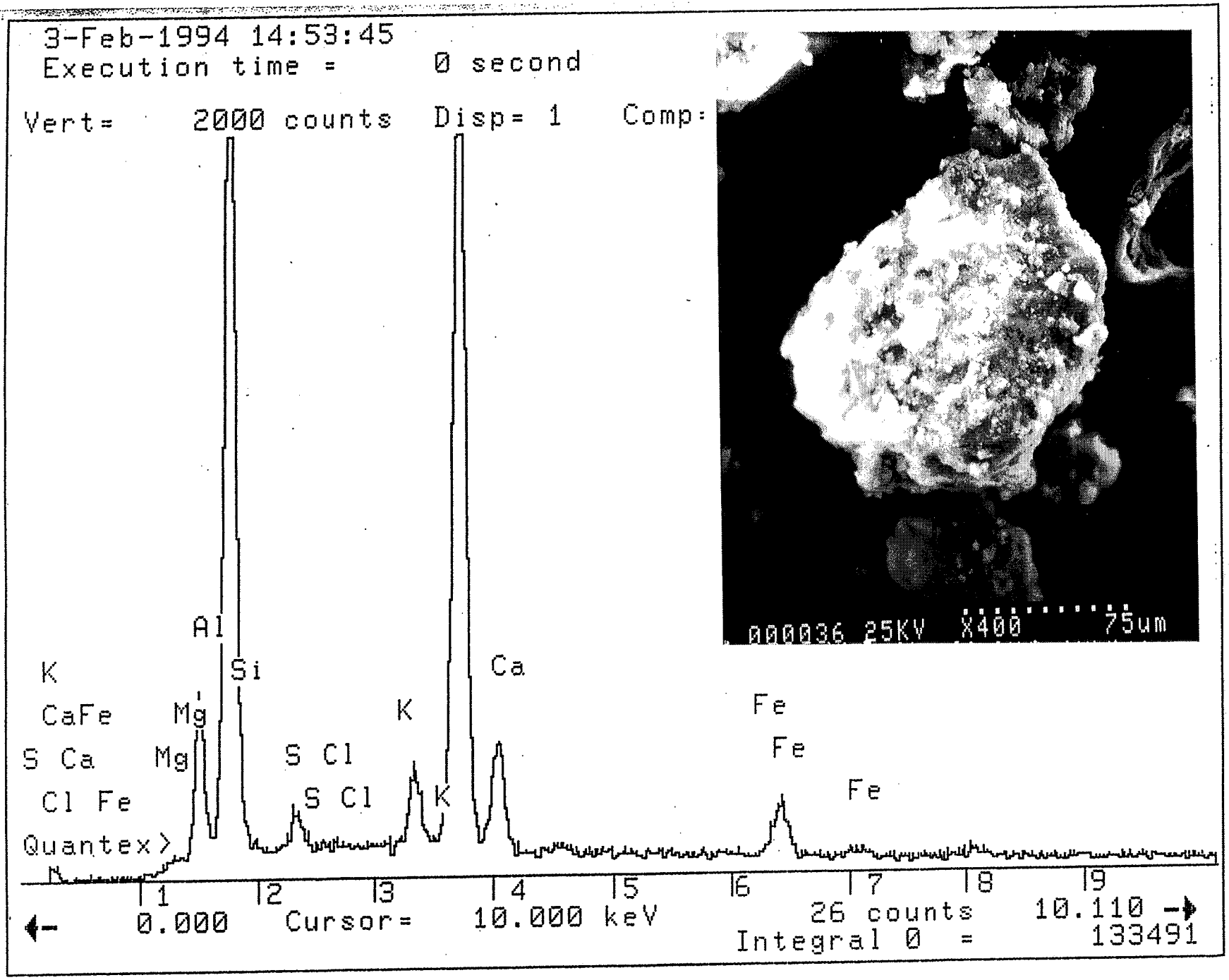

Fig. 9.29 - EDS Spectrum and SEM Micrograph of Sample NE 5'-7'

Typical EDS and SEM micrograph
of sample N.E (5'–7')

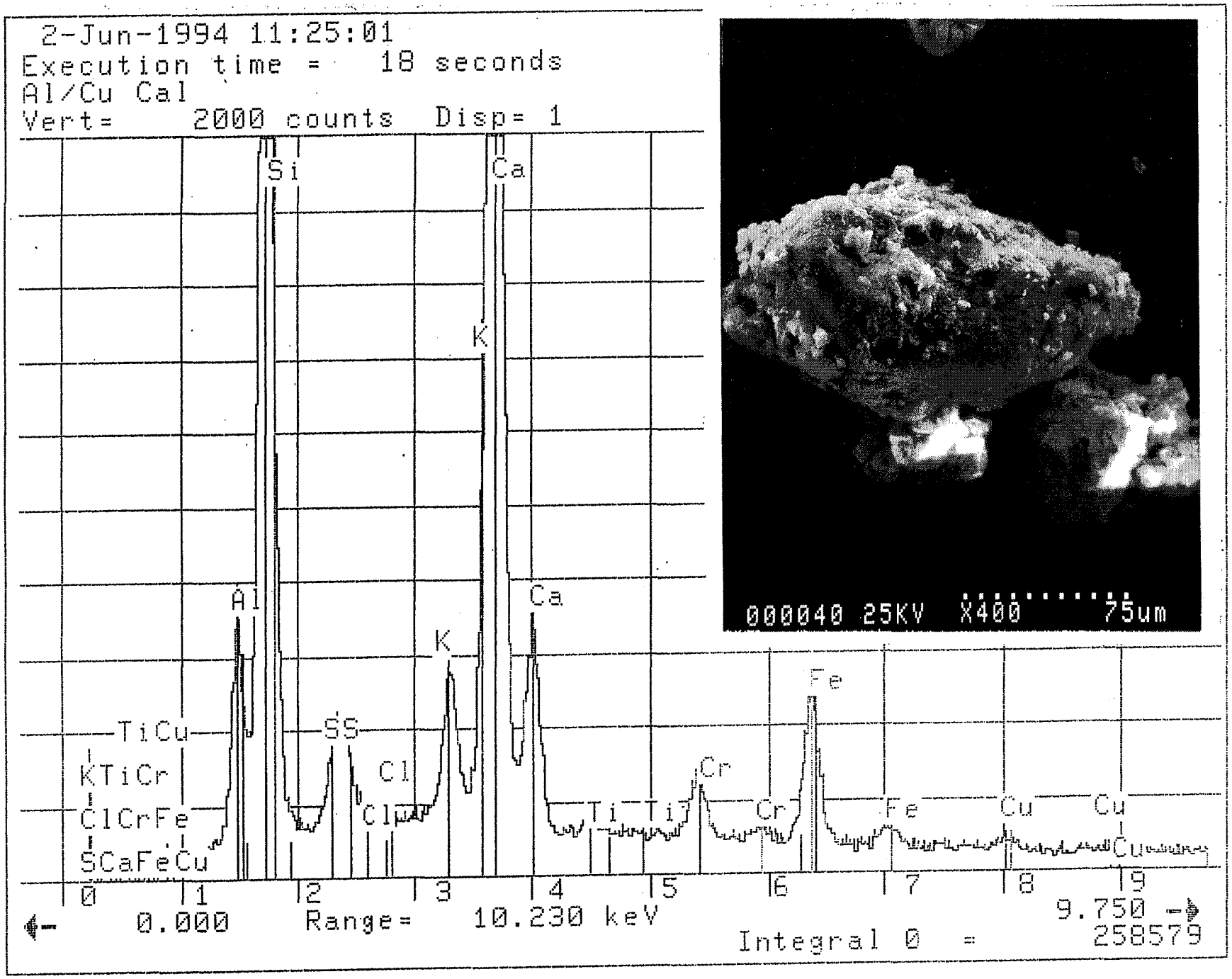

Fig. 9.30 - EDS Spectrum and SEM Micrograph of Sample SE 0'-2'

Typical EDS and SEM micrograph of sample (SE 0–2)

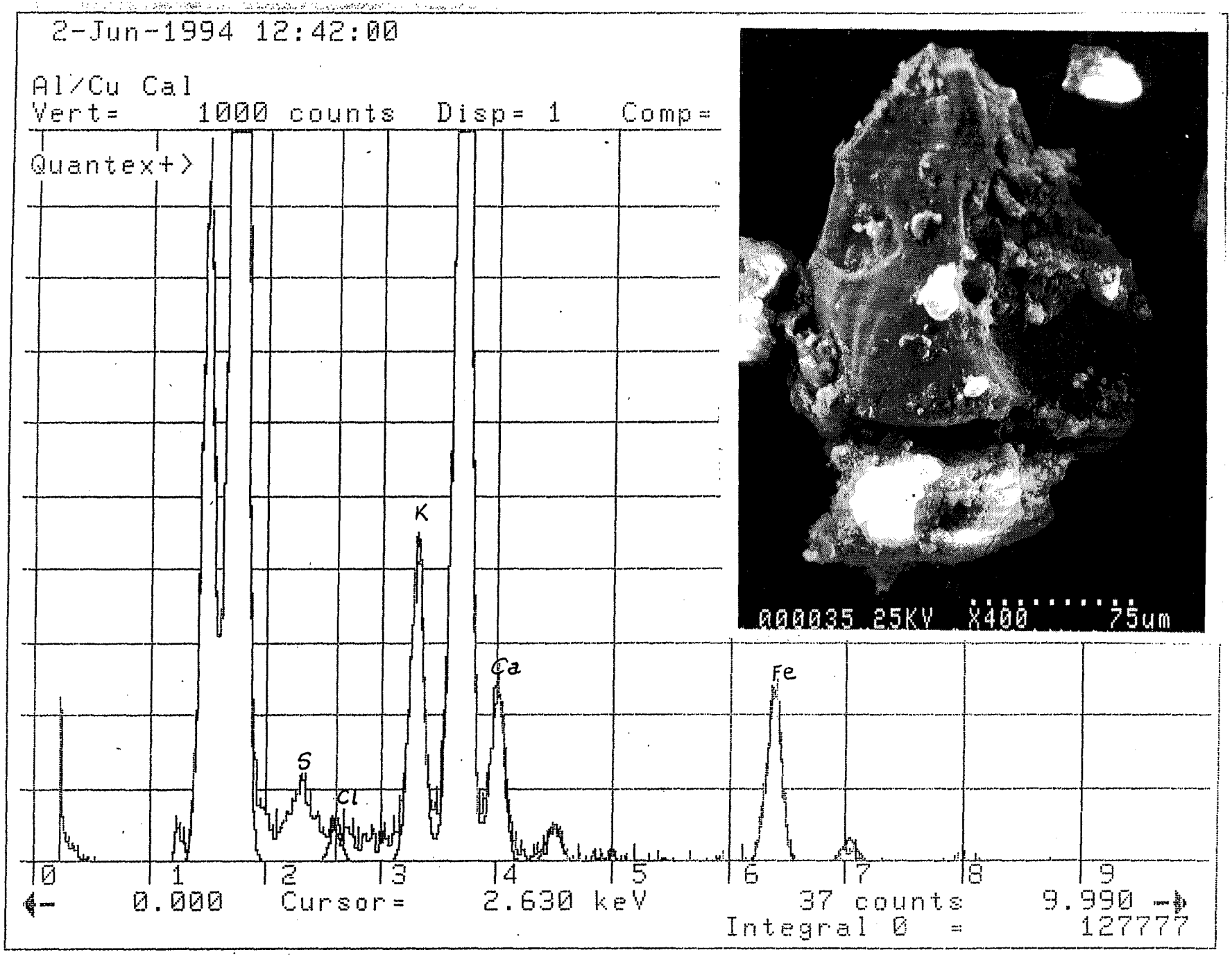

Fig. 9.31 - EDS Spectrum and SEM Micrograph of Sample NW 2'-4'

Typical EDS and SEM micrograph of sample (NW2-4)

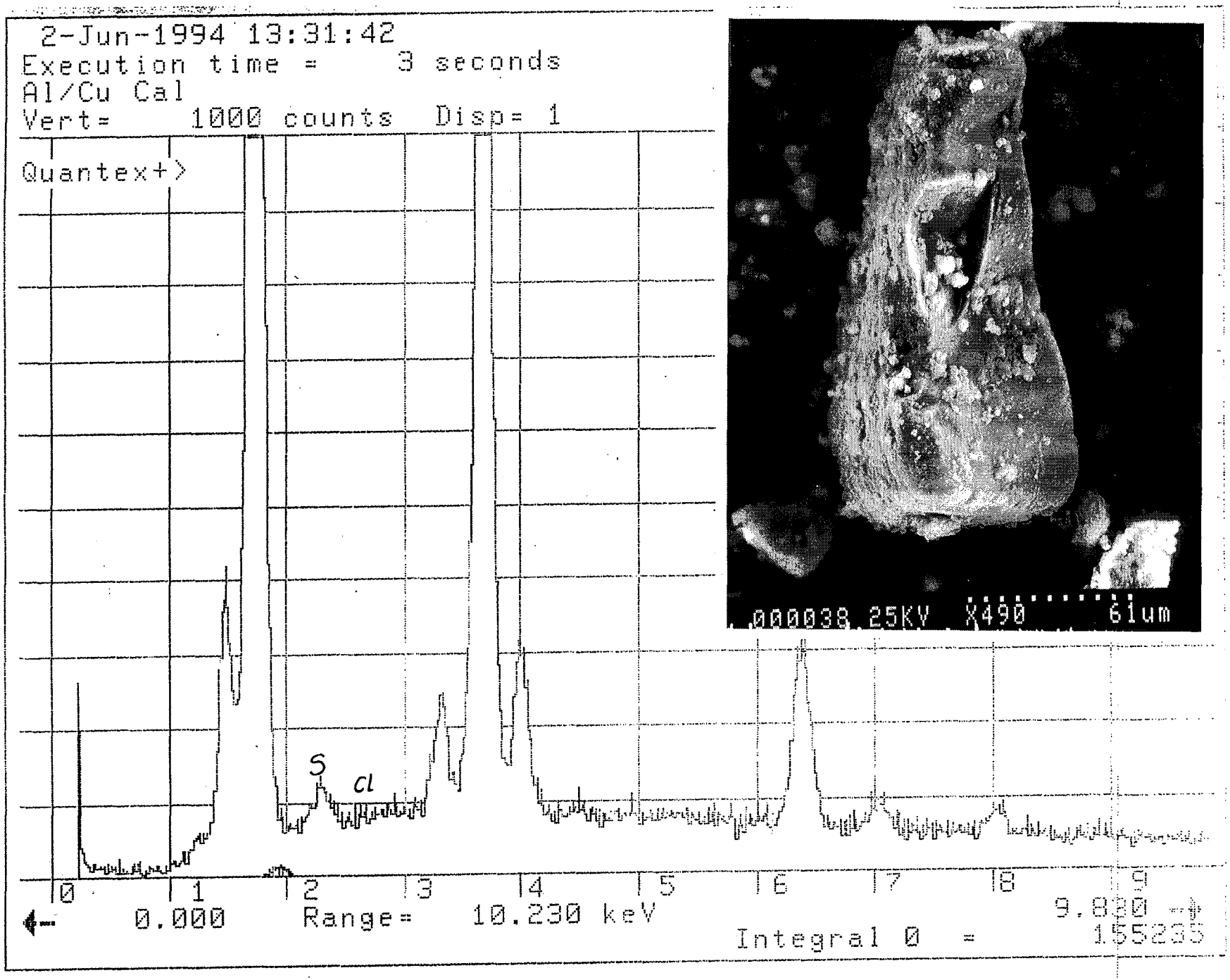

Fig. 9.32 - EDS Spectrum and SEM Micrograph of Sample NE 4'-6'

Typical EDS and SEM micrograph of sample (SN 4–6)

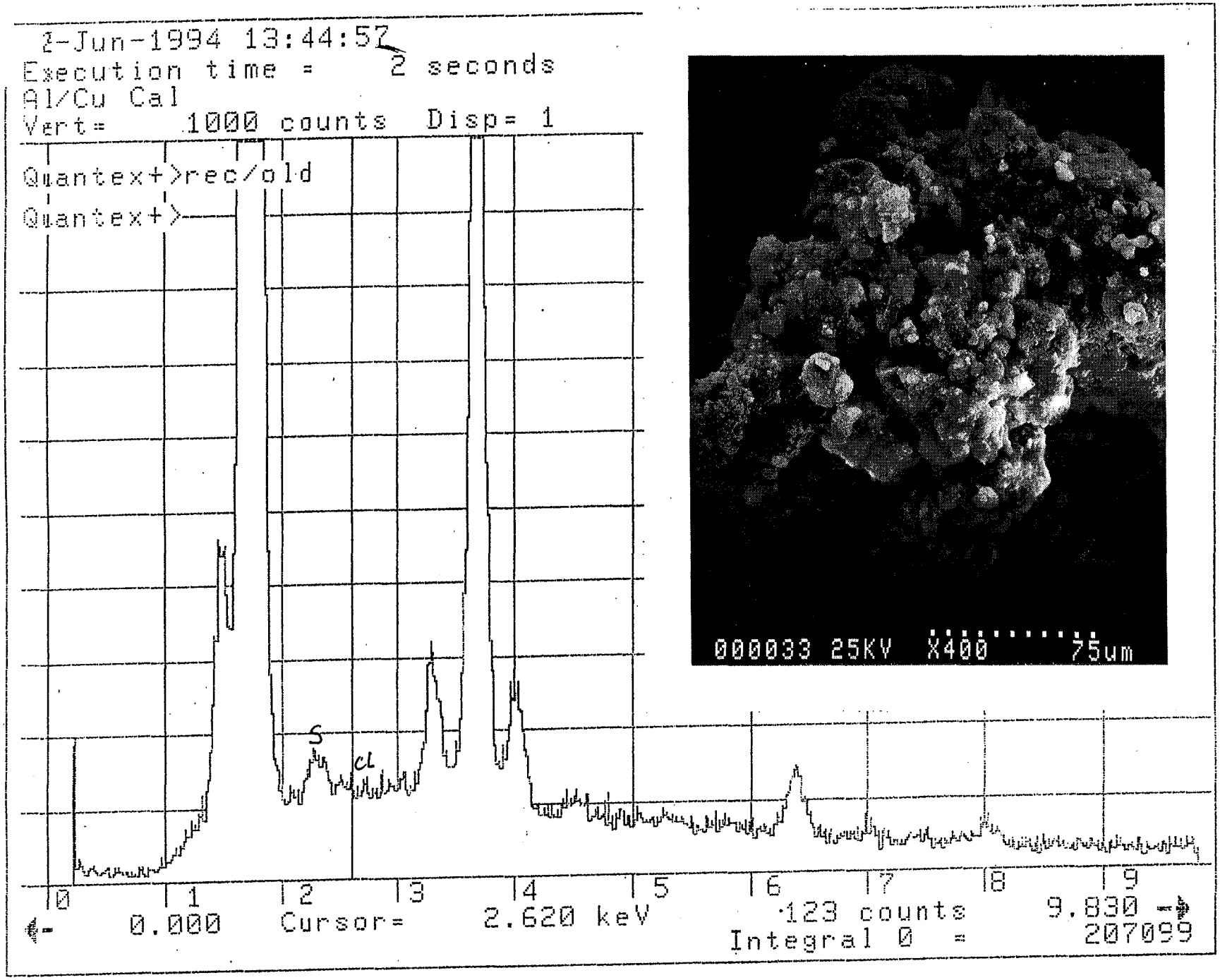

Fig. 9.33 - EDS Spectrum and SEM Micrograph of Sample NE 2'

Typical EDS and SEM micrograph of sample (NE -2)

10. CONCLUSIONS

The study has had a number of conclusions, of which the primary one is that the addition of cement to retaining wall backfill does not need to be discouraged or discontinued from a corrosion point of view, so long as reasonable concentrations of cement are used. The addition of cement to backfill in the usual quantities (i.e. 7% or more) is sufficient to raise the pH environment to values close to normal concrete (i.e. pH 12 to 13). At these levels, no consistent acceleration of corrosion was measured -- if anything, corrosion rates were less than for unstabilized fill, and were found to be acceptable, so long as cement contents exceeded low minimum values of a few percent. Such values are normally exceeded in practice -- certainly at this site, where actual cement contents were found to vary from 7% close to the facing units, to 18% in the middle of the stabilized cross-section. Under these conditions, measured laboratory corrosion rates were below commonly accepted threshold values of 0.01 mm/year, giving a design life in excess of 100 years.

Very small amounts of cement addition, however, of the order of 1% to 4% producing a pH environment significantly below 12, could cause limited acceleration of corrosion. This can be seen by examining the general trend for corrosion rates of galvanized specimens under different conditions displayed in Figures 10.1 through 10.4. It is, therefore, advisable to control minimum cement levels and to encourage efficient mixing.

Similar behavior was also observed for crushed concrete fill, for which the high natural pH levels had previously been assumed to render the material unacceptable. Laboratory test data on this material indicate that it has no disadvantages as far as corrosion is concerned, and that the use of crushed concrete in backfill can, therefore, be allowed. There seems to be no reason why the specifications for backfill cannot be relaxed to allow this material to be used.

The possibility of corrosion cells occurring between regions of different cement content was investigated. Large local variations in cement content were certainly measured in the flll behind the field retaining walls, as indicated above, but tests did not show the presence of such "corrosion cells" to have a major contributory effect to corrosion rate in the laboratory.

High corrosion rates were observed primarily as a result of the presence of high concentrations of inorganic ions. These can increase corrosion rates by a factor of 10 to 100. Laboratory corrosion rate values measured under these conditions were of the order of 0.1 to 1 mm/year, which would correspond to reduction in design lives to as little as 10 to 1 years. In the laboratory, this was simulated with sodium chloride solution, although at the field problem site in District 12, this was attributed to a particularily high concentration of sulfates. These results, therefore, support the recent amendments to backfill corrosivity specifications, requiring specific measurements of chloride and sulfate concentrations, rather than just using backfill resistivity as a general overall measure, as previously done.

It was also noticeable in the course of the fieldwork, that the intact strength of field samples close to the facing units was low. This was initially attributed to sub-standard cement content, but subsequent tests showed this not to be the case. Consequently, compaction densities close to the wall face were almost certainly low (as is the natural tendency of reinforced earth contractors), and this probably exacerbated the corrosion environment at the wall face by allowing easier penetration of surface water and atmospheric oxygen. It might be desirable to find some way of encouraging more effective compaction close to facing units in the future.

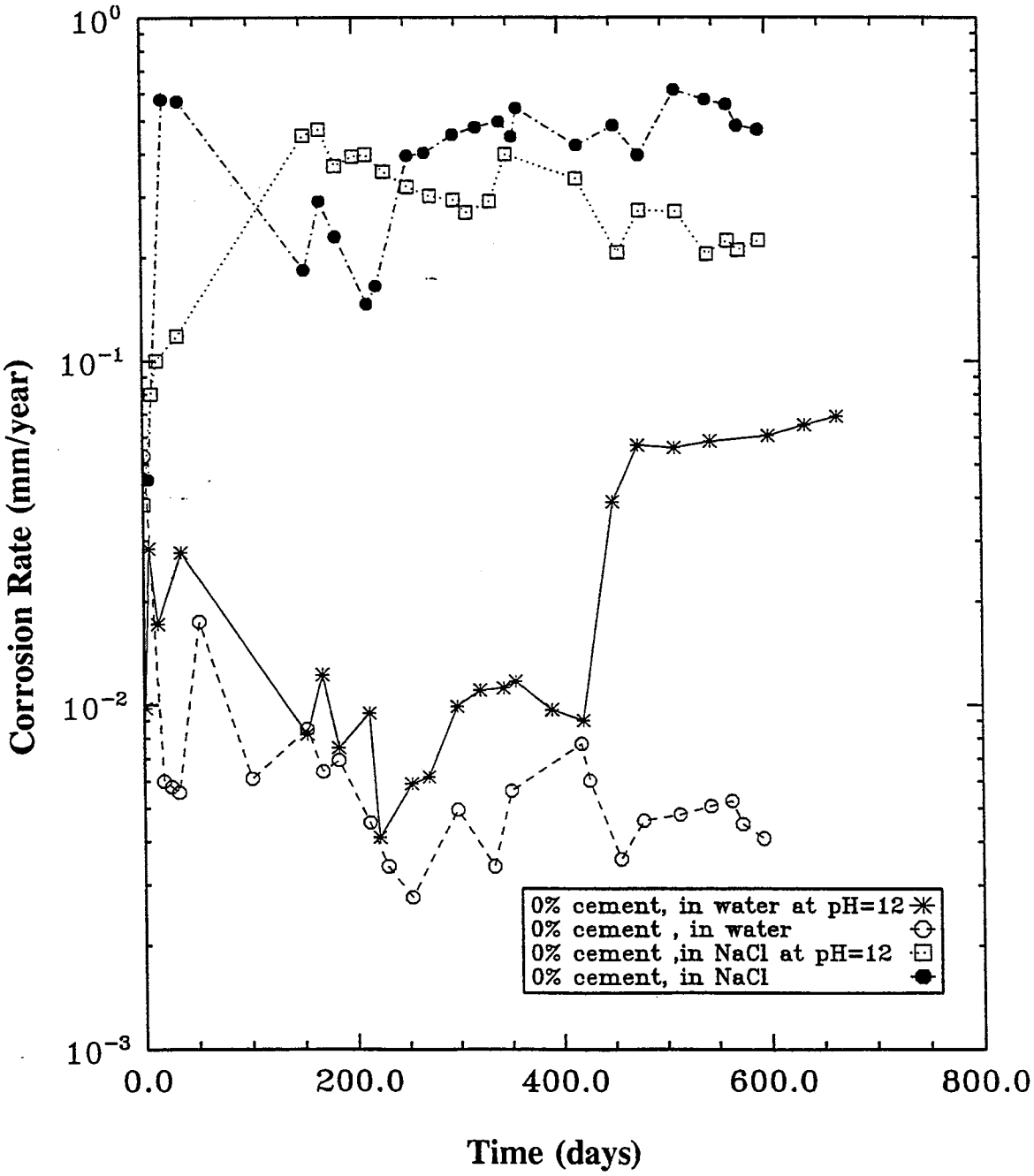

Comparison of the Corrosion Rates vs Time of galvanized steel with 0% cement content.

Fig. 10.1 - Corrosion Rates of Galvanized Specimens in Different Conditions, 0% Cement

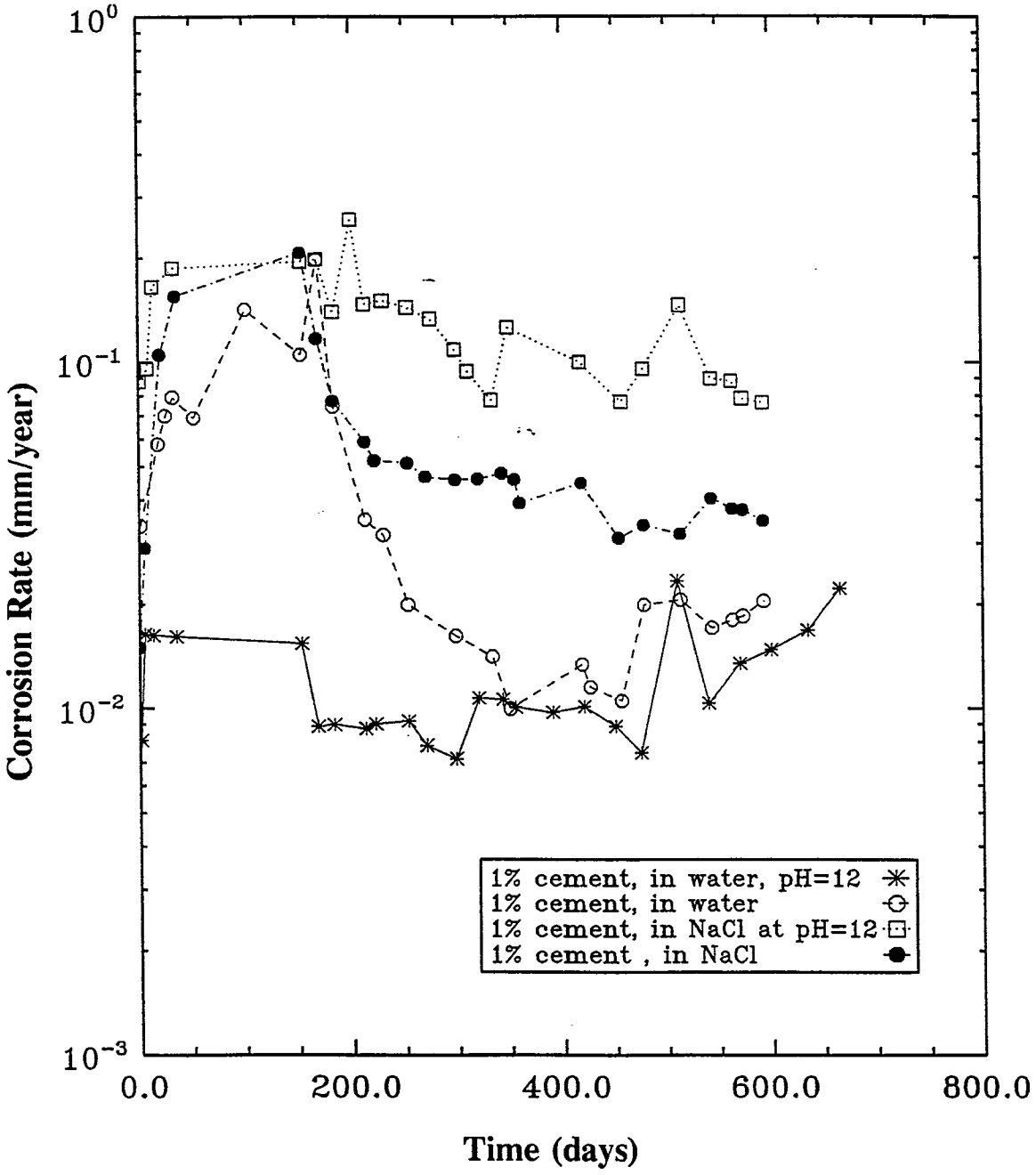

Comparison of the Corrosion Rates vs Time of galvanized steel with 1% cement content.

Fig. 10.2 - Corrosion Rates of Galvanized Specimens in Different Conditions, 1% Cement

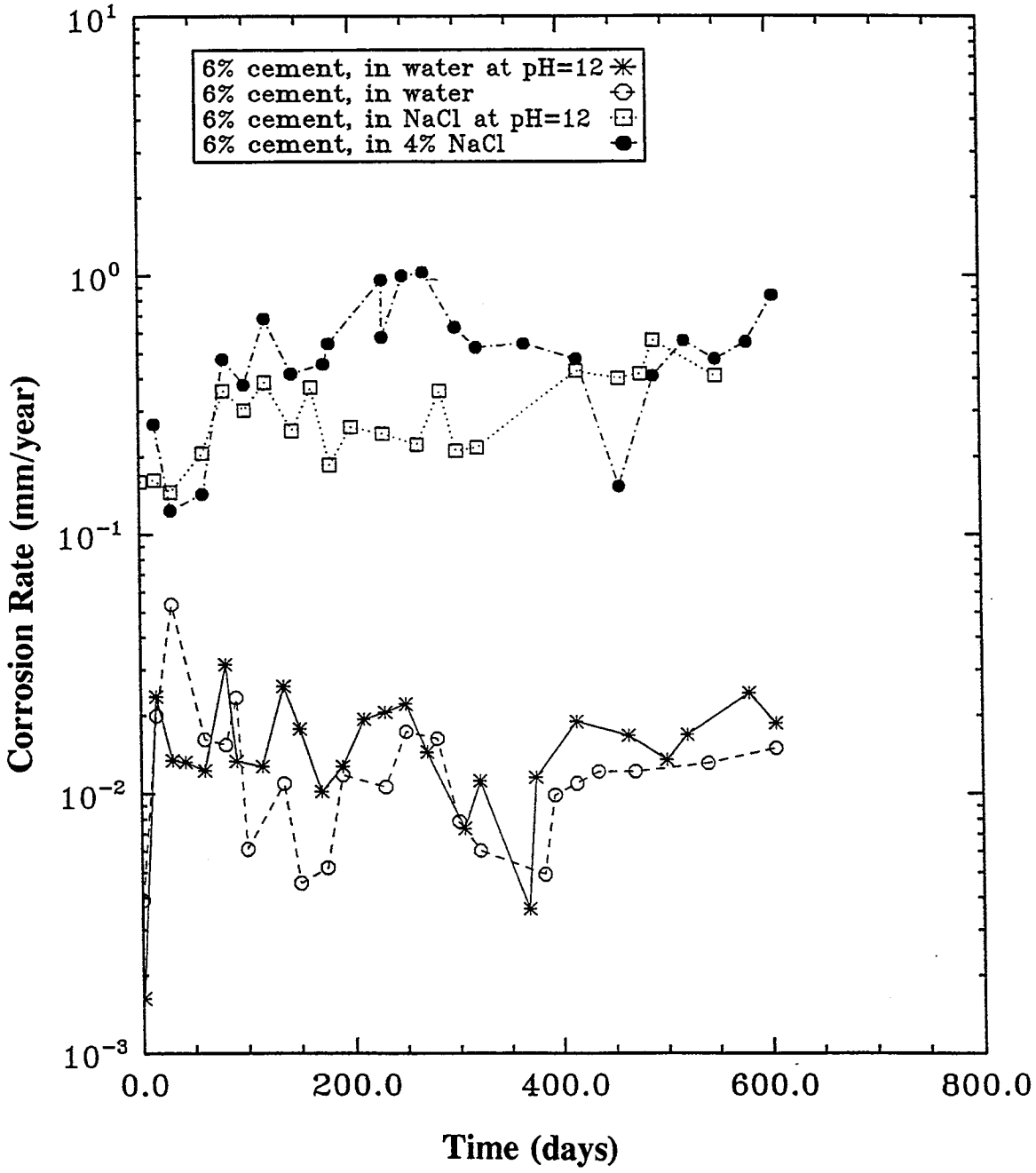

Comparison of the Corrosion Rates vs Time of galvanized steel with 6% cement content.

Fig. 10.3 - Corrosion Rates of Galvanized Specimens in Different Conditions, 6% Cement

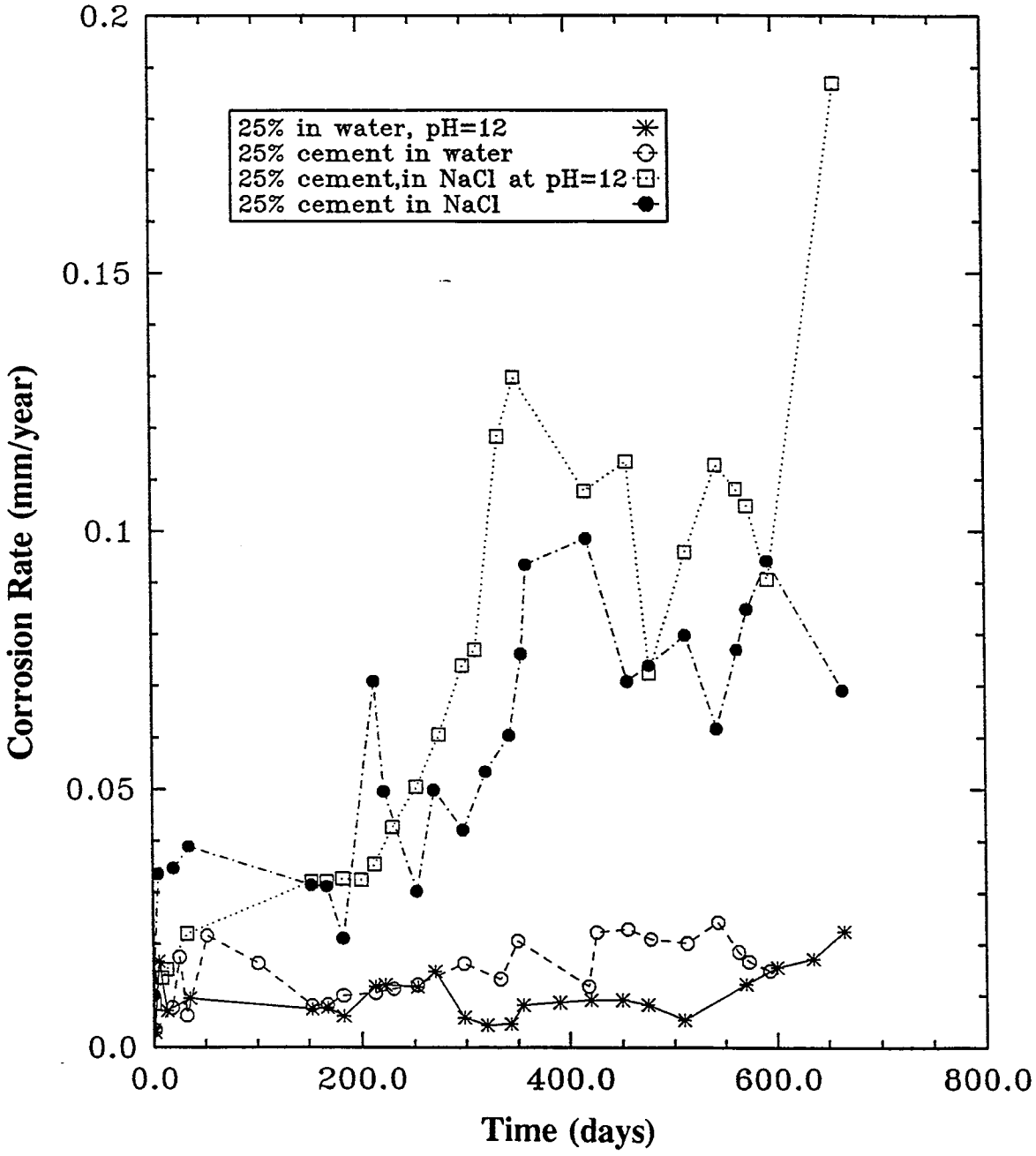

Comparison of the Corrosion Rates vs Time of galvanized steel with 25% cement content.

Fig. 10.4 - Corrosion Rates of Galvanized Specimens in Different Conditions, 25% Cement

11. REFERENCES

Andrade, C., Castelo, V., Alonso, C., Gonzales, J.A., (1984). "Determination of the Corrosion Rate of Steel Embedded in Concrete by the Polarization Resistance and AC Impedance Methods," ASTM Special Technical Publication 906, Symposium on Corrosion Effects of Stray Currents and Techniques for Evaluating Corrosion of Rebars in Concrete, edited by Victor Chaker, Williamsburg, VA.

Bernsted, J., (1983). "Advances in Cement Technology," edited by S.N. Ghosh, Pergamon Press, New York, NY.

Blight, G.E. and Dane, M.S.W., (1989). "Deterioration of a Wall Complex Constructed of Reinforced Earth," Geotechnique, Vol. 39, No. 1, pp. 47-53.

Clear, K.C., (1981). "Time to Corrosion of Reinforcing Steel in Concrete Slabs, Volume 4: Galvanized Reinforcing Steel," Report FHWA-RD-82-28, Federal Highway Administration, McLean, VA.

Darbin, M., Jailloux, J.M., and Montuelle, J., (1978). "Performance and Research on the Durability of Reinforced Earth Reinforcing Strips," A.S.C.E. Symposium on Earth Reinforcement, Pittsburgh, Pennsylvania.

Elias, V., (1990). "Durability/Corrosion of Soil Reinforced Structures," Report FHWA-RD-89-186, Federal Highway Administration, McLean, Virginia.

Gonzales, J.A. and Andrade, C., (1979). "An Advanced Study on the Behavior of Galvanized Rebars in Carbonated and Non-Carbonated Concrete," Revista de Metalurgia, Vol. 15, No. 2, pp. 83-90.

Hill, G.A., Spellman, D.L., Stratfull, R.F., Tonini, D.E., Cook, A.R., and Cornet, I., (1976). "Laboratory Corrosion Tests of Galvanized Steel in Concrete," Transportation Research Record 604, pp. 25-37.

Hutchinson, F.E. and Olson, B.E, (1967). "The Relationship of Road Salt Applications to Sodium and Chloride Ion Levels in the Soil Bordering Major Highways," Highway Research Record 193, Washington, D.C.

Prior, G.A. and Berthouex, P.M., (1967). "A Study of Salt Pollution of Soil by Highway Salting," Highway Research Record 193, Washington, D.C.

Swamy, R.N., (1990). "In-Situ Behavior of Galvanized Reinforcement," Fifth International Conference on Durability of Building Materials, Brighton, U.K.

Tuuti, K., (1982). "Corrosion of Steel in Concrete," Swedish Cement and Concrete Research Institute, Stockholm, Sweden.

APPENDIX

The appearance of thirteen of the samples (ten galvanized steel and three mild steel rods) after 650 days of exposure under various conditions, are shown in the following 26 figures on pages 124 to 136. The zinc protected galvanized steel samples still appeared reasonably intact, but it was noticeable that the mild steel specimens showed advanced corrosion and buildup of iron oxide (Fe_3O_4) on the surface after 650 days of exposure.

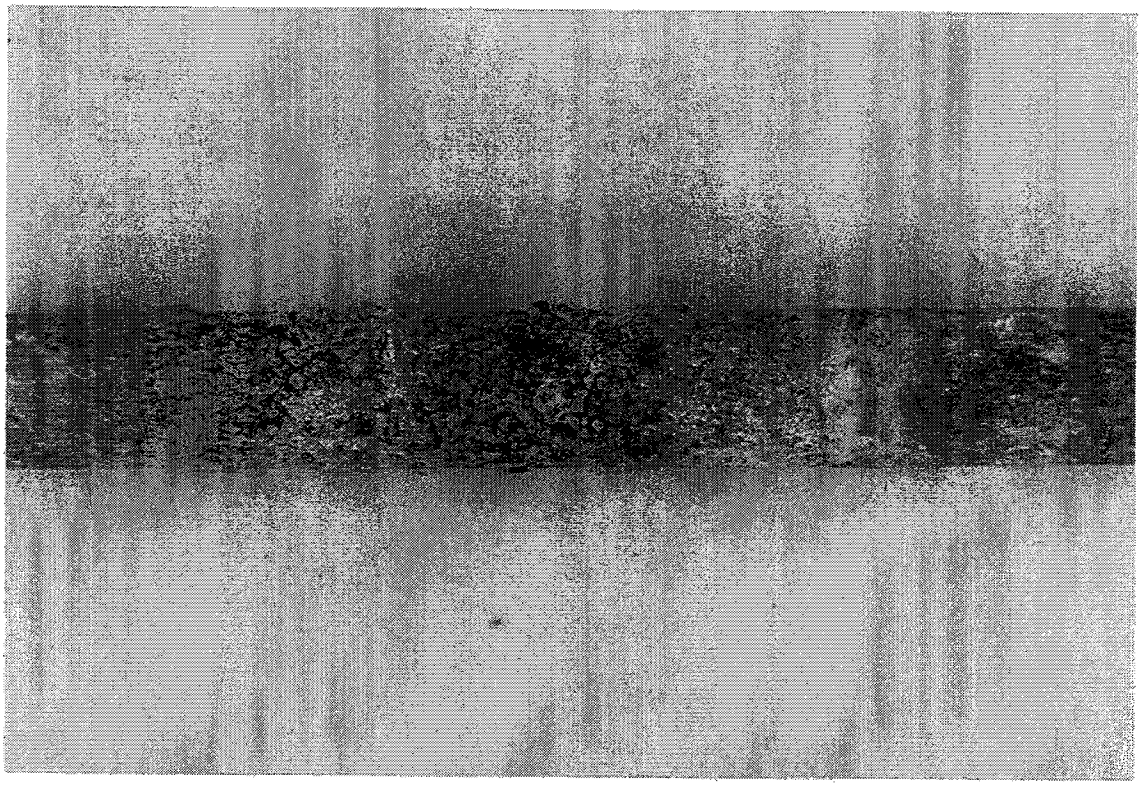

Fig. A1 - Appearance of galvanized steel rod (from soil/water mixture with 1% cement) in NaCl, after 650 days.

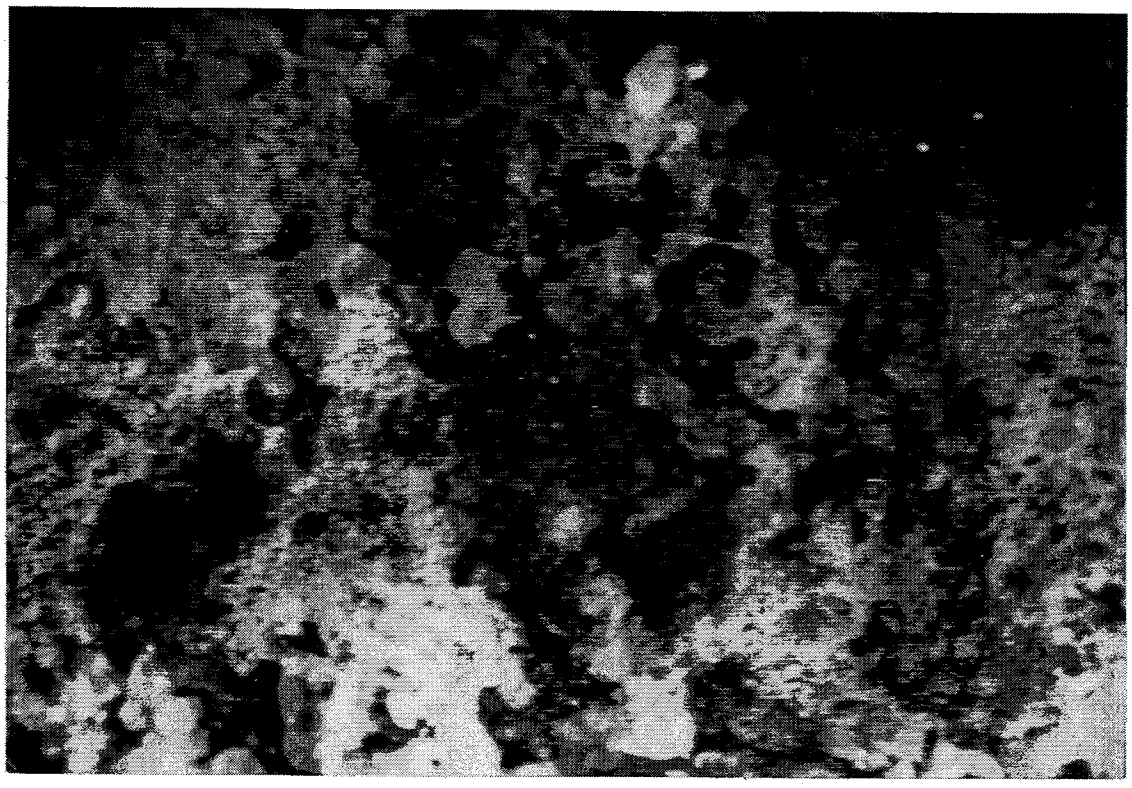

Fig. A2 - Microstructure (x40) of the sample.

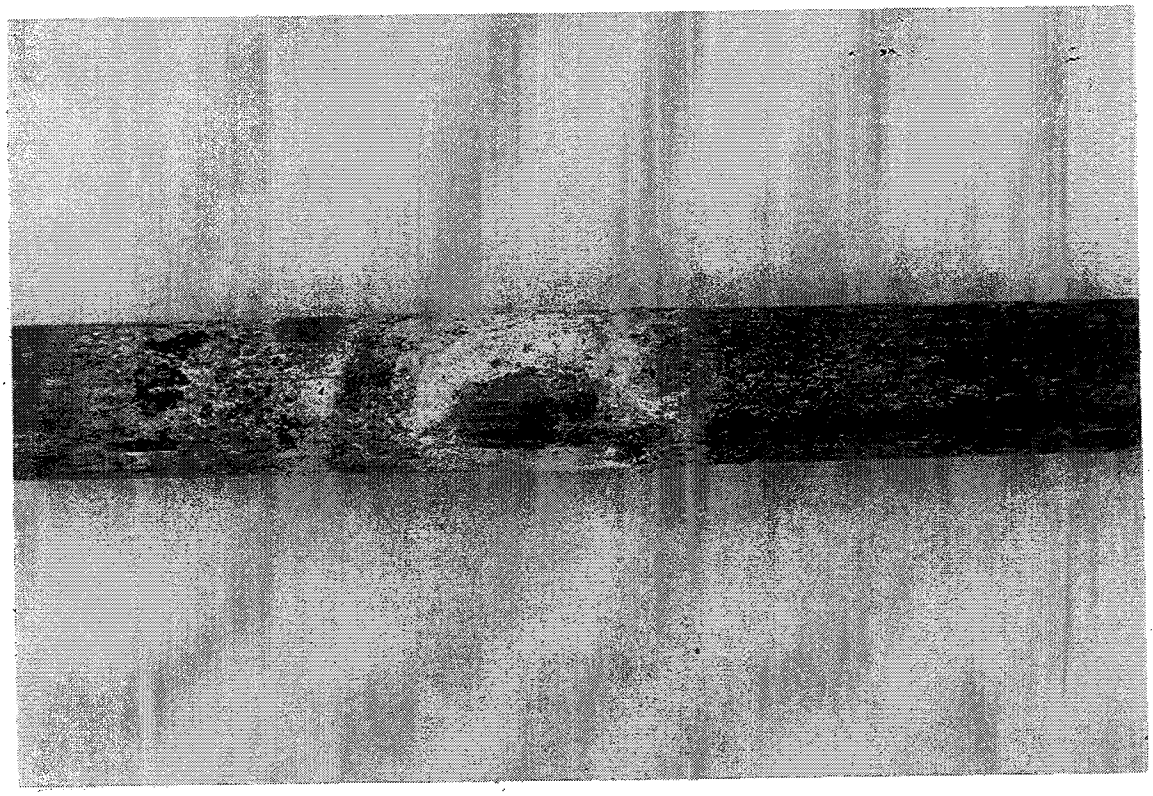

Fig. A3 - Appearance of galvanized steel rod in sand with 1% cement in NaCl, after 650 days.

Fig A4. - Microstructure (x42) of the sample.

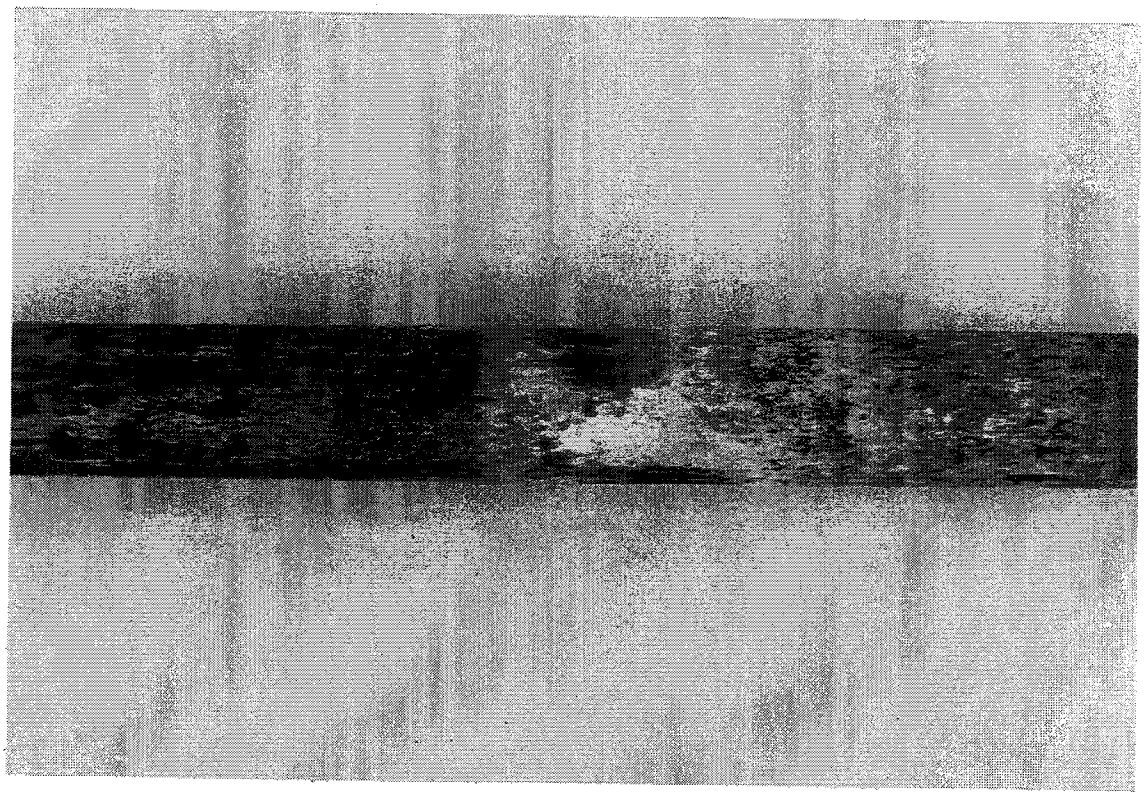

Fig. A5 - Appearance of galvanized steel rod (from soil/water mixture with 13% cement) in water, after 650 days.

Fig. A6 - Microstructure (x42) of the sample.

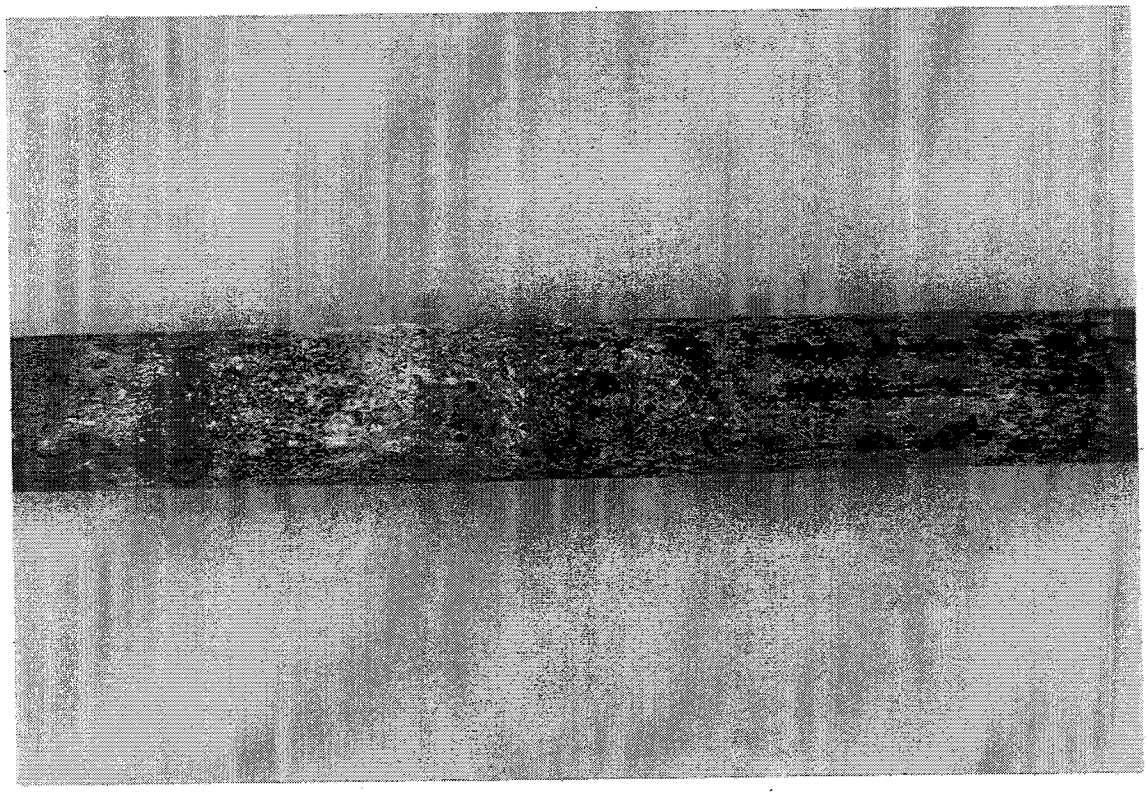

Fig. A7 - Appearance of galvanized steel rod in soil/water mixture with 1% cement in water, after 650 days.

Fig. A8 - Microstructure (x42) of the sample.

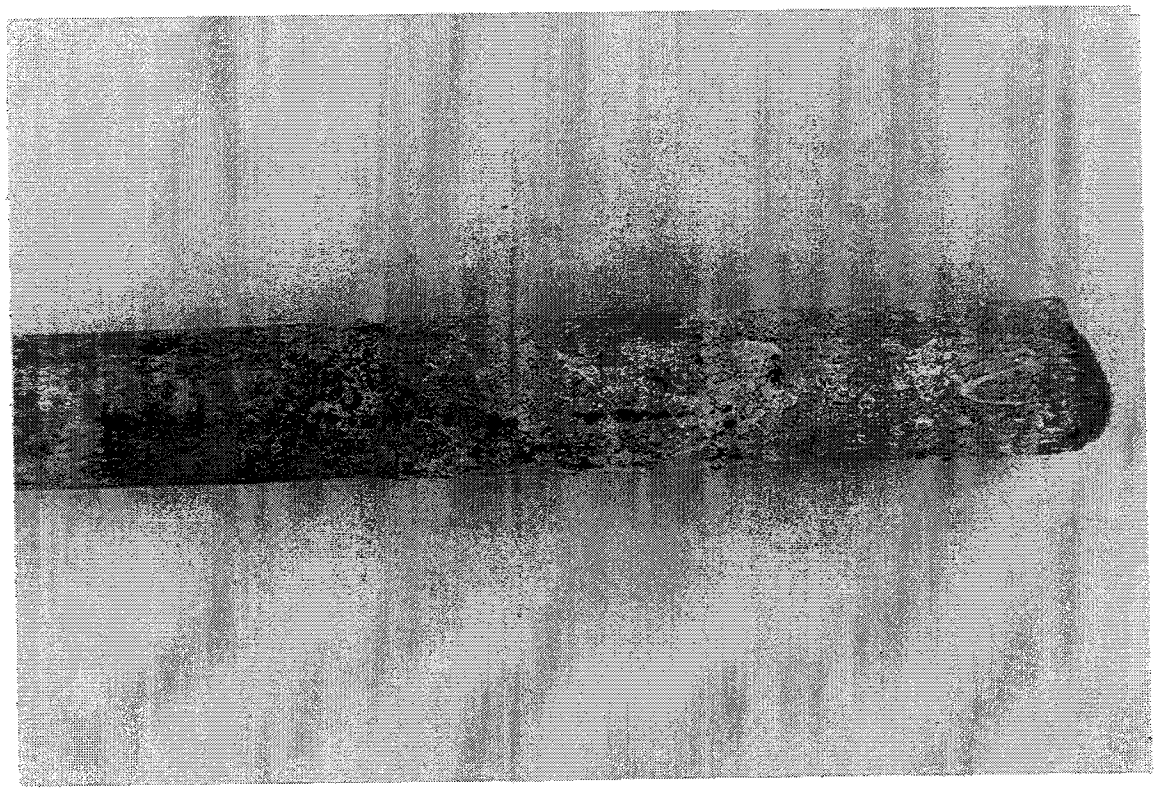

Fig. A9 - Appearance of galvanized steel rod in sand with 4% cement in water, after 650 days.

Fig. A10 - Microstructure (x42) of the sample.

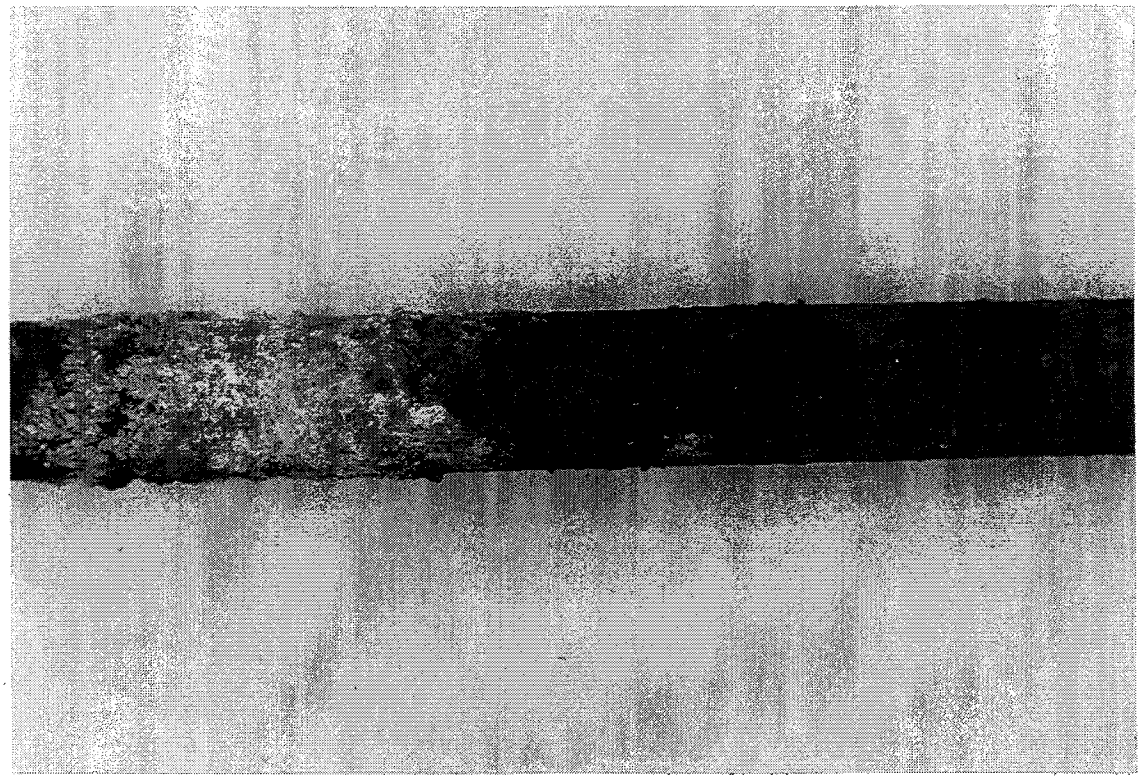

Fig A11 -Appearance of galvanized steel rod in soil/water mixture with 0% cement in NaCl, after 650 days.

Fig. A12 - Microstructure (x42) of the sample.

Fig. A13 - Appearance of galvanized steel rod in soil/water mixture with 0% cement in water at pH=12, after 650 days.

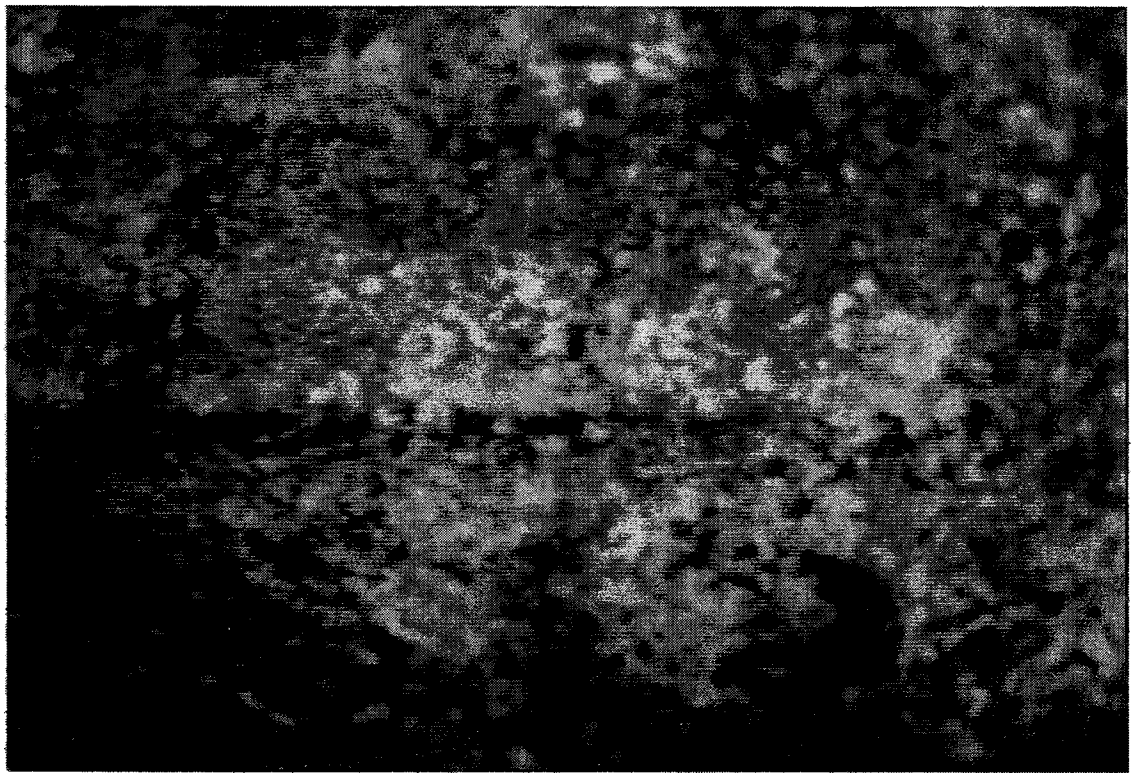

Fig. A14 - Microstructure (x42) of the sample.

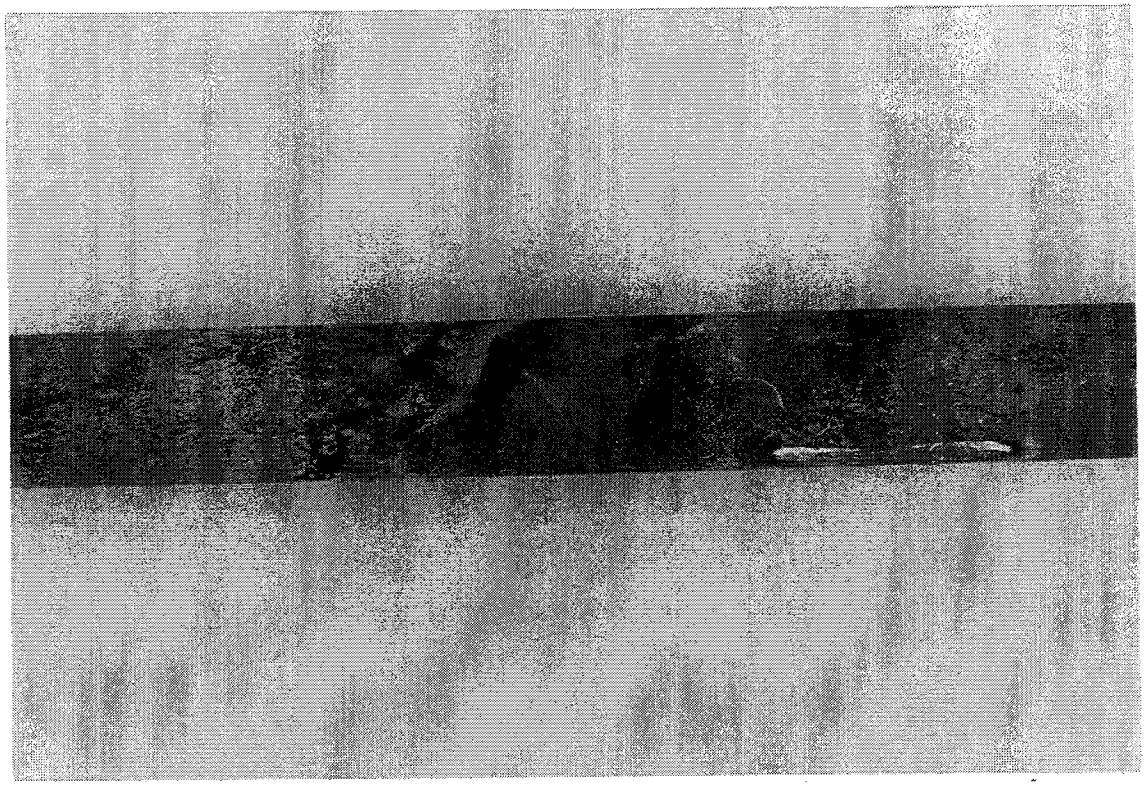

Fig. A15 - Appearance of galvanized steel rod (in sand/water mixture with 0% cement) in water, after 650 days.

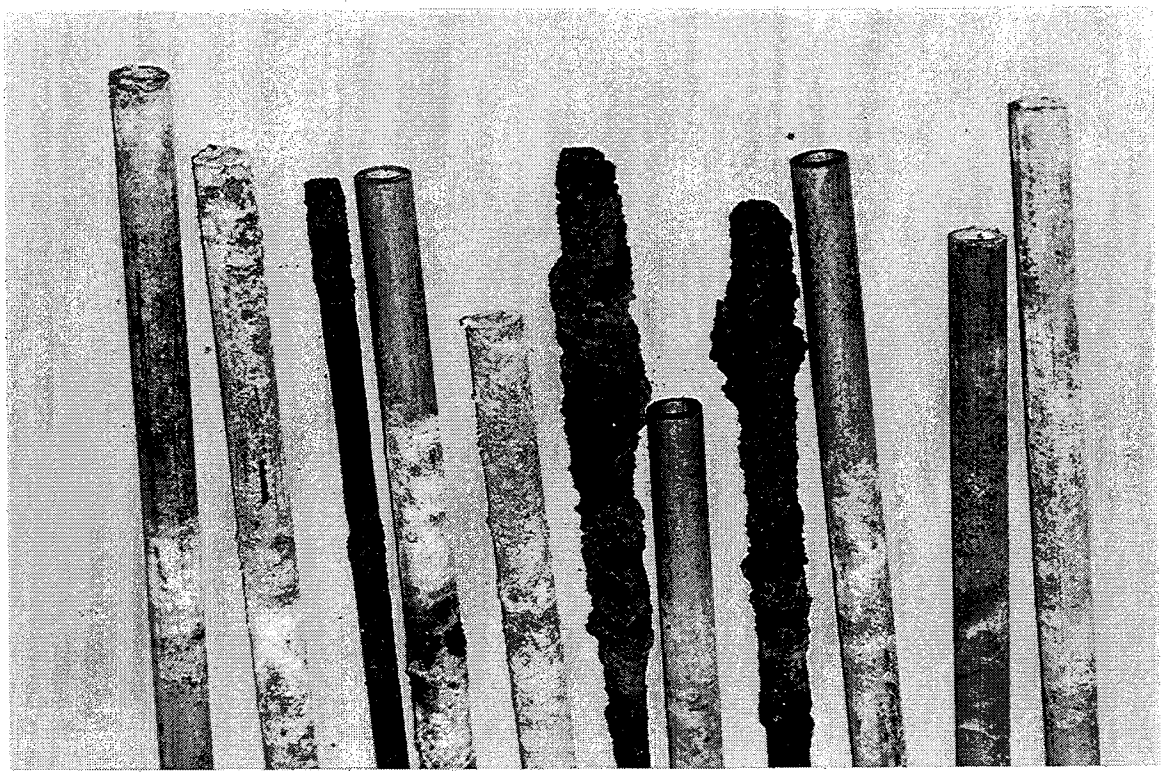

Fig A16 - Extent of corrosion after 650 days for different samples.

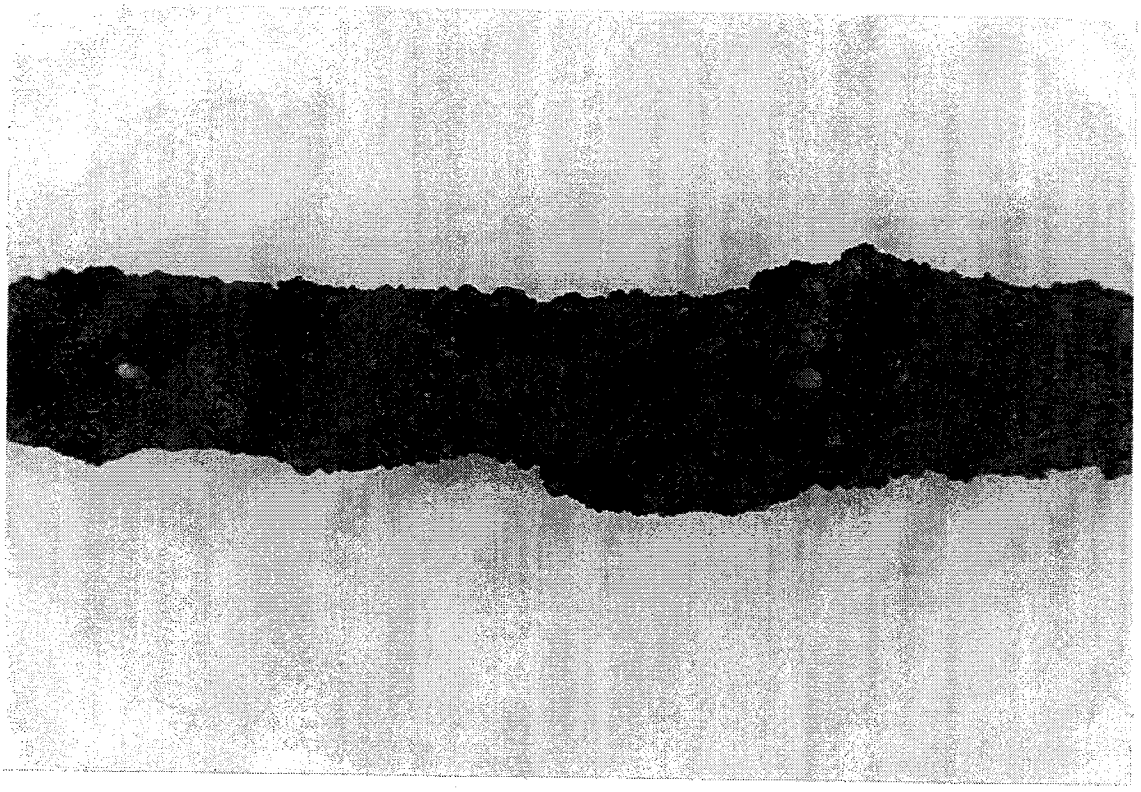

Fig. A17 - Appearance of steel rod in soil/water mixture with 0% cement in water, after 650 days.

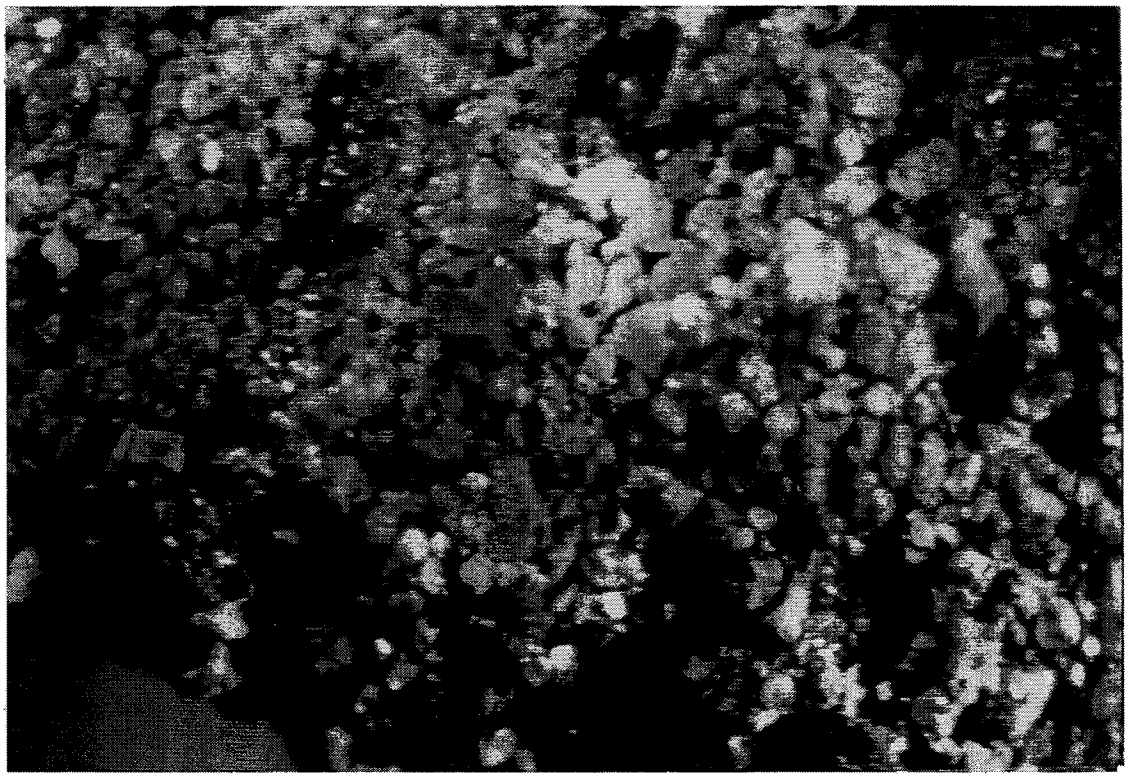

Fig. A18 - Microstructure (x42) of the sample.

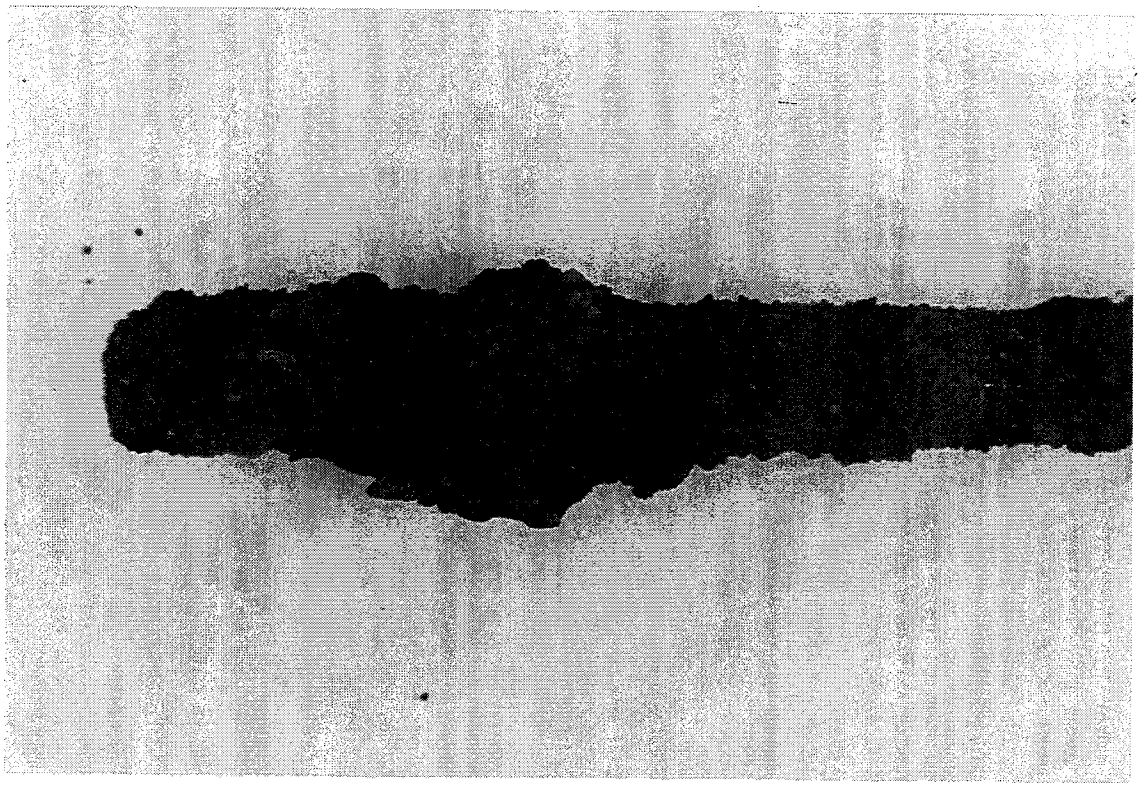

Fig. A19 - Appearance of steel rod in soil/water mixture with 0% cement in water at pH=12, after 650 days.

Fig. A20 - Microstructure (x42) of the sample.

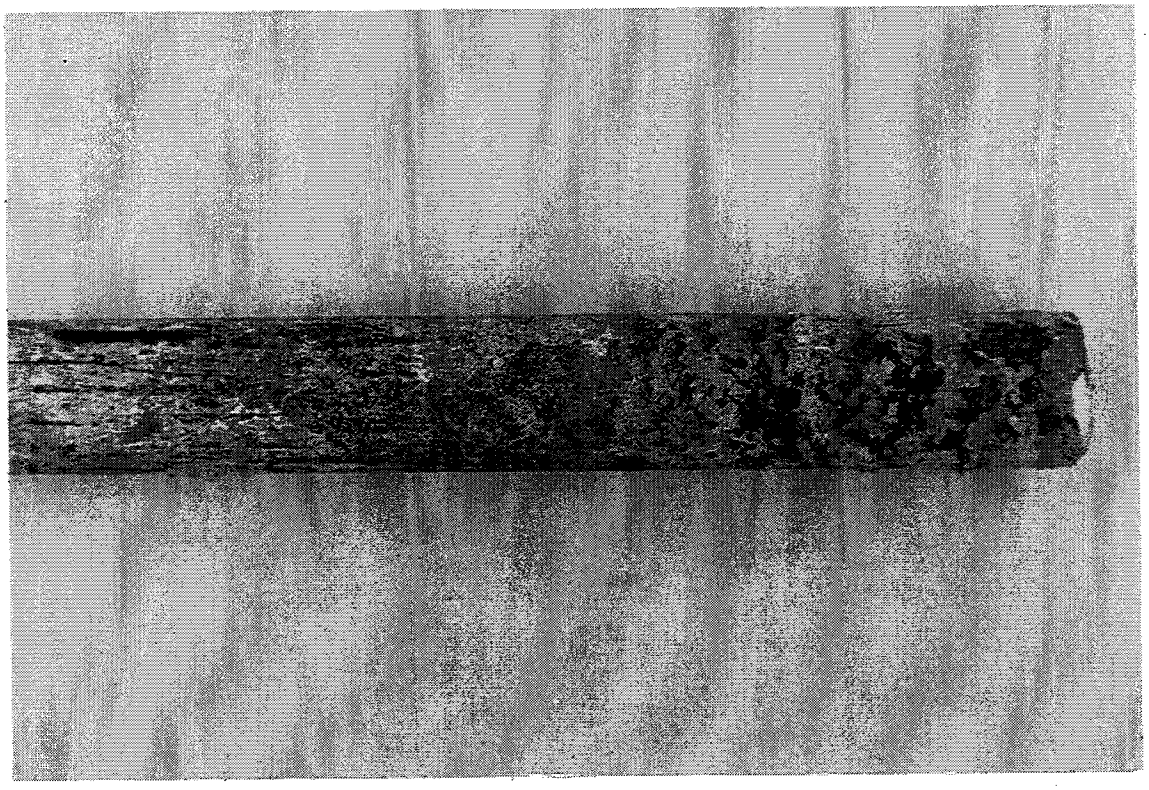

Fig. A21 - Appearance of galvanized steel rod in crushed concrete/water mixture with 0% cement in NaCl, after 650 days.

Fig. A22 - Microstructure (x42) of the sample.

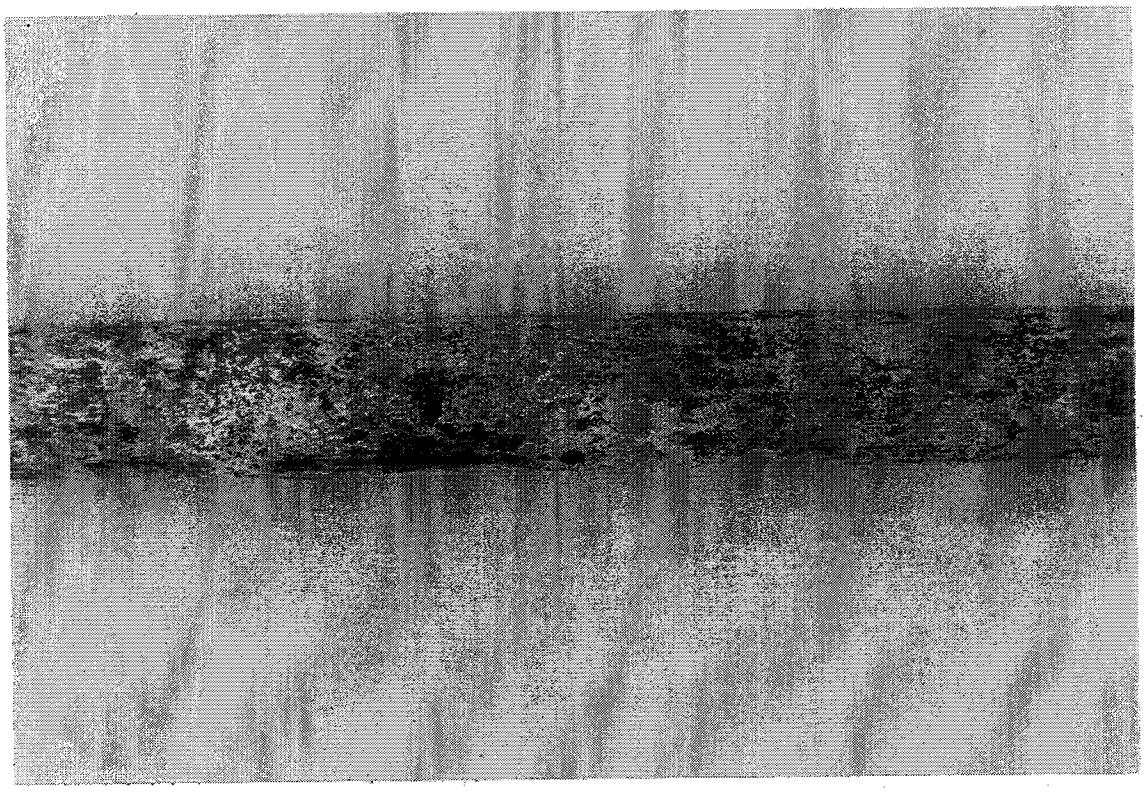

Fig. A23 - Appearance of galvanized steel rod in crushed concrete/water mixture with 0% cement in water, after 650 days.

Fig. A24 - Microstructure (x42) of the sample.

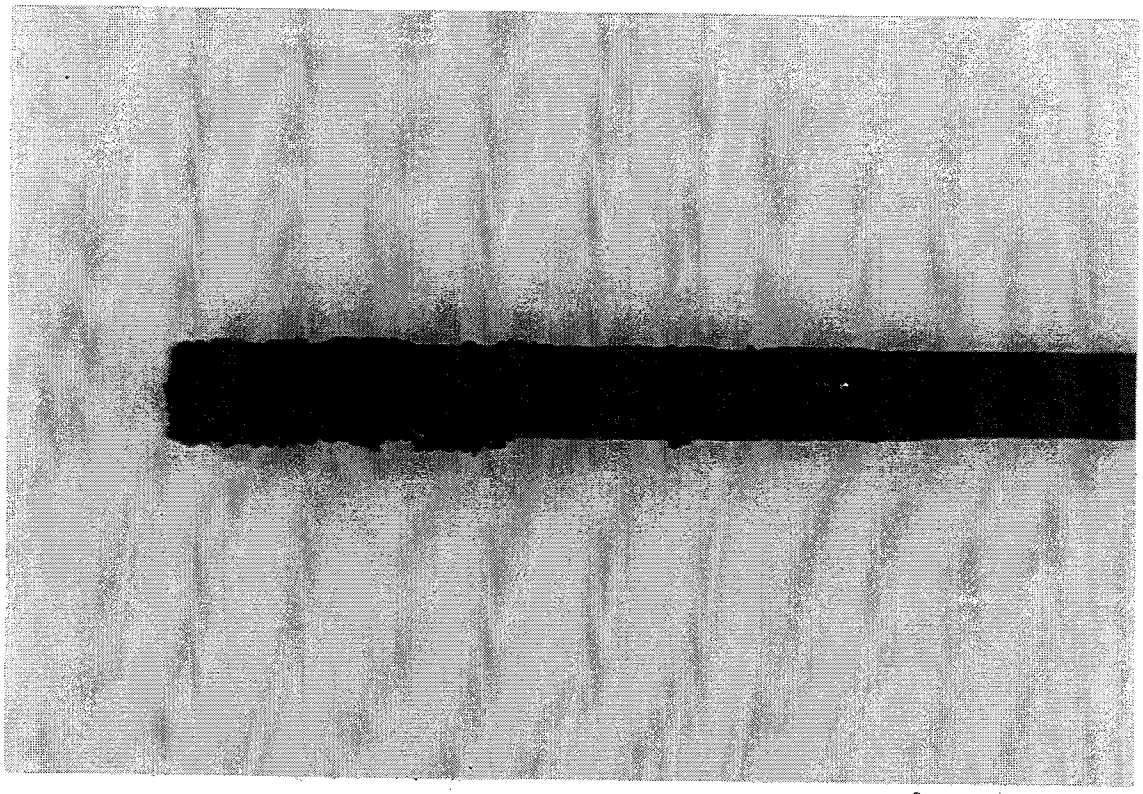

Fig. A25 - Appearance of steel rod in soil/water mixture with 1% cement in water at pH=12, after 650 days.

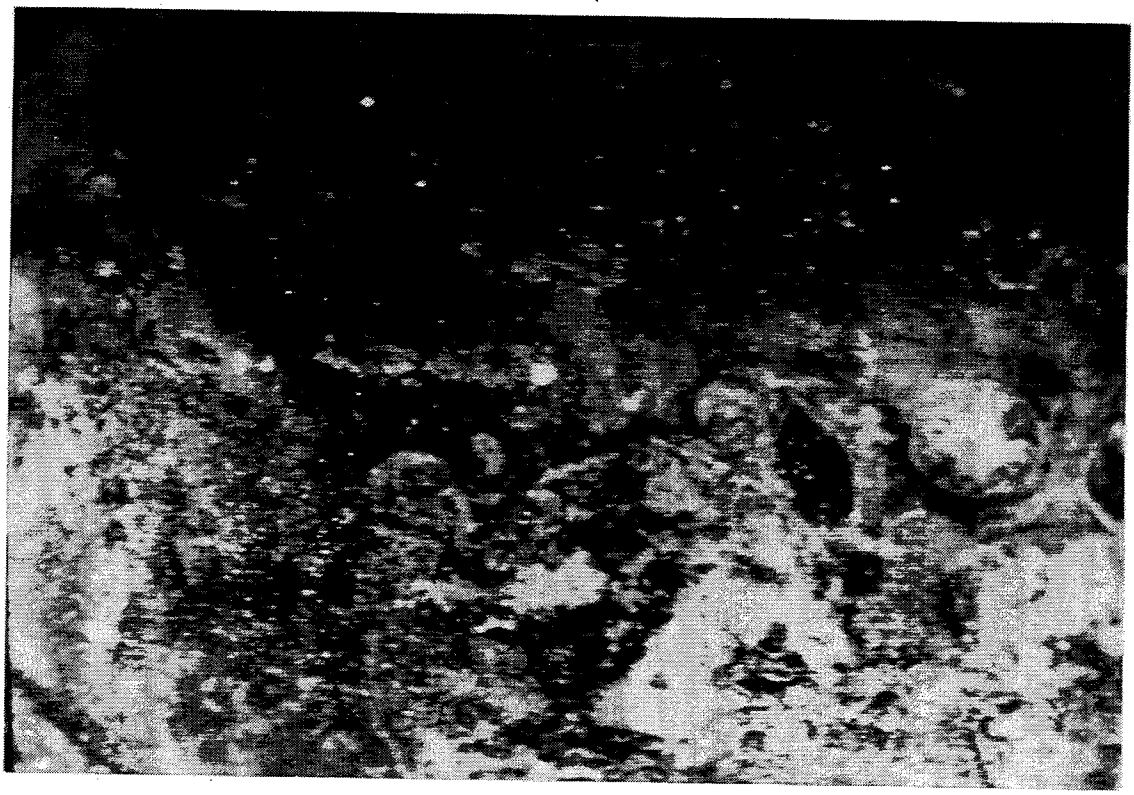

Fig. A26 - Microstructure (x42) of the sample.